# DEHYDRATION OF AQUEOUS ACETONITRILE SOLUTIONS BY EXTRACTIVE DISTILLATION USING DEEP EUTECTIC SOLVENTS

# Ph.D. THESIS

*by*

**BANDHANA SHARMA**

**DEPARTMENT OF CHEMICAL ENGINEERING**
**THAPAR INSTITUTE OF ENGINEERING AND TECHNOLOGY**
**(Deemed to be University)**
**PATIALA -147004**

**March, 2020**

# DEHYDRATION OF AQUEOUS ACETONITRILE SOLUTIONS BY EXTRACTIVE DISTILLATION USING DEEP EUTECTIC SOLVENTS

**A THESIS**

***Submitted in partial fulfilment of the requirements for the award of the degree***

***of***

**DOCTOR OF PHILOSOPHY**

***in***

**CHEMICAL ENGINEERING**

***by***

**BANDHANA SHARMA**

**DEPARTMENT OF CHEMICAL ENGINEERING**
**THAPAR INSTITUTE OF ENGINEERING AND TECHNOLGY**
**PATIALA- 147004, PUNJAB, INDIA**
**March, 2020**

## CANDIDATE'S DECLARATION

I hereby certify that the work which is being presented in the thesis entitled **"DEHYDRATION OF AQUEOUS ACETONITRILE SOLUTIONS BY EXTRACTIVE DISTILLATION USING DEEP EUTECTIC SOLVENTS"** in partial fulfillment of the requirements for the award of the degree of Doctor of Philosophy and submitted in the Department of Chemical Engineering, Thapar Institute of Engineering and Technology, Patiala is an authentic record of my own work carried out during a period from July 2014 to March 2020 under the supervision of Dr. Neetu Singh, Associate Professor, Department of Chemical Engineering and Dr. J. P. Kushwaha, Associate Professor, Department of Chemical Engineering, Thapar Institute of Engineering and Technology, Patiala.

The matter presented in the thesis has not been submitted by me for the award of any other degree of this or any other Institute.

Bandhana Sharma.

**(BANDHANA SHARMA)**

---

This is to certify that the above statement made by the candidate is correct to the best of our knowledge.

**Dr. Neetu Singh**
**Supervisor**

**Dr. J. P. Kushwaha**
**Supervisor**

# Abstract

The increasing concern about environmental issues and the requirement to reduce the negative influence of industrial processes has directed the attention of scientific community towards the development of novel "green solvents". This growing demand for green solvents has spurred the development of environmentally benign solvents.

Separation of azeotropic mixtures is of particular interest for scientific community because it represents separation limit by conventional distillation. Extractive distillation is the most applied technique for the separation of azeotropic/close boiling mixtures. Application of non-toxic and biodegradable solvents in extractive distillation is today's need, due to the environmental concern. From the last two decades, application of ionic liquids (ILs) as an entrainer for azeotropic mixture separation, significantly encouraged the researchers due to their distinctive prominent features. Gradually, the use of ILs for separation applications became restricted due to complex synthesis process, difficulties in purification, high cost, potential toxicity and poor degradability.

Recently, Deep Eutectic Solvents (DESs) which are ionic liquids (ILs) analogues have appeared as a promising substitute to conventional volatile organic solvents. Unlike ILs, DESs offer inexpensive and easy synthesis, less toxicity and good biodegradability. Due to the multi-tasking nature of DESs, these have been applied to many chemical processes. DESs are combination of two (or more) components, commonly a hydrogen-bond acceptor (HBA) and a hydrogen-bond donor (HBD), which forms a eutectic mixture. Because of the strong hydrogen-bonding impact, these have much lower melting temperature than those of starting original substances. Due to these unusual chemical and physical properties, DESs are currently getting remarkable attention as "greener" means for a wide variety of applications.

This study focuses on the separation of a common industrial waste, acetonitrile (ACN) + water mixture via extractive distillation. Due to the very high market demand of ACN, its separation from water mixture is of special interest for researchers. However, its recovery from waste effluents is often difficult as ACN + water solution forms a minimum-boiling azeotrope of composition of 67.4 mole% ACN at 76.5 ˚C and standard atmospheric pressure. Many conventional solvents like; ethylene glycol, butyl acetate and dimethyl sulfoxide (DMSO) have been used earlier for dehydration of acetonitrile. Although, high entrainer requirement, uneven

mixing of ethylene glycol with the mixture and recycling issue of butyl acetate (because of its high volatility), restricts the application of these entrainers.

Few imidazolium based ionic liquids (ILs) have been used for separation of this azeotropic mixture. 1-butyl-3-methylimidazolium chloride ([Bmim][Cl]), 1-butyl-3-methylimidazolium tetrafluoroborate ([Bmim]-[BF4]), and 1-butyl-3- methylimidazolium dibutyl phosphate ([Bmim][DBP]) have been used for this purpose. In spite of many extraordinary physicochemical properties of these ILs, its toxic nature, non-biodegradability and high cost of synthesis and purification became the main barrier in its extensive utilization in separation processes.

The main objective of this thesis was to synthesize different types of DESs and examine its viability as entrainer for separation of ACN + water mixture by extractive distillation. Two different classes of DESs i.e. sugar based DESs and natural DESs were prepared by considering different types of HBDs and HBAs. Glycolic Acid and Malic acid were used as HBD and choline Chloride and Tetramethylammonium chloride were used as HBA in different molar ratios for this purpose. Two sugar based DESs glycolic acid + choline chloride 3:1 (GC 3:1) and glycolic acid + tetramethylammonium chloride 3:1 (GTM 3:1) and two natural DESs malic acid + choline chloride 1:1 (MC 1:1) and malic acid + tetramethylammonium chloride 1:1 (MTM 1:1) were synthesized. These were characterized for relevant chemical, physical and thermal properties like, FT-IR spectroscopy, $^{1}$H NMR spectroscopy, Thermogravimetric analysis, viscosity, density and moisture content.

These synthesized DESs were utilized as entrainer for vapor–liquid equilibrium (VLE) studies of ACN + water mixture via extractive distillation. A modified Othmer type recirculation still was employed for VLE studies. Isobaric VLE studies for pseudobinary systems (ACN + DES, water + DES) and pseudoternary systems (ACN + water + DES) were performed at atmospheric pressure. Studied pseudobinary systems include, ACN + GC3:1, ACN + GTM 3:1, ACN + MC1:1, ACN + MTM 1:1, water + GC 3:1, water + GTM 3:1, water + MC1:1 and water + MTM 1:1. Pseudoternary VLE data were generated for systems ACN + water + GC 3:1, ACN + water + GTM 3:1, ACN + water + MC1:1 and ACN + water + MTM 1:1 for different DES molar compositions (5%, 10%, 15% mol/mol).

From results it was observed that, addition of these DESs (GC 3:1, GTM 3:1, MC1:1 and MTM 1:1) created a significant salting-out effect by increasing the relative volatility of ACN to water, and could eventually remove the azeotrope. However, this effect was better in case of sugar based DESs (GC 3:1, GTM 3:1) as compared to natural DESs (MC 1:1, MTM 1:1). MTM 1:1 could not break the azeotrope at lowest studied dose (5% mol/mol) but at higher dosage it could successfully break the azeotrope. Nonetheless, exceptional solubilizing and stabilizing properties of NADESs (due to uncommon intermolecular adjustment in its matrix), natural & biodegradable starting compounds and non-corrosive nature adds more value to be used as entrainer. Although all four DESs were capable in breaking the ACN + Water azeotrope (at different dosage) but GTM 3:1 presented the highest relative volatility at a given concentration. Comparing the performances of simple sugar based DESs with NADES, the simple DESs were performing better than NADESs following the trend GTM 3:1> GC 3:1 > MC 1:1 > MTM 1:1. The high viscosity of MC1:1 and MTM 1:1 is a limiting factor in separation processes, but by manipulating its properties it can be used as entrainer in future.

Further, experimental results (for pseudobinary & pseudoternary systems) were validated employing nonrandom two-liquid (NRTL) model with minor deviations. The average absolute deviation in vapor phase mole fraction of ACN in case of GC 3:1, GTM 3:1, MC 1:1 and MTM 1:1 was 0.009, 0.007, 0.002 and 0.001 respectively. The average absolute difference for the equilibrium temperature of GC 3:1, GTM 3:1, MC 1:1 and MTM 1:1 was 0.42 K, 0.45K, 0.15 K and 0.45 K respectively.

Both types of DESs were also retrieved successfully and reused till five cycles with no notable change in chemical properties but slight decrease in performance of NADESs was observed.

# ACKNOWLEDGEMENTS

I express my indebtedness to the "**ALMIGHTY**" for all his blessing, kindness and potency to follow the path of success.

I would like to express my sincerest regards and gratitude to my supervisors **Dr. Neetu Singh** and **Dr. J.P. Kushwaha**, Department of Chemical Engineering, Thapar Institute of Engineering and Technology (Deemed to be University), for providing me such a valuable research opportunity and for their countless guidance, knowledge and motivation during the course of my research. They have been invaluable in the constructive input to this work. It's been a great honour to work under their guidance.

I am extremely thankful to Prof. Prakash Gopalan, Director, Thapar Institute of Engineering and Technology (Deemed to be University), Prof. Rafat Siddiqui, Dean of Research & Sponsored Projects and Prof. Haripada Bhunia, Head, Department of Chemical Engineering for extending the opportunity to undertake this doctoral research. I am also thankful to Prof. R.K. Gupta, Former Head of Chemical and Engineering Department for his valuable suggestions throughout the course of this research work.

I am also thankful to my doctoral committee members Dr. Sanghamitra Barman, Associate Professor, Department of Chemical Engineering, Dr. S.K. Ahuja, Associate Professor, Department of Chemical Engineering and Dr. Amjad Ali, Professor and Head, School of Chemistry & Biochemistry, for advising and guiding me towards the right direction. The generous support of all the staff members of Department of Chemical Engineering is greatly appreciated. I would like to thank entire staff of SAI Labs, TIET, Patiala and SAIF Labs, PU, Chandigarh for facilitation in analytical analysis.

My sincere thanks to Dr. Vijay Luxami, Associate Professor, School of Chemistry and Biochemistry, Dr. Parminder Singh, Assistant Professor, Department of Chemical Engineering, Thapar Institute of Engineering and Technology (Deemed to be University) for their valuable help, and to Soumen Ghosh, for helping me with Gas Chromatography Techniques.

This thesis would never be possible without immense love and support of my father-in-law Ram Lubhaya Sharma and my mother-in-law Veena Sharma. I am also thankful to my brother-in-law Rohit Sharma and my sister-in-law Poonam Sharma for their constant support through out my Ph.D. journey.

I would like to thank my colleagues Sehaspreet Kaur Toor, Ravneet Kaur, Kamaljit Singh, Meenakshi, Metali Sarkar, Steffi Talwar, Parminder Kaur and Suman Duhan for providing all the encouragement and support at various stages of my work.

I express my deepest gratitude to my parents Charanjiv Lal Sharma and Sapna Sharma and my sister Vanita Sharma and Brother Abhinav Sharma for their love, never ending support, and encouragement. I would cherish every moment where my parents were so keen and curious to know about the details and progress of my work, which boosted my confidence.

Last but definitely not least It is my privilege to thank my husband Gaurav Sharma who supports in every phase without questioning my capability and hearty thankful for his eternal support, love and courage to achieve my goals, and daughter Inaayat Sharma for being a good baby throughout my research period and making it possible to complete what I started and would like to dedicate this thesis to them.

Bandhana Sharma

**(BANDHANA SHARMA)**

# CONTENTS

# LIST OF TABLES

# LIST OF FIGURES

# NOMENCLATURE

**ABBREVIATIONS**

| | |
|---|---|
| ACN | Acetonitrile |
| HPLC | High performance liquid chromatography |
| LCMS | Liquid chromatography-mass spectrometry |
| COSMO-RS | Conductor like screening model for real solvents |
| VOCs | Volatile organic compounds |
| LLE | Liquid–liquid extraction |
| SALLE | Salting out liquid–liquid extraction |
| PSD | Pressure swing distillation |
| IL | Ionic liquid |
| FT-IR | Fourier transform infrared spectroscopy |
| RTILs | Room temperature ionic liquids |
| AAILs | Amino acid ionic liquids |
| DES | Deep eutectic solvent |
| HBD | Hydrogen bond donor |
| HBA | Hydrogen bond acceptor |
| DWC | Divided wall column |
| TGA | Thermogravimetric analysis |
| DMSO | Dimethyl sulphoxide |
| NMR | Nuclear magnetic resonance |
| GC | Gas chromatograph |
| IPA | Isopropanol |
| NRTL | Non-random two-liquid model |
| VLE | Vapor–liquid equilibrium |
| TMAC | Tetramethylammonium chloride |
| NADES | Natural deep eutectic solvent |

**List of symbols**

| | |
|---|---|
| $A_i, B_i, C_i$ | Antoine equation constants of component $i$ |

| | |
|---|---|
| $OF$ | Objective function |
| $g$ | Interaction parameters in NRTL equation, J/mol |
| $P$ | Total pressure in the system, kPa |
| $p_i^{sat}$ | Saturation vapor pressure of pure liquid i, kPa |
| $x_i$ | Mole fraction of component $i$ in liquid phases |
| $x_i^{'}$ | Mole fraction of component $i$ in the liquid phase on DES-free basis |
| $y_i$ | Mole fraction of component $i$ in vapor phases |
| $T$ | Equilibrium boiling temperature, K |
| $T_b$ | Boiling points of pure substance at 101.32 kPa, K |
| $V^L$ | Liquid molar volume |
| $w_i$ | Mass fraction of Component $i$ |
| $u$ | Uncertainty |
| $PE_i$ | Pointing effect of component $i$ |
| D | Average value |
| d | Maximum value |
| 1 | Acetonitrile |
| 2 | Water |
| 3 | DES |

**Greek letters**

| | |
|---|---|
| $\alpha$ | Non-randomness parameter in NRTL equation |
| $\alpha_{12}$ | Relative volatility of component 1 and 2 |
| $\gamma_i$ | Activity coefficient of component $i$ in the liquid phase |
| $\phi_i^V$ | Fugacity coefficient of component $i$ |
| $\phi_i^S$ | Fugacity coefficient of saturated pure component $i$ |
| $\beta$ | Distribution ratio |
| $S$ | Selectivity |

| | |
|---|---|
| ρ | Density |
| μ | Viscosity |

**Superscripts**

| | |
|---|---|
| *cal* | Calculated value |
| exp | Experimental value |
| *L,V* | In the liquid phase; in the vapor phase |
| *s* | Saturation |
| *E* | Extract |
| *R* | Raffinate |

**Subscripts**

| | |
|---|---|
| *i* | Component *i* |
| n | Data point |

*Chapter – 1*

# INTRODUCTION

## 1.0 GENERAL

Acetonitrile (ACN), an important organic solvent, is widely used in many fields such as pharmaceuticals, liquid chromatography, organic synthesis and in photosensitive materials. ACN is classified as simplest nitrile in terms of functional group with chemical formula $CH_3CN$. The Chemical structure of ACN is illustrated in Figure 1.1 (https://pubchem.ncbi.nlm.nih.gov/compound/Acetonitrile).

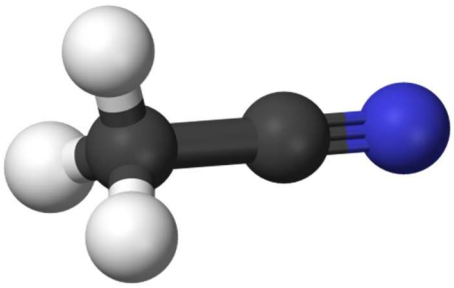

**Figure 1.1 Chemical structure of Acetonitrile**

(Where white balls represent Hydrogen, grey balls represent Carbon and blue ball represents Nitrogen)

Due to its polar aprotic behavior, it is mainly used for the purification of butadiene, (Xu et al., 2002) as well as in the synthesis of many pharmaceuticals drugs and photographic films (Srinivasu et al., 2002). Due to the unique properties of ACN like, low viscosity, low chemical reactivity and high dipole moment (3.84 D), a broad range of ionic as well as non-polar solvents dissolve in it. Because of this nature, it acts as mobile phase in HPLC (Gu et al., 1994, Dhamole et al., 2010) and LCMS (Rosen et al., 2002). There are two types of acetonitrile available in the market i.e. “analar grade” which is 99.9% refined and mainly used in HPLC, and the other is “technical grade” which can be used by chemical industries for the synthesis of different organic compounds like amides, amines, carboxylic acids, amidines,

esters, ketones, aldehydes and many more (Marcotte et al., 2003). High permittivity of ACN makes it an eligible solvent for use in battery fields (Imanishi et al., 1999, Kurzin et al., 2006) and in cyclic voltammetry (Yang et al., 1991). Moreover, ACN has applications in the synthesis of photosensitive materials and also enhances the enzyme's catalytic efficiencies (Gupta et al. 2000). It is also used in various extractive purification processes, organic compound analysis as well as biochemical reactions (Kittaka et al. 2007) e.g., it is used as a solvent to produce insulin, antibiotics and some natural occurring pesticides. The physical properties of ACN are given in Table 1.1 (Miyanaga et al. 1992).

**Table 1.1 Physical Properties of Acetonitrile (ACN)**

| Property | Value |
|---|---|
| Molar mass | 41.0524 g/mol |
| Boiling Point | 81.6°C |
| Melting Point | -41.7°C |
| Density | 0.786 g/ml |
| Refractive Index | 1.3442 D |
| Surface Tension | 29.29 dyne/cm |
| Dipole moment | 3.44 Debye |
| Dielectric Constant | 36.0 |
| Heat of Vaporization | 7.94 kcal/mol |
| Heat of Fusion | 1.95 kcal/mol |
| Heat of Combustion | -300.3 kcal/mol |
| Thermal Conductivity | 213 mJ/m/sec/°C |

Source:- Miyanaga et al. 1992

### 1.1 Production Routes

ACN is mainly produced by the catalytic ammoxidation of propylene which is used as a substitute process in place of acetylene based technology. In a fluidized bed reactor, Propylene and ammonia are reacted in the presence of air and produces acrylonitrile. During the synthesis of acrylonitrile, ACN and hydrogen cyanide are produced as by-products

(Presson et al. 1982). At commercial scale, ACN is available under different grades like, reagent grade, high purity grade and chemical grade. The majority of acrylonitrile producers produce ACN as co-product by ammoxidation of propylene and ethane using metal zeolite catalyst (Li et al., 1998). During the production of 100 litres of acrylonitrile by ammoxidation of propylene, it produces 2 to 4 litres of ACN as by-product (http://www.ineos.com/businesses/ineos-nitriles). But there are only few acrylonitrile production plants in existence that isolate ACN and make it available for the sale. ACN is also produced by organic synthesis on laboratory scale.

**1.2 Acetonitrile: An Excellent Solvent**

ACN is considered as Pseudo-universal solvent because it can dissolve a wide range of organic compounds in the pharmaceutical and chemical industries without violating their chemical structure. Due to the presence of stable C-C bonding in the ACN, it is highly inert in nature and it can be hydrolyzed only in severe condition. Therefore it acts as a very promising reaction solvent. The studies like Conductor-like Screening Model (COSMO) and Sigma profiles were employed to study the favorable solvation properties of ACN as compared to the other organic solvents (McConvey et al., 2012). The charge distribution of ACN as well as polarity found in COSMO qualitative analysis resembled with the respective properties of water molecules which leads to the solvation of a wide range of the polar as well as non-polar compounds in it. The comparison of the physical properties of ACN with other polar organic solvents is demonstrated in Table 1.2 (McConvey et al., 2012).

**1.3 Shortage of ACN**

In 2008, the decreasing supply of ACN, as a byproduct during the production of acrylonitrile, enhanced the cost of ACN. As the demand of the acrylonitrile was very low in 2008, the supply of the ACN also reduced by 50% due to the lower production of acrylonitrile (Majors et al., 2009). At the same time, the worldwide supply of ACN was shut because of the Olympics held in china to minimize air-pollution. Secondly, In September 2008, in the coast of Texas, Hurricane Ike temporarily shut down which was one of the main producers in Texas and this shortage prolonged till 2009. There was no direct route for the production of ACN, due to which the supply of ACN decreased and there was a remarkable rise in the price

of ACN. The problem rose to such limit that it was known as "The Great Acetonitrile Shortage" or "The Great Acetonitrile Drought" (Lowe et al., 2009).

**Table 1.2 Characteristic Properties of ACN as a solvent as compared to the other polar organic solvents**

| Property | Molecular weight (g/mol) | Boiling Point ($^oC$) | Density (g/ml) | Kinematic Viscosity ($10^6$ $m^2/s$) at 20$^oC$ | Dielectric constant at 20$^oC$ | Miscibility with water |
|---|---|---|---|---|---|---|
| Acetonitrile | 41.5 | 81.6 | 0.783 | 0.49 | 35.94 | miscible |
| Methanol | 32.04 | 64.50 | 0.791 | 0.75 | 32.66 | miscible |
| Hexane | 86.18 | 68 | 0.655 | 0.44 | 1.89 | immiscible |
| THF | 72.11 | 67.0 | 0.88 | 0.62 | 7.58 | miscible |
| DMSO | 78.14 | 189.0 | 1.1 | 2.0 | 46.45 | miscible |
| DMF | 73.09 | 153.0 | 0.948 | 0.98 | 36.7 | miscible |
| DCM | 84.93 | 39.7 | 1.325 | 0.33 | 8.93 | Immiscible |
| Acetone | 58.08 | 56 | 0.791 g/ml | 0.41 | 20.7 | miscible |

Source:- McConvey et al., 2012

### 1.4 Acetonitrile Production Statistics

Presently, the ACN producers are divided throughout the world. To produce ACN for upto 60% of global capacity, there are only few competitors including INEOS Ltd. in the United States, Formosa, CNPC Jilin Chemical Group in China, Asahi Kasei Ltd. in Japan, PetroChina, Secco and Sinopec in China. Around 40 to 50% supply of ACN throughout the world is done by INEOS (http://www.ineos.com/businesses/ineos-nitriles/news/ineos-nitriles-breakthough-secures-global-supply-of-acetonitrile), producing about 34,000 tons of ACN per annum (http://www.chemmarket.info/en/home/article/2902). USA is the main producer of ACN, followed by China, United Kingdom, Brazil, Germany and France which are the top producer countries of ACN. World consumption is expected to continue to rise at a rate of

about 6% per year in the next five years. The highest growth rates of consumption of ACN (about 9–10% per year) is anticipated for China and India, since the production of generic medicines, engineered drugs and pesticides are increasing day by day in these countries. The report represents the world consumption of ACN in 2017-2018 (Figure 1.2) (https://www.ihs.com/products/acetonitrile-chemical-economics-handbook.html), where India stood on fourth place due to the large amount of consumption in pharmaceutical and analytical industries (Miyanaga et al., 1992).

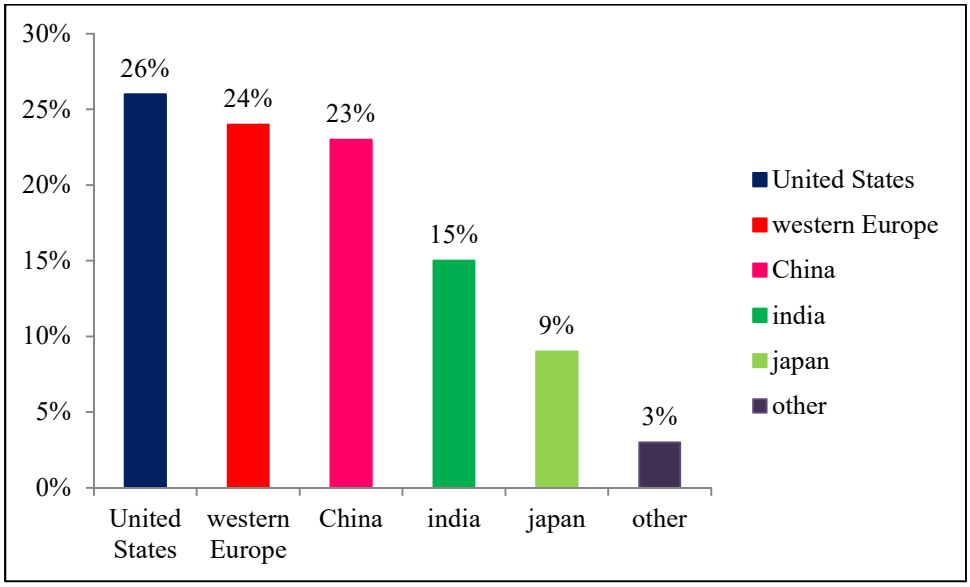


**Figure 1.2 World consumption of Acetonitrile in 2017-2018**

Source:- Miyanaga et al., 1992

### 1.5 Environmental and health impacts of ACN

Acetonitrile is a solvent that is frequently used in the industrial processes, especially in chemical and pharmaceutical industries. Many pharmaceutical industries consume a huge amount of ACN for the purification of peptide drugs in the columns of liquid chromatography. Due to this, the mixture of ACN and water release as waste stream from pharmaceutical industries. As the ACN + water mixture forms homogenous minimum boiling

azeotrope and its separation is not simple, so it was a regular practice to drain the effluent out of the plant without treatment. As the process capacity expands, the cost of the disposed waste solvent and fresh ACN purchase affects the economy of the plant (Kim et al., 2004, Boczkaj et al. 2014). In Environment, the ACN reacts with acid, water and air which results in the production of flammable vapors and harmful toxic fumes. Even the reaction of ACN with strong oxidizing agents like nitric acid, sodium peroxide and chromic acid leads to the explosion as well as causing fire (Pirkanniemi et al., 2002). The regular exposure of ACN for a certain period of time affects the human nervous system, circulatory as well as respiratory system. In humans the concentration of acetonitrile above 500 ppm through inhalation can cause mucous membrane irritation and the longer exposure can cause weakness, nausea and convulsions. The effects can be confusion, abnormal salivation, rapid breathing, vomiting and rapid heart rate which results in coma and it can also lead to death (http://www.npi.gov.au/resource/acetonitrile). The reaction of ACN with other organic compounds can produce photochemical smog. It also affects the fertility of the soil.

**1.6 Recovery of ACN from spent stream**

Like other water soluble organic solvents such as isopropanol, ethanol, tert-butanol etc. the separation of ACN + water mixture is very difficult task because the two components i.e. ACN and water represents similar boiling points and form azeotrope at a given concentration, which does not allow the separation by conventional distillation (Gmehling et al., 1994). ACN + water mixture forms a minimum-boiling azeotrope of composition of 82.2 mass% (67.4 mole %) acetonitrile at 76.5 ˚C temperature and atmospheric pressure (Maslan et al., 1956). The phase diagram of ACN + water azeotropic mixture is dependent upon temperature and pressure. In Figure 1.3, the VLE of a binary mixture is represented by means of $T-x,y$ (temperature-composition) in case of ACN + water azeotropic mixture (Othmer et al., 1947). There are number of processes available for the separation of ACN + water azeotropic mixture. The different types of separation processes for the production of anhydrous ACN is mentioned below:

1) Liquid–Liquid Extraction
2) Membrane Processes
3) Hybrid Membrane Processes (Pervaporation-Distillation)

4) Extractive Distillation
5) Azeotropic Distillation
6) Pressure-swing Distillation
7) Other Processes

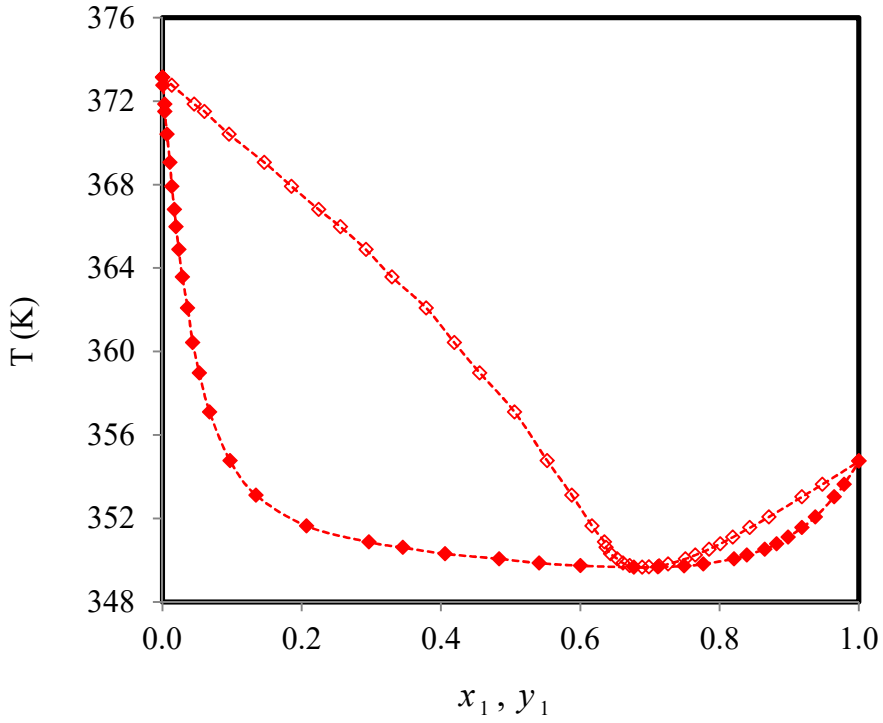


**Figure 1.3 Temperature−composition (T−x,y) diagram for the acetonitrile (1) + water (2) system at 101.3 kPa.**

*Chapter – 2*

# SEPARATION OF AZEOTROPIC MIXTURES – A LITERATURE REVIEW

## 2.0. GENERAL

Scientific community has found several ways to separate the close boiling point azeotropic mixtures that cannot be separated by the simple distillation. In this segment of thesis, the commonly used techniques to separate ACN + water azeotropic mixtures will be discussed. For the separation of azeotropic mixtures, the most common techniques that are available can be categorized into four different groups:

*(i)* Membrane processes

*(ii)* Liquid-liquid extraction.

*(iii)* Adsorption Processes

*(iv)* Enhanced distillation techniques.

## 2.1. Membrane Processes

In membrane-based processes, the most implemented membrane process to separate the azeotropes is pervaporation. Pervaporation is a separation technique in which the separation of the liquid azeotropic mixture is processed with the help of a thick membrane by dragging a vacuum to the permeate side of the membrane, so that the permeate pass through the membrane (Kishore et al., 2003, Tsuru et al., 2000, Aptel et al., 1976). In case of pervaporation separation technique, the chemical potential gradient is the main driving force that maintain across the membrane. The chemical potential gradient can be created by maintaining the partial pressure of the azeotropic feed higher than the permeate vapor pressure (which is usually maintained with the help of vacuum pump) (Kober et al., 1917). The efficiency of membrane processes depend upon a number of factors associated with the membrane i.e. good permeability, stability, reasonable useful time, high selectivity, easy fabrication & packaging, chemical & mechanical compatibility with the processing environment, stability and capability to endure large pressure differences (Mishra et al., 2016, Arif et al., 2017). In chemical industries, membrane separation processes for azeotropic separation are adequately used (de Haan et al., 2007). In general, membrane processes are less

capital intensive, easily operated, controlled and maintained. Still, for large scale operation, it requires many parallel units that are still to be explored. The schematic diagram of membrane process is presented in Figure 2.1.

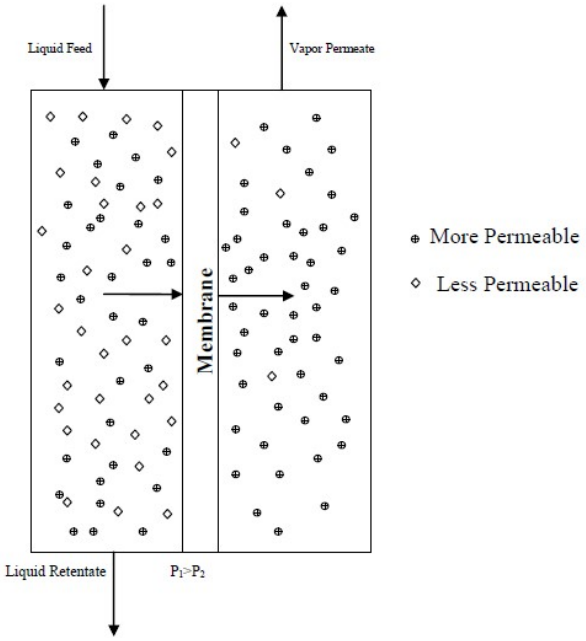


**Figure 2.1. Schematic Diagram of membrane process**

Hoof et al. (2006) used the commercially available NaA type zeolite membrane that was supplied by Mitsui engineering to eliminate the azeotrope from ACN + water, methylethylketon + water and isopropanol + water azeotropic mixtures. The dehydration capability of this membrane was compared for each solvent independently with other commercially available polymeric membranes that were supplied by the different suppliers known as Celfa and Sulzer. The optimum temperature to perform all the experiments was set at 70˚C. In case of all the solvents that were tested, the best dehydration properties were shown by the zeolite membrane in the region of azeotrope and below the region of azeotrope for the water concentration. In case of dehydration of isopropanol, the polymeric Celfa membrane (CMC-VS-11V) performed satisfactorily with excellent results. The Mitsui membranes gave the higher fluxes as well as the selectivity of the solvent although the

concentration of water feed was low, which could be possible to pervaporate up to low concentration of water feed. Pfenning and Woermann (1987) conducted some experiments based upon hyperfiltration for the separation of ACN + water azeotropic mixtures with the help of specially prepared phenolsulfonic acid (PSA) membranes. The transportation properties of the membranes were also reported. They used the cation exchanging membranes that were heterogeneous membranes grafted with the polystyrene sulfonate on the foil of polyethene. Khayet and co-workers (2008) used Sulzer Pervap 4060 membranes for pervaporation process to productively separate acetone + water, ethanol + water and ACN + water binary azeotropic mixtures as well as multicomponent azeotropic systems. By using different feed concentrations, they conducted pervaporation experiments for organic azeotropic mixture of ACN and water that ranges from 0.5 to 10 weight% by varying the feed temperature from 30ºC to 60ºC. They controlled the temperature of the feed side by placing thermostat where pervaporation experiment was performed. The permeation flux and organic selectivity were analyzed by varying the operating temperature as well as feed composition. The pervaporation was carried out for the low concentration wastewater solution of acetonitrile, acetone and ethanol. The results showed that concentrations of the organic solvent in permeate increased with the trend: acetone > acetonitrile > ethanol. The solvent's solubility with the water played a vital role in the pervaporation process because the size of the studied azeotropic solvents was following the same order. Therefore the trend follows by the solvents in case of overall mass transfer coefficient was given: acetone > acetonitrile > ethanol. The increment of the overall mass transfer coefficient was due to rise in temperature whereas the overall mass transfer coefficient was also correlated with the organic feed concentration. For the dehydration of ACN, polyvinyl membranes (PVA) were used by Scholtz and Grimsehl (2002). Naidu et al. (2005) prepared a mixed matrix membrane that was based upon two types of zeolites ZSM-5 and Na-Y. To synthesize these membranes, sodium alginate was used as dispersion medium and polyvinyl–alcohol–polyaniline matrix was formed to dehydrate the azeotropic mixture of ACN + water. A crosslinking agent glutaraldehyde was used to modify the prepared mixed matrix membrane. To enhance the membrane's hydrophilic nature, the higher flux values were played an important role. As the

amalgamation of hydrophilic nature, zeolites in sodium alginate was manipulated, due to which the flux increased with huge rate. Taking higher amount of aniline for the preparation of semi-IPN membranes proved that pervaporation performance of these membranes in terms of selectivity and flux values was higher rather than the preparation of the membranes processed by adding small amount of the aniline. Mandal and co-workers (2011) used PVA-iron oxide based nanocomposite membrane for the elimination of azeotrope from ACN + water solution. They concluded that membranes prepared by adding excess concentration of iron particles gave higher value of flux of water in case of all the feed mixtures selected for the study. On the other hand, in terms of the value of pervaporation separation index (PSI), PVA membrane matrix that contains 10% by weight iron oxide named as PVA–Fe-10 offered greater value of PSI than PSI values obtained in case of nanocomposite metal oxide. Diffusion selectivity and sorption calculations signified that the results obtained in case of sorption selectivity for ACN + water mixture was very higher than diffusion selectivity. They concluded that the sorption method could be more preferable than diffusion to dehydrate the azeotropic mixture of ACN + water by means of pervaporation process. The dehydration performance of alginate due to its well-known water-soluble properties was found better than PVA along with other polysaccharides membranes e.g. chitosan as well as cellulose ones (Adoor et al., 2007). Due to high swelling nature of sodium alginate membrane, the mechanical strength as well as the separation factor of the system decreased. Many modifications (cross linking (Bhat et al., 2006), blending (Bhat et al., 2007), and grafting (Rehm et al., 2009) and by adding fillers (Nigiz et al., 2012)) had been done for the improvement of the membrane properties. Hosseini and co-workers (2017) performed pervaporation for the dehydration of ACN via mixed matrix membrane (MMM) that consisted NaA zeolite in different amounts i.e. 10, 20 and 30% by weight diffused in the alginate (Alg) matrix that were explored at different temperature and water concentrations. The prepared membranes were modified by cross linking agent (sulfosuccinic acid). They concluded that the addition of nano zeolite increased the value of flux and membrane factor of sodium alginate up to 123% and 169%. Secondly, use of MMM for the dehydration of ACN containing water (30% by weight) gave better performance than alginate membrane.

## 2.2. Liquid-liquid Extraction (LLE)

Liquid-liquid extraction, also recognized as *extraction*, *liquid extraction* or *solvent extraction*, is a substitute process in place of distillation depends upon solubility differences of the azeotropic mixtures instead of relative volatility differences. Sometimes calculations and modification of relative volatilities are complicated processes, so LLE technique is the best alternative to separate the azeotropic mixture. Industrially, Liquid extraction was explored since 1930. The liquid extraction is mainly used in the petrochemical industry (Sorensen et al., 1979). In case of liquid extraction process, the azeotropic feed (carrier and solute) is mixed with the second liquid phase that is known as *solvent*. The solvent is partially miscible or immiscible with the carrier whereas the solvent and solute forms a miscible true solution with each other. The two phases are developed after mixing of both the streams occurs. The phase that is rich in solvent is termed as *extract*, while another liquid phase is termed as *raffinate*. A simplified design of a liquid-liquid extraction process of a binary azeotropic mixture is illustrated in Figure 2.2. In the given figure, the feed and the solvent enter the column at opposite streams in order to improve mass transfer. If the feed is allowed to enter from the top of the extraction column, the raffinate will be automatically obtained at the bottom of the column and at the top of the column the extract has been collected. If the solvent is not absolutely miscible in the carrier, there is no need to implant the raffinate distillation column.

The phenomenon of liquid extraction works upon the thermodynamic equilibrium of the components of the azeotropic mixtures. The separation via liquid extraction mainly depends on the thermodynamic partition equilibrium of the components of the mixture into the two liquid phases of the azeotropic mixture (liquid-liquid equilibrium (LLE) data). There is distribution ratio ($\beta$) and selectivity (S) in liquid extraction which states the feasibility of a distillation process.

The distribution ratio ($\beta$) is the ratio of the mole fraction or mass fraction of a component *i* of an azeotropic mixture present in the extract phase and the mole fraction or mass fraction of the same component of the azeotropic mixture present in the raffinate phase.

In general, the distribution ratio refers to the ratio of the distribution of solute among the extract phase and raffinate phase. The distribution ratio may be expressed in mass fraction and can be calculated using Equation 2.1.

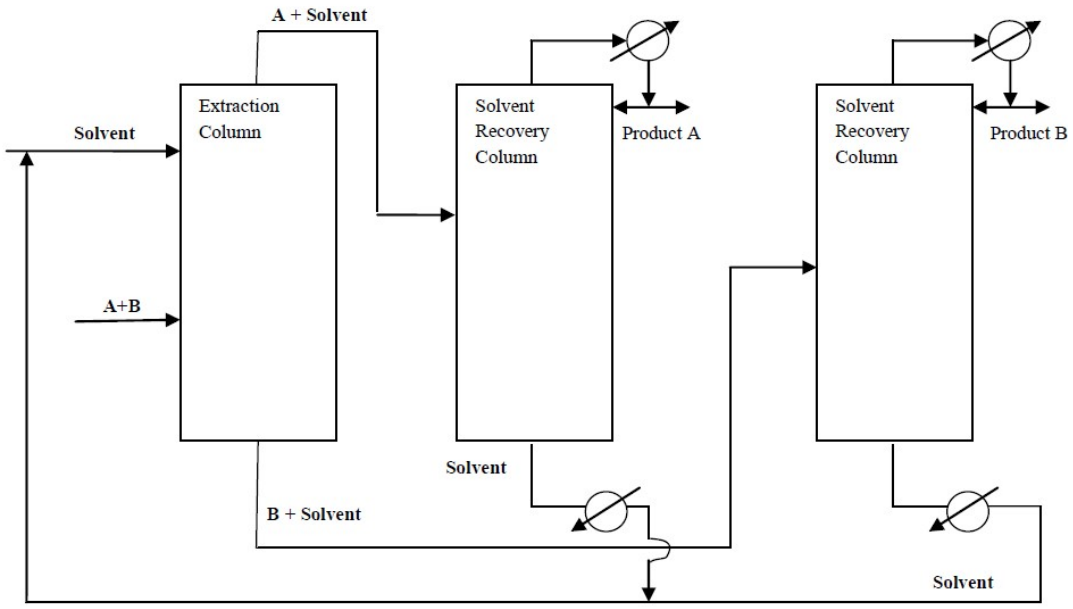


**Figure 2.2. Schematic Diagram of a Liquid-Liquid Extraction Process of Ternary System**

$$\beta_i = \frac{w_i^E}{w_i^R} \tag{2.1}$$

Where $w_i$ refers as the mass fraction of component $i$ and the superscripts $E$ and $R$ is the extract and raffinate phase, respectively.

The selectivity in case of liquid-liquid extraction is similar to the relative volatility calculated in extractive distillation which expresses the affinity of the solvent for the solute and the carrier. Similarly like relative volatility, higher the value of the selectivity, the separation of azeotrope will be easier. If the value of selectivity is unity, the separation of the azeotropic mixture will be impossible.

Selectivity can be calculated as the ratio of the solute $i$ distribution ratio with the carrier $j$ distribution ratio and it may be expressed in the form of Equation 2.2.

$$S = \frac{\beta_i}{\beta_j} \tag{2.2}$$

The solvent selected for the liquid extraction plays an important role. To select an efficient solvent the following properties has to be considered:

1. **Distribution ratio or partition ratio (*β*)**:- The solute distribution ratio signifies that the urge of the solvent to make a bond with the solute. Higher the value of solute distribution ratio, lesser amount of solvent to feed ratio requires in case of extraction.
2. **Selectivity (*S*)**:- The selectivity is the ratio of two components that exist in the extract-solvent phase divided by the ratio of the same components present in the feed-solvent phase. Selectivity values higher than unity are needed for the extraction to be feasible. A high value of the selectivity implies less equilibrium stages. The selectivity values are generally higher for concentrations of dilute solute.
3. **Density**: - Higher the density difference between the phases of extract and raffinate, easier will be the phase separation.
4. **Viscosity**: - Lower viscosity leads to the formation of smaller drops during the mixing, which leads to the higher specific surface area.
5. **Recoverability**: - The solvent should be easily recovered from the raffinate as well as the extract phase. The solvent recovery is usually carried out by distillation process, so there should be significant difference in the volatility of the solvent.
6. **Availability and cost**: - The availability of the solvent should be approachable and reasonably priced to compensate the loss of the solvent.
7. **Thermal and chemical stability***:* -For the recycling of the solvent, it should be thermally and chemically stabilized.
8. Some other properties like corrosivity, biodegradability, eco-friendly nature, flammability must be considered.

The extraction of ACN from acetonitrile and water solutions by LLE technique was studied by C.V. Rao et al. (1978).They used xylene, chlorobenzene, and n-butylacetate as solvent and found that these solvents had excellent solvent properties for the azeotrope elimination. These solvents were non-volatile in nature due to their high boiling points and

difference between the density of water and reported solvents except chlorobenzene was significant. The mutual solubility data produced for these solvents as well as tie-line data signified that for LLE separation process, these solvents were suitable. It was cleared that area of heterogeneity observed in case of the studied solvents followed the pattern: xylene < chlorobenzene < n-butyl acetate. For the extraction from aqueous acetonitrile D.S. Rao and co-workers (1979) used toluene, isoamyl alcohol, methyl isobutyl ketone, and methyl ethyl ketone. They generated ternary liquid equilibrium data at 30ºC temperature for the systems ACN + water + toluene, ACN + water + isoamyl acetate, ACN + water + methyl isobutyl ketone, ACN + water + methyl ethyl ketone and ACN + water + isoamyl alcohol. The tie-line data generated for the three systems (ACN + water + methyl isobutyl ketone, ACN + water + isoamyl acetate, ACN + water + toluene) were correlated by Othmer-Tobais and Hand method. But in case of other two systems (ACN + water + methyl ethyl ketone and ACN + water + isoamyl alcohol), the area of heterogeneity was observed to be very less. The selectivity of the solvents followed the order methylisobutyl ketone < isoamyl acetate < toluene. Due to the availability and cheap cost of toluene, it was used as the prior solvent for extraction of ACN.

Sugaring-out is another successful technique used to dehydrate ACN from the azeotropic mixtures of ACN + water. In this method, monosaccharide or disaccharide sugars are used which makes a strong hydrogen bond with water which forces ACN to break bond with water. Wang et al. (2008) reported sugaring-out method in which a monosaccharide and disaccharide sugar had been used that worked on the principle of phase separation method to obtain pure acetonitrile from ACN + water azeotropic mixture. They observed by adding monosaccharide sugar i.e. glucose, fructose or xylose, arabinose as well as disaccharide sugar like maltose or sucrose into an ACN + water azeotropic mixture resulted in the occurrence of two phase separation, when concentration of sugar surpassed threshold amount of sugar. The upper phase of the mixture was found to be rich in ACN whereas the water content was found higher in lower phase. By the addition of sugar resulted in the increment of ACN concentration in the upper phase. The upper phase concentration of the ACN was >40%.When the concentration of glucose was less than 35g/L, the concentration of ACN in

the upper phase was found to be less than 40%. The ACN concentration was achieved up to 80% using glucose as an extracting agent with concentration greater than 25 g/L by Sudan I extraction test.

Salting-out also shows the same effect like sugaring-out technique in which salts are used in place of mono-sugars or polymeric sugars. In analytical chemistry, the implementation of the salting-out effect is very widespread that can be used to increase the relative volatility of the analytes in extraction processes, to instigate the protein's precipitation used in biological samples or to develop the recoveries of the organic compounds in liquid-liquid extractions. Salting-out assisted LLE is a profitable process for the preparation of the samples that can be used for the HPLC-UV analysis during the development of the analytical methodologies. Some new extraction methodologies like QuEChERS are based upon the SALLE concept. Valente et al. (2013) proposed LLE that was based upon the salting out technique in ACN + water azeotropic mixture. The different entrainers used in the salting-out process, their effect, concentration of the salts and the volume ratio of the ACN + water azeotropic mixtures were the main parameters that were studied thoroughly. The salts were divided into three main groups used for the phase separation and the extraction nature of the salts: (i) Carbonates and sulfates, ii) Chlorides and acetates and (iii) magnesium sulfate. Out of the studied salts, NaCl showed greater influence on the extraction of the α-dicarbonyls fraction. Takamuku et al. (2007) investigated the separation of the phases of ACN + water mixtures using different chlorides of alkali metals (MCl, M= $Li^+$, $Na^+$, and $K^+$) as an extracting agents at 298 K. The Phase diagrams of ternary system of ACN + water + alkyl chloride demonstrated that phase separation of the azeotropic mixture of ACN + water occurred even at lower salt concentration following the trend: NaCl > KCl > LiCl. The trend of the phase separation of ternary system of ACN + $D_2O$ + MCl followed the same pattern as the ACN + water + alkyl chloride ones, but the concentrations observed in phase separation of $D_2O$ systems was lesser for each salt than the ACN + water systems. The experiments based upon small-angle neutron scattering (SANS) were performed on the ACN + water + alkyl chloride systems for the clarification of the ACN + water + alkyl chloride phase separation at a mesoscopic scale as a function of concentration of the salt

before phase separation. Due to the results produced by the SANS experiments in terms of Ornstein–Zernike correlation length, they concluded that by increasing the concentration of the alkyl chloride salts (NaCl > KCl > LiCl), the clusters of $D_2O$ were more rapidly developed which was in the favor of phase separation. Ligette et al. (1990) proposed that with addition of NaCl, the ACN + water phase separation was induced at 298K. Similarly, Gu and Shih (2004) also recovered 60% of acetonitrile from HPLC effluent stream containing azeotropic mixture of ACN and water using different derivatives of Phosphate salts. Dhamole et al. (2010) also compared the salting out effect using $K_2HPO_4$ salt and sugaring out effect using glucose monosaccharide at 6° C temperature and at mole fraction 0.012. The results illustrated that there was not any considerable difference observed between the recovery of protein and composition of ACN. The recovery of protein was found to be 96% (w/v) in case of salting out and 98% (w/v) in sugaring out technique. On the basis of operational methods, it was concluded that the environmental pH was not changed by the addition of sugars, but the addition of salt i.e. $K_2HPO_4$ increased the pH effectively (9.2–9.5) and corrosion of the vessels also occurred by the use of salts.

## 2.3 Adsorption Processes

In adsorption processes, the molecular sieves are utilized in which the selective adsorption of the water occurs on the basis of molecular size difference among water and ACN molecules. A molecular sieve is a substance in which there are number of small pores of a particular and consistent size. For the adsorption process, the synthetic zeolite in the form of pellet can be utilized for the adsorption purpose, other than that many adsorbents derived from plant i.e. cornmeal, straw, and sawdust can be used. Normally the zeolites are composed of minerals of alumino silicate or synthetic compounds enclosed by the open structures in which the diffusion of small molecules like clays, micro porous charcoal particles, active carbon as well as porous glasses takes place. The adsorption of smaller size molecules occurs due to the passage through the pores whereas the larger molecules cannot pass through the pores. Assche and co-workers (2011) worked on the dehydration of ACN from the water + ACN mixtures using twenty-nine adsorbents based upon different adsorption categories, including zeolites, metal–organic frameworks (MOF), activated carbon and silica gel in batch

adsorption experiments. The separation ability of the reported adsorbents for dehydration of acetonitrile from water was determined by studying data produced by the experimental batch isotherm with the help of a breakthrough model. The diffusion coefficient estimated for the acetonitrile and water as well as the water isotherms (296 K) results was reported for potential adsorbents. Among all the studied adsorbents, 4A zeolite was found to be the most eligible adsorbent because the separation of ACN from water content took place up to 40% by weight via fixed bed adsorption column. The breakthrough curves obtained were also compared with the numerical as well as analytical models that were implemented in fixed bed adsorption.

## 2.4 Enhanced Distillation Techniques

The mixtures that are having relative volatility close to unity (≈1) can be separated by the special distillation techniques. The enhanced distillation techniques consist of the following distillation techniques.

*(i)* Pressure Swing Distillation

*(ii)* Homogenous & Heterogeneous azeotropic distillation

*(iii)*Extractive distillation

*(iv)* Other enhanced distillation techniques

### 2.4.1. Pressure Swing Distillation (PSD)

Pressure Swing Distillation is a distillation technique in which the pressure dependence property of the azeotropic mixtures is used for the separation of the azeotropic mixtures. The pressure swing distillation is totally implemented upon those solvents that are highly pressure-dependent azeotropic mixtures. These azeotropic mixtures consist of {tetrahydrofuran + water mixture}, {acetonitrile + water mixture}, and {methanol + acetone mixture}. The schematic diagram of pressure swing distillation process is depicted in Figure 2.3.

The component A mixture is separated in the first column in its purest state i.e. obtained at the bottom of the distillation column whereas the azeotropic mixture is collected at the top of the distillation column which acts as feed for the second distillation column. Both columns are maintained at different pressures. The azeotropic point of the mixture shifts due

to which the pure component B is collected in the second column in the bottom stream and again top is the azeotropic mixture at pressure 2 which is again recycled to the first column.

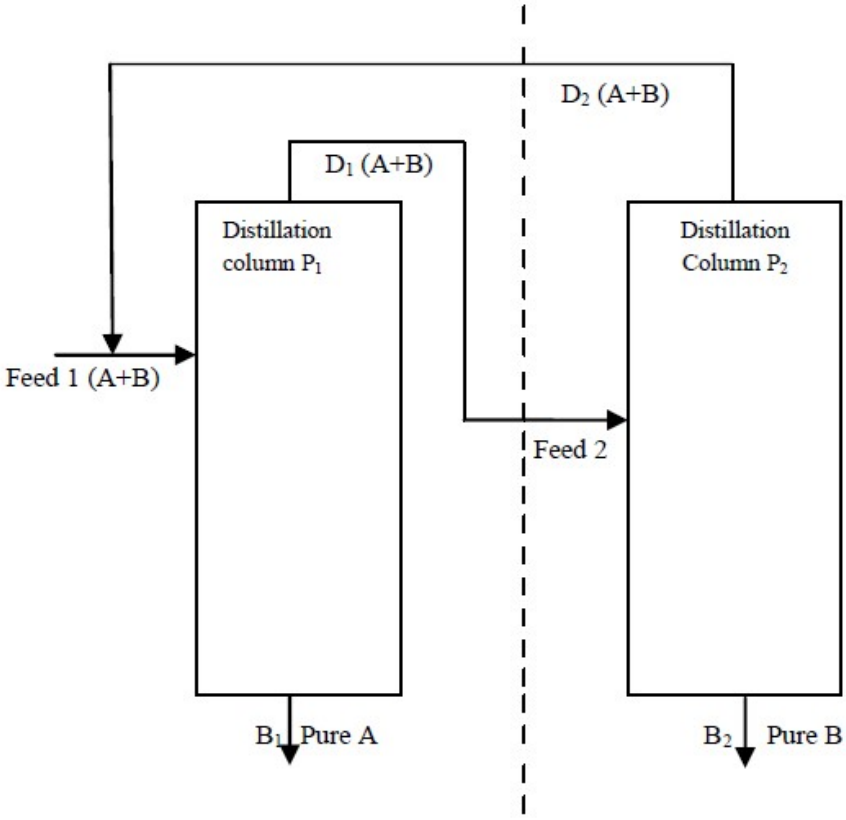


**Figure 2.3. Schematic Diagram of Pressure-Swing Distillation of a minimum boiling point azeotropic mixture**

On the basis of the nature of the azeotropic mixtures i.e. minimum boiling azeotrope or maximum boiling azeotrope as well as on the concentration of feed, the distillation cycles may vary but the theory of the process remains same for the distillation. Repke et al. (2004) analyzed the separation of a homogenous ACN + water azeotropic mixture via pressure swing distillation based upon thorough dynamic modeling of the system. There were two controlling structures that were considered for the study. The foremost aim of the research was to analyze instability in the concentration of the feed and the impact of the disturbance on the performance of the mass and heat integrated distillation column process. The analysis

showed that the process performance of the system was stable by the implementation of the control structures. Kim et al. (2013) performed a computational study by PSD to eliminate azeotrope of ACN from ACN + water azeotropic mixtures in which they separated 99.9 mol% of ACN from the ACN + water azeotropic mixture. Yu et al. (2014) studied the pressure swing distillation as well as extractive distillation to separate ACN and water azeotropic mixture. The binary parameters obtained by the experimental VLE data were simulated in the Aspen Plus® software using Wilson model separately in case of two separation processes. The theoretical plates, feed location and reflux ratio were analyzed that had an effect on separation efficiency and energy consumption of the system. They compared the results of PSD technique and extractive distillation and concluded that the azeotropic mixture of ACN + water was significantly separated by both the processes and the purity percentage in both the processes was up to 99.5%. During the comparison of both techniques, the extractive distillation is found to be the most promising technique due to its energy saving process which influences the economy of the system.

**2.4.2. Azeotropic Distillation**

In this technique, a third component commonly known as entrainer is used. Entrainer forms an azeotrope with one of the component of the azeotropic mixtures, and facilitates the separation of the azeotropic mixtures (Perry's et al., 1934). Azeotropic distillation can be categorized as homogenous azeotropic distillation in which there is only one liquid phase and heterogeneous azeotropic distillation in which there are more than one liquid phase present. The Simplified schematic diagrams of homogeneous azeotropic distillation and heterogeneous azeotropic distillation sequences are given in Figure 2.4. As shown in Figure 2.4, the component having low boiling point is collected as distillate at the bottom of the first distillation column (same as extractive distillation, in which the third component used is a component which is having high boiling point that is obtained at the bottom of the first distillation column). For both homogenous process as well as heterogeneous process, a sequence with two distillation columns' is required. The feed stream mixed with the entrainer recycle and the entrainer make-up enters into the first distillation column. At the bottom of the first column, the less volatile component A is obtained almost in its purest form, the distillate

of the first column that can forms an azeotrope with the component B is treated in a different way in case of homogeneous and heterogeneous azeotropic distillation.

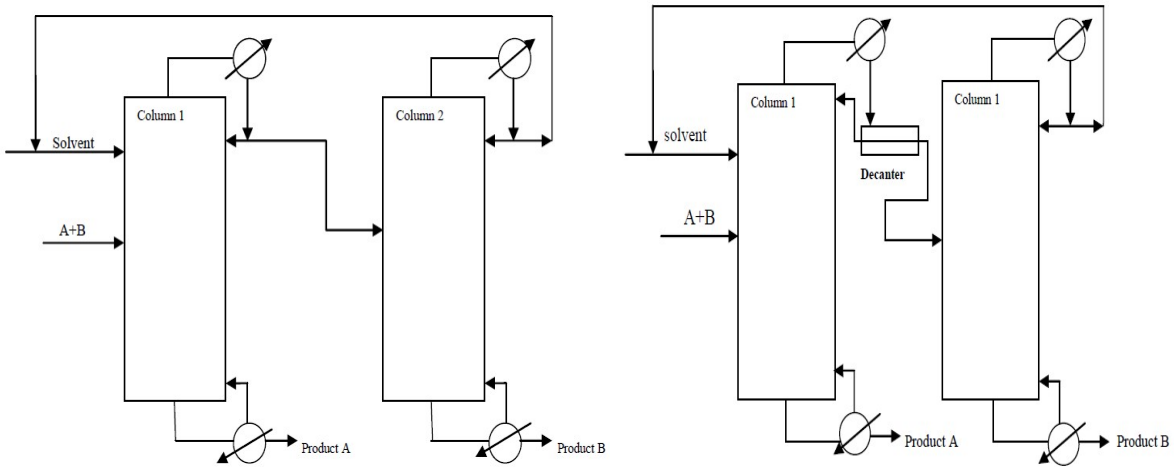


**Figure 2.4. Azeotropic Distillation configuration a) Homogenous, b) Heterogenous Azeotropic distillation**

In the homogeneous azeotropic distillation, the distillate obtained is fed into the second distillation column. In the second distillation column, the most volatile component of the distillate mixture is collected at the bottom of the second column and the entrainer that is obtained as distillate is again recycled to the first column. In case of heterogeneous azeotropic distillation, as the head product condenses, the formation of two immiscible liquid phases occurs. The separation of these two immiscible liquid phases has been done in a decanter. The entrainer-rich phase is collected as reflux of the first column whereas the component B-rich phase is collected in the second column, the purest component B is obtained at the bottom of the column and the entrainer is collected at the top of the column and recycled back to the first column.

### 2.4.3 Extractive Distillation

Extractive distillation is a separation method in which third component is added to the azeotropic mixture which is partially miscible with one of the binary mixture which will alter

the relative volatility of the azeotropic components (Perry's et al., 1934). A diagrammatic representation of an extractive distillation sequence of a minimum-boiling azeotropic mixture is shown in Figure 2.5.

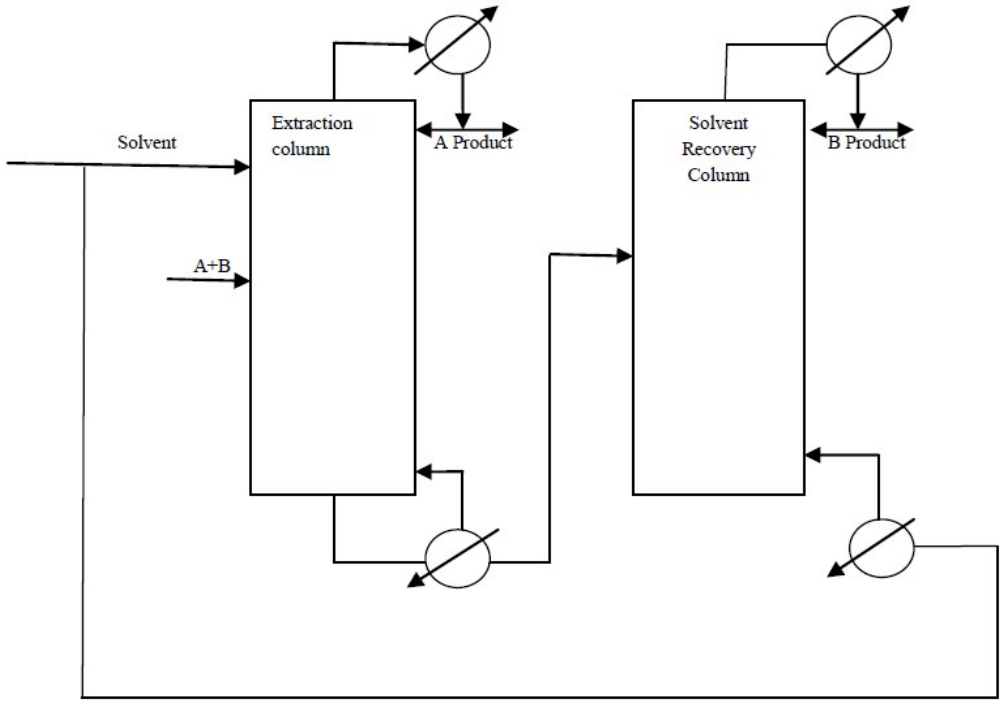


**Figure 2.5. Schematic diagram of Extractive distillation**

As shown in Figure 2.5, there are two distillation columns present in this separation technique. The solvent is added in the first column that is few trays beneath the top, to facilitate a high concentration of the solvent throughout the column. The less volatile component passes through the bottom of the first distillation column. The most volatile component (A) is collected as distillate at the top of the first distillation column. Alternatively, the bottom product obtained in the first distillation column acts as feed in the second distillation column, and the second component of the azeotropic mixture is collected

as distillate into the second distillation column, whereas the solvent collected at the bottom of the second distillation column again recycled and taken back to the first distillation column. The properties of suitable entrainer for extractive distillation should have high relative volatility taken at moderate concentrations, it does not form azeotrope with any of the component of the azeotropic mixtures, it should be easily separated from the components of the azeotropic mixture, high melting point and thermally stable, non-toxic in nature, economically feasible, readily available, noncorrosive. Some azeotropic mixtures that are industrially separated by extractive distillation are listed in Table 2.1.

**Table 2.1. Azeotropic mixtures industrially separated via extractive distillation**

| **Mixture** | **Entrainer** |
|---|---|
| Acetonitrile + water | Ethylene glycol, DMSO, DMF |
| Acetone + methanol | Aniline, water , ethylene glycol |
| Benzene + cyclohexane | Aniline |
| Butanes + butenes | Acetone |
| Isopropanol + water | Ethylene glycol |
| ethanol + water | Glycerin, ethylene glycol |

#### 2.4.3.1 Extractive Distillation with Organic Solvents

Extractive distillation with organic solvents is used to dehydrate ACN from ACN + water mixture. This method uses solvent that are less volatile or non-volatile in nature. The solvents alter the relative volatility of one of the feed component than another one, so that azeotropic mixture separation will take place. The solvent used for the extractive distillation is known as extractive distillation solvent. Acosta-Esquijarosa et al. (2006) worked on heterogeneous batch distillation feasibility to eliminate azeotrope from the azeotropic mixture of ACN from water in a batch rectifier. The main aim of the research was to split the azeotropic mixture by adding ethylene glycol that was partially miscible with one of the component of the azeotropic mixture which manipulated relative volatility of the components of the azeotropic mixture. Same researchers used acrylonitrile as entrainer for the

heterogeneous batch distillation and yield recovery of ACN up to 80% (Rodriguez-Donis et al. 2001, Rodriguez-Donis et al., 2001). On the other hand, they also used acrylonitrile which is produced as the co-product of acetonitrile which reduced acetonitrile shortage problem. Rodriguez–Donis et al. (2003) continued the prior study on the heterogeneous batch distillation and extractive distillation, the separation of the azeotropic mixture had been evaluated by the use of heterogeneous entrainers. Different entrainers were used for the extractive distillation by the simulation using UNIFAC method, hexyl amine and butyl acetate was recognized as potential entrainers used for the separation of the ACN + water mixture by heterogeneous batch distillation. Kurzin et al. (2004) measured isothermal VLE data using tetrabutylammonium bromide for the ACN + water system at different constant salt molalities ((0.20, 0.40. 0.60, 0.80, and 1.00) $mol.kg^{-1}$). The data had been evaluated by the gas chromatography at two different temperatures i.e. 25ºC and 50ºC. The correlation of the experimental data for ACN + water systems was done by NRTL model. They also measured isothermal VLE data using tetraproylammonium bromide for the ACN + water system at different constant salt molalities ((0.20, 0.40. 0.60, 0.80, and 1.00) $mol.kg^{-1}$). The mole fraction of the samples was determined by headspace gas chromatography by varying the temperatures (25ºC and 50ºC). Two thermodynamic models NRTL and UNIFAC were used for the correlation of the experimental data. Mean absolute deviation of acetonitrile vapor phase compositions for NRTL and UNIFAC models were observed 0.006 and 0.007, respectively. Zhang et al. (2013) used DMSO to estimate the Isobaric VLE data for the dehydration of ACN + water Mixtures via extractive distillation at atmospheric pressure. They generated Isobaric VLE data for the binary systems ACN + water, water + DMSO, ACN + DMSO, and VLE data for ternary system ACN + water + DMSO were calculated at atmospheric pressure. The experimental results were correlated by the thermodynamic models i.e. Wilson, UNIQUAC and NRTL models, respectively. They concluded that the experimental studies showed good agreement with theoretical studies when correlated with above mentioned models. Out of three implied models, Wilson demonstrated better results than other models. As an entrainer, DMSO enhanced the relative volatility of the ACN + water system and the azeotrope of ACN + water system was successfully eliminated. The

DMSO produced a solvent effect which made bond with water and resulted dehydrated ACN. Due to the good selectivity and less viscosity, it was found to be a good entrainer for the dehydration of azeotropic mixtures (ACN + water) by extractive distillation. The main drawback of using DMSO was that it readily penetrated into the skin which led to many severe diseases like bronchial cancer, skin cancer. Also, it had an unacceptable odor. The risks associated with the use of organic solvents, has driven the research in the area of green chemistry (Kumar et al., 2012).

**2.4.3.2Extractive Distillation with Novel Solvents**

**2.4.3.2.1 Ionic Liquids (ILs)**

Ionic Liquids are the salts of anion and cation compounds with melting point below the boiling point of water. In several chemical and pharmaceutical industries, ionic liquids are one of an efficient alternative solvent with exceptional solvent properties.

The following properties of ILs make them suitable as new green solvents.

1. **Volatility: -**Due to its negligible vapor pressure, it is considered one of the significant green solvent in separation processes. Although many researchers for several years claimed that ILs are not volatile at all and the vapor pressure cannot be estimated, but some researchers proved that at high temperature and low pressure, they can be easily vaporized (Rebelo et al., 2005, Paulechka et al., 2005, Earle et al., 2006, Bonhote et al. 1996).
2. **Melting point & Boiling point: -**The ionic liquids have very low melting point whereas the boiling point of ILs is comparatively very high than the conventional organic solvents due to which it can be used as solvents with broad temperature range.
3. **Decomposition temperature:-**The decomposition temperatures of some ILs were found to be up to 400°C. If the size of cation remains same but the size of the anion increases, it will decrease the melting point of the ionic liquid (Aparicio et al., 2010).
4. **Density:** - The density of the ILs is generally lies in the range of 1.05 to 1.35 g/ml (Ludwig et al., 2008). The density is the main property of ILs which is least influenced by the temperature and the impurities present in the solvent.

5. **Viscosity: -**The ionic liquids are more viscous than the traditional organic solvents that are considerably used in pharmaceutical and chemical industries which create many problems like mixing, limiting mass transfer and pumping. The impurities like water and temperature affects the viscosity of the ILs.
6. **Solubility:-** The modification of the anions and cations in the ionic liquids can enhance the solubility of the ILs e.g. anion phosphoushexaflorate $[PF_6]^-$ do not allow the ILs to be soluble in water whereas chloride ions $Cl^-$ makes ILs completely miscible in water. In ILs, the cations are capable to donate the H-bond to polar or dipolar solutes, whereas the anions always accept the H-bond (depending on the structure of the anion (Gathergood et al. 2006). Therefore in liquid extraction the modification of the ILs according to the solubility is very important.

There are many other important factors like non-flammable nature of the ILs as well recyclability, non-toxic behavior, biodegradability, high ionic conductivity; electrochemical stabilization of ILs against redox reactions and their negligible vapor pressure makes them suitable for separation processes. But the toxicity of many ILs has still to be explored (Gathergood et al., 2004, Docherty et al., 2005, Plechkova et al., 2008).

**i) Applications**

There are many applications of ILs available in the literature (Ghandi et al., 2014, Rodriguez et al., 2011, Brennecke et al., 2001, Wilkes et al., 2002). The first ILs was used in electrochemistry as an electrolyte (known as low temperature liquid electrolyte) (Olivier-Bourbigou et al., 2010). The significant properties of ILs like broad range operating temperature, electrochemical properties, low dielectric constant and high conductivity make them attractive in batteries and fuel cell's applications. They can also used as solvents in the synthesis of organic compounds as well as used as catalysts in organic chemistry (Welton et al., 2004, Zhang et al., 2011, Welton et al., 1999, Tan et al. 2010). There are many other applications of ILs like synthesis of nano-particles, decomposition of lignocellulosic biomass (Tadesse et al., 2011, Brandt et al., 2013, Valkenburg et al., 2005) as well as heat transfer fluids (Pena-Pereira et al., 2014). The applications of ILs in different fields are illustrated in Figure 2.6.

**ii) Applications of ILs in separation technology**

There are several publications that have presented the applications of ILs in separation technology (Flieger et al. 2014, Han et al., 2010) along with azeotrope breaking particularly (Orchillés et al., 2010, Rocha et al., 2013). They are also used in many other fields like metallurgy processes, recovery of the important ingredients of plants, gas separation processes like $CO_2$ capture, separation of chiral compounds (Flieger et al., 2014). However ILs are associated with many issues that has to be solved before they can be used in large scale applications e.g. high prices of ILs, thermodynamic data, lack of safety, handling, and environmental issues, recyclability and degradation nature of ILs.

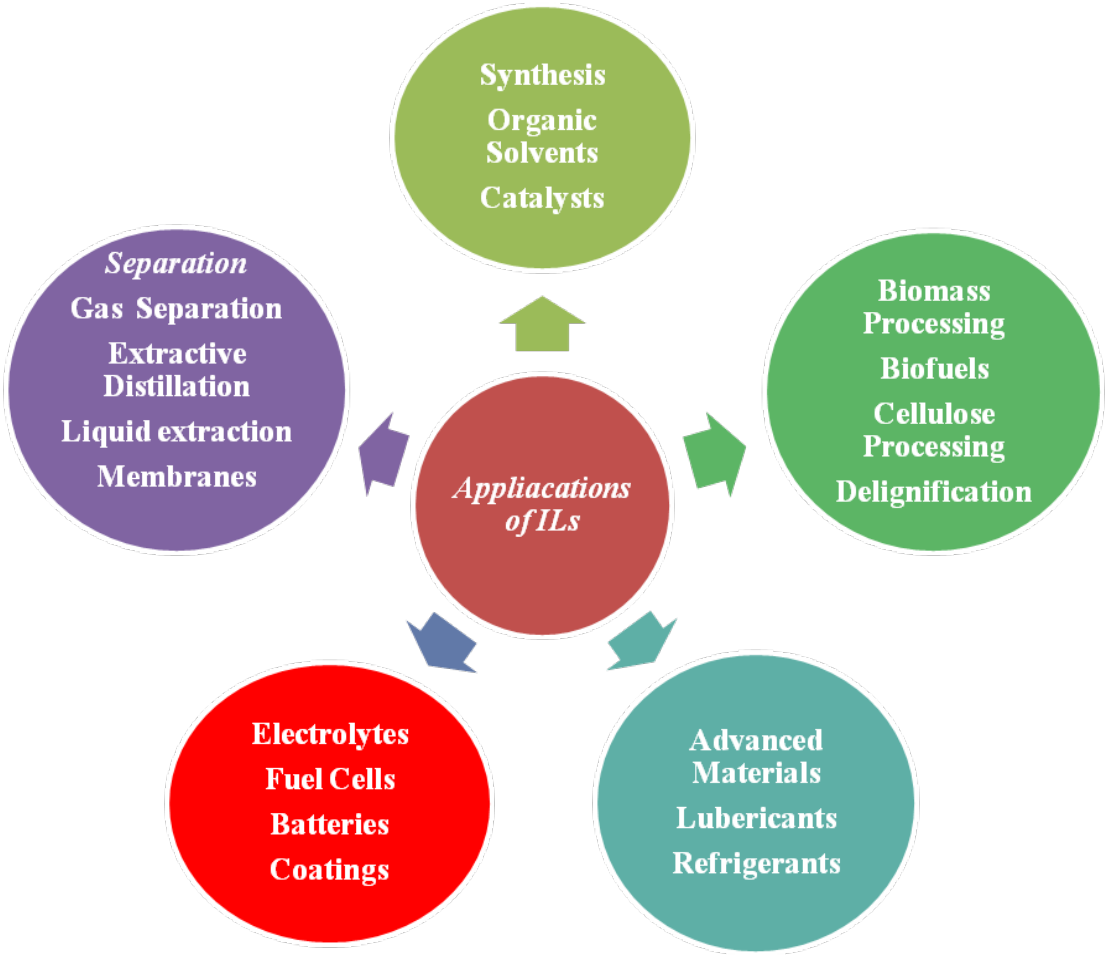


**Figure 2.6. Applications of Ionic Liquids (ILs)**

As discussed above the ILs are latent applicant for the recovery of metals, like metal oxides and processing of minerals and ores, electrodepositing of metals and extraction and separation of metal ions (Parmentier et al., 2016) as well as promising alternatives of polymers. ILs are also used in the extraction of many biomolecules like alkaloids, vitamins, proteins, antibiotics and proteins from different biological flora or fauna (Meindersma et al., 2006).

ILs have been used as entrainer (extraction agents) for azeotropic mixtures separation by different separation techniques like LLE process, extractive distillation and azeotropic distillation.

In extractive distillation, ILs as entrainers has several advantages. Due to the low or negligible vapor pressure of the ILs, the distillate can be obtained in its pure state and the chances of solvent loss are reduced. Due to the interactions of anions and cations, ILs is thermally and chemically stable in nature. They are less corrosive, easy to handle, biodegradable and environmental friendly as compared to traditional volatile organic compounds. The ILs are designed to target specified task. To select an eligible and significant solvent, there are many group contribution methods such as UNIFAC as well as other predictive tools like COSMO-RS that can be used.

The main drawbacks of using these solvents in separation processes are the high price of the initial components used for the synthesis of ILs. The purification and recovery methods of these solvents are also very difficult due to which ILs cannot be used in large scale processes. But as the demand of ILs increases, the price may be reduced (Orchillés et al., 2010).

Many researchers (Calvar et al., 2007, Jiang et al., 2007, Zhao et al., 2006, Kulajanpeng et al., 2014) had worked on the generation of VLE data for the ternary mixtures (e.g. ACN + water + IL, ethanol + water + IL) at different conditions. The ILs successfully eliminated the azeotrope from the mixtures. The studied ILs worked on the phenomenon of salting out effect which increases the relative volatility of one of the component of the azeotropic mixtures which makes the azeotrope displace or eliminate the azeotrope

completely. Viscosity also plays a significant role in the separation processes. If the viscosity of ILs is very high, it inhibits the mass transfer.

Li et al. (2012) studied the phase behavior of the ternary system ACN + water + ILs via COSMO-RS method. The effect of cations and anions behavior on the azeotropic mixture of ACN and water was studied in detail. They concluded that, for the dehydration of ACN, the anions like $[OAc]^-$ and $Cl^-$ efficiently enhanced the relative volatility of the ACN + water system which resulted in the elimination of the azeotrope, but in case of cations, no major effect was observed in the vapor–liquid phase diagram of ACN + water system. The commonly used imidazolium-based ILs e.g. 1- Ethyl-3-methylimidazolium acetate ([EMIM][OAc]) and 1-Ethyl-3-methylimidazoliumchloride ([EMIM] Cl) were the potential entrainer for the extraction of the ACN from the ACN + water azeotropic mixture. The results showed that the hydrogen bonding formed between ILs and water as compared to the ACN was large, which eliminated the azeotrope successfully. Fang et al. (2013) first time used room temperature ionic liquids (RTILs) as entrainer to eliminate the azeotrope of ACN + water mixture. They used 1-Ethyl-3-methyimidazolium tetrafloroborate ([EMIM][$BF_4$] ) and 1-Ethyl-3-methylimidazolium nitrate ([EMIM][$NO_3$]). The experimental results illustrated that both [EMIM][$BF_4$] as well as [EMIM][$NO_3$] were found potential entrainers which increased the relative volatility and broke the azeotrope successfully. In their further study, they generated isobaric VLE data for the azeotropic mixture of ACN + water using different ILs like 1-Butyl-3-methylimidazolium tetrafloroborate ([BMIM][$BF_4$]), 1-Butyl-3-methylimidazolium dibutylphosphate ([BMIM][DBP]) and 1-Butyl-3-methylimidazolium chloride ([BMIM][Cl]) at atmospheric pressure. The results showed that [BMIM][$BF_4$] was unable to the enhance the relative volatility of ACN + water azeotropic mixture, but ionic Liquids, like [BMIM][DBP] and [BMIM][Cl] effectively enhanced the relative volatility of ACN and successfully broke the azeotrope completely. [Bmim][Cl] performed better than [Bmim] [DBP]. The experimental results of VLE data of ACN + water + IL systems were correlated by Non-radom-two-Liquid (NRTL) model. The results showed that the correlated data of ACN + water + IL obtained by the NRTL model gave average deviation of 5.17%. Further, Fang and his co- workers used salt effect models (Furter model and improved Furter

model) to correlate the experimental data of the ACN + water containing same ionic liquids. The overall average relative deviation observed in case of Furter model was 5.43% whereas in case of improved Furter model, it was 4.68%. The results showed that salt effect models like Furter model and improved Furter model both validate the correlation of ACN + water + IL systems and increased the relative volatility of the ACN. Li et al. (2015) studied the effect of ionic liquids that were made up of 18 different amino acid (AAILs) for the dehydration of ACN + water by COSMO-RS method. They concluded that all AAILs had the capability to eliminate the azeotrope by enhancing the relative volatility of the ACN + water. The ionic liquid synthesized by using the amino acid Proline {1-Ethyl-3-methylimidazolium proline ([EMIM][Pro])} was the most eligible entrainer at a given condition for the elimination of the azeotrope. The VLE data of ACN + water + [EMIM][OAc] and ACN + water + [EMIM][Pro] were generated to validate the feasibility taking the mole fraction of ionic liquid (0.05 and 0.10) at atmospheric pressure. The enhancement of relative volatility of ACN was observed by using two ILs as an entrainer which successfully breaks the azeotrope even at the lower mole fraction 0.05. The experimental VLE data obtained in case of ACN + water + [EMIM][OAC] and ACN + water + [EMIM][Pro] was correlated by COSMO-RS at atmospheric pressure.

**2.4.3.2.2. Deep Eutectic Solvents (DESs)**

Deep eutectic solvents (DESs) are the mixtures composed of one or multiple hydrogen bond donors (HBDs) or Lewis bases and one or multiple hydrogen bond acceptors (HBAs) or Lewis acids which when mixed in a definite ratio, it forms a liquid having lower melting point (eutectic) than their initial components. The lowering of melting point is due to the formation of hydrogen bonding between the HBD and HBA.

**i) History**

The deep eutectic solvents were first reported by Abbott and co-workers (2003). In their work, they discussed solid-liquid behavior of the mixtures that were mainly formed by the substitution of the quaternary ammonium salts with different amides. A significant depression in freezing point was observed by Abbott and co-workers (2004) in the initial components that were used to synthesize the mixture. The hydrogen bonding interactions

between the HBD and HBA were responsible for particular type of behavior which lowers the lattice energy of the DESs. They also predicted that solvents that will have the capability to form hydrogen bonding will be highly soluble in the DESs e.g. ethanol, water are highly soluble in DESs whereas acetone, hexane, acetonitrile are purely immiscible in DESs. This publication was considered as the initiating point in the history of DESs.

As their publication, in which the urea:choline chloride mixture were used in a molar ratio (2:1) (*reline*), was the most notable and explored DES. Although after one year, on the basis of the same principle, *i.e*., taking a complex of a halide salt and the charge between the halide anion and the hydrogen bond donor delocalized, they showed that other HBDs like carboxylic acids are also capable to form DESs (Abbott et al., 2007). The classification of DESs was done by grouping the DESs in four different categories (Irfan et al., 2018). The new categorization of the DESs was also published by Abbott and co-workers, and defined DESs with the help of a general formula $R_1R_2R_3R_4N^+X^-Y^-$, in which $Y^-$ can be classified as given in Table 2.2. Besides, there is also one more category i.e. Type IV DES, that is mainly made up of metal halides (*e. g.* $ZnCl_2$) mixed with different types of HBDs e.g. urea, or ethylene glycol.

**Table 2.2. Classification of DESs, according to the halide salt derivative complexing agent**

| DES | Type Y |
|---|---|
| Type I | $MCl_x$, M= Zn, Sn, Fe, Al, Ga |
| Type II | $MCl_x.yH_2O$, M= Cr, Co, Cu, Ni, Fe |
| Type III | $R_5Z$, Z= $CONH_2$, -COOH, -OH |

Source :- Irfan et al., 2018

A lot of research has been done on the new classes of DESs, physiochemical characterizations, new applications, and primary studies associated with DESs (Zhang et al., 2012, Hayyan et al., 2012, Sergey et al., 2015, Artemiy et al., 2018). Alternatively, the most significant studies were the preparation of DESs using different HBAs, *e.g.*, halide salts based

of phosphonium-ions (Kareem et al., 2010), amino acids (Rocha et al., 2013), and availability of huge variety of HBDs, *e.g.*, sugars, glycerol and ethylene glycol (Abbott et al., 2011, Van et al., 2015) and the expansion of hydrophobic DESs.

**ii) Preparation and Properties of DESs**

The physicochemical properties of the DESs resembles with ILs such as low volatility. But the preparation of DESs is easy and prepared by the cheaply available acids and bases, overcoming the main drawback of the ILs for large scale applications. The preparation of DESs can be done by three different methods:

1. Heating method (Abbott et al., 2006)
2. Grinding method (Florindo et al., 2014)
3. Freeze drying (Garcia et al., 2015)

The commonly used method for the preparation of DESs is heating method. In heating method, both the initial components are mixed in a beaker and heated & stirred until it forms a clear liquid. Usually, the temperature of the heating components varies from 40-80 °C. In the grinding method, in a mortar the initial components are taken and grinded until the initial components mix well and turn into a clear liquid.

At last, in the freeze drying method initial components are prepared in their aqueous solution form and mixed. After that, the mixture is frozen and consequently freeze-drying of the mixture is done until it forms a clear liquid. The water presents in the liquid is evaporated in a rotary evaporator.

Recent studies revealed that the method adopted to synthesize the DESs influenced the physiochemical properties of the DESs mixture. It is mainly happened in the DESs prepared by dicarboxylic acids and choline chloride compounds (Mulyono et al., 2019). The high temperature during the preparation of the DESs promotes the esterification of the dicarboxylic acids due to the change in the pH of the synthesized DESs. The esterification can be inhibiting by preparing the DESs at lower temperatures and moisture absence. Hence, esterification process should only be considered in those hydrogen bond donors and hydrogen bond acceptors that have capability to do esterification. So, heating method can be considered most favorable method in the preparation of most of the DESs, Even though in case of that

reaction in which the reaction will be promoted by temperature, other methods of preparations can also be considered.

The adjustable properties of DESs are highly remarkable than ILs, because with the modification of the HBD nature, the cationic and anionic properties of the HBA and HBD as well as varying the molar ratio of the DESs mixture, the properties of the DESs can also be modified or designed.

There is huge range of DESs with exceptionally high melting points. But only those DESs can be considered whose melting point should be lower or close to the ambient temperature for industrial applicability. The possible HBD and HBA that can be used to form DESs are listed below (Table 2.3).

**Table 2.3. HBDs and HBAs that can be combined to form a DES**

| S. No. | Hydrogen Bond Donors (HBDs) | Hydrogen Bond Acceptors (HBAs) |
|---|---|---|
| 1. | Acetamide | Ethylammonium chloride |
| 2. | Oxalic acid | Nicotinic acid |
| 3. | Malonic acid | Ethyl(2-hydroxyethyl)-dimethylammonium chloride |
| 4. | Malic acid | Trimethylammonium chloride |
| 5. | Xylitol | Betaine |
| 6. | Urea | Choline nitrate |
| 7. | 1,1-dimethylurea | Tetramethylammonium chloride |
| 8. | D-isosorbide | Choline chloride |
| 9. | Tartaric acid | Choline tetrafluoroborate |
| 10. | Tricaballylic acid | Tetraethylammonium bromide |
| 11. | Thiourea | Chlorocholine chloride |
| 12. | Trifluoroacetamide | Tetraethylammonium bromide |
| 13. | Benzoic acid | Chlorocholine chloride |
| 14. | Itaconic acid | Histidine |
| 15. | Citric acid | Alanine |

| S. No. | Hydrogen Bond Donors (HBDs) | Hydrogen Bond Acceptors (HBAs) |
|---|---|---|
| 16. | Imidazole | 2-fluoroethyltrimethylammonium bromide |
| 17. | 2-imidazolinone | Acetylcholine chloride |
| 18. | Benzamide | Choline fluoride |
| 19. | 4-hydroxybenzoic acid | Benzyldimethyl(2-hydroxyethyl)-ammonium chloride |
| 20. | Cinnamic acid | Proline |
| 21. | Ethylene glycol | Diethyl(2-hydroxyethyl)-ammonium chloride |
| 22. | Propylene urea | Lidocaine |
| 23. | Resorcinol | (phenylmethyl)triphenylphosphnium chloride |
| 24. | Phenylacetic acid | Methyltriphenylphosphonium bromide |
| 25. | D-sorbitol | Tetrabutylammonium chloride |
| 26. | Lactic acid | Zinc chloride |
| 27. | 1,3-dimethylurea | |
| 28. | Levulinic acid | |
| 29. | Gallic acid | |
| 30. | Caffeic acid | |
| 31. | 1-methylurea | |
| 32. | Glycerol | |
| 33. | Succinic acid | |
| 34. | Hexanoic acid | |
| 35. | Coumaric acid | |
| 36. | Stearic acid | |
| 37. | Adipic acid | |
| 38. | Oleic acid | |
| 39. | Suberic acid | |

| S. No. | Hydrogen Bond Donors (HBDs) | Hydrogen Bond Acceptors (HBAs) |
|---|---|---|
| 40. | Linoleic acid | |
| 41. | Decanoic acid | |

The nature of HBD and HBA as well as the molar ratio of HBD and HBA influenced the melting point of the DESs. The studies revealed that if the same HBD mixed with HBA of choline salt derived, the trend of melting point decreased as follows:-

$F^- > NO_3^- > Cl^- > BF_4^-$

It clearly explained the correlation of the strength of hydrogen bond and the melting point (Kareem et al., 2010).

In case of HBD i.e. for quaternary ammonium salts and carboxylic acids, lesser the molar mass of the acid, higher the depression in the melting point observed. However, in DESs the effect of different HBD compounds like carboxylic acid, amine, polyol, on the melting point has yet to be explored in future. At last, considering the effect of the molar ratio of DES, Abbott et al. (2004) explained that for the solvation of one molecule of choline chloride, there must be two molecules of carboxylic acid requires. While only one dicarboxylic acid molecule is required to solvate one molecule of Choline chloride. So the formation of DESs by mixing choline chloride with a carboxylic acid and dicarboxylic acid develops a eutectic composition (i.e. HBD: HBA) with molar ratio of 2:1 and 1:1 respectively. Recently, to predict the melting point of choline chloride based DESs, some researchers developed some predictive models like quantitative structure-activity relationship (QSAR) (Garcia et al., 2015).

The decomposition temperature plays significant role which defines solvent's operational liquid range. The decomposition temperature of the initial components defines the decomposition temperature of the DESs which lies in the range of 400-500 K. The other important property of DESs is density which helps for the process designing and to develop the appropriate equations of state (EoS). The density of most of the DESs lies between 1.0 to 1.35 $g/cm^3$ at room temperature and at atmospheric pressure, although the nature of HBD and HBA and their molar ratio also affect the performance of the DESs. The density of many

DESs had been studied and reported by many researchers (Gutierrez et al., 2009). The moisture content and synthesis method also affect the density (Van et al., 2015). The main applications of DESs are listed in Figure 2.7.

DESs were used as solvents in many separation processes like LLE, extractive distillation in many azeotropic mixtures (Rodriguez et al., 2015, Rodriguez at al., 2015), $CO_2$. But there is no study that has been proposed for the separation of ACN + water mixture using DESs.

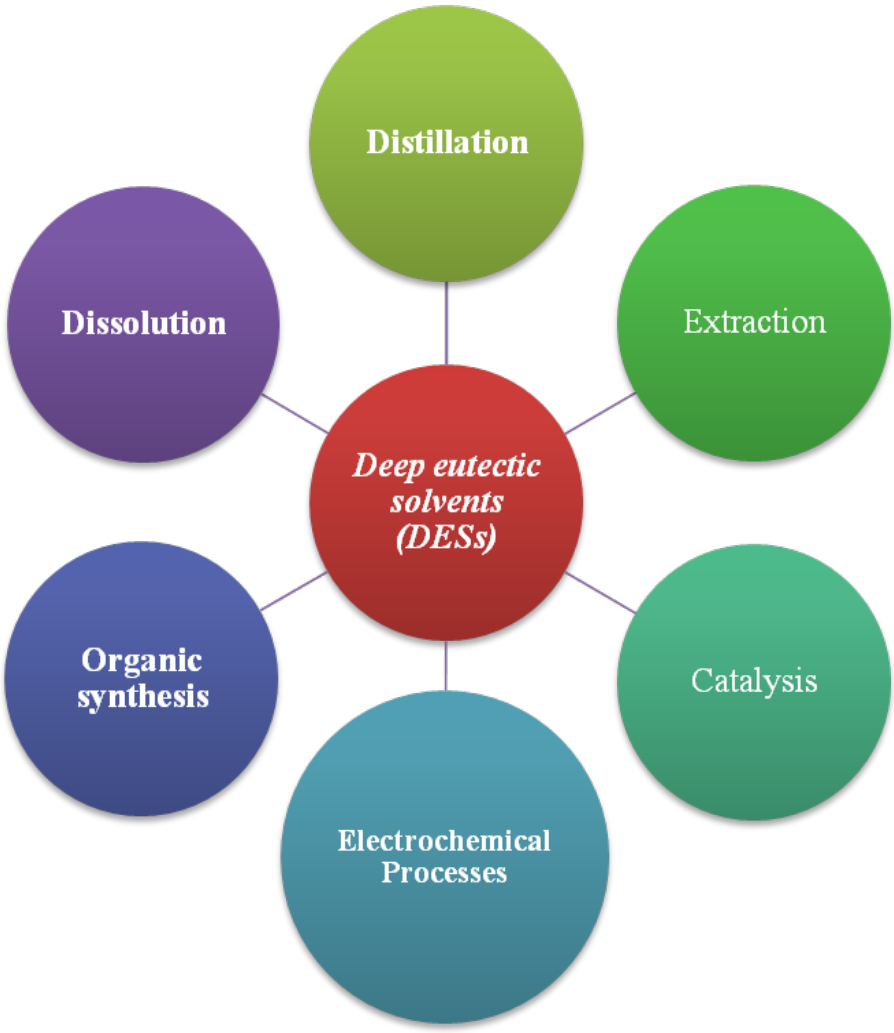


**Figure 2.7. Applications of Deep eutectic Solvents (DESs)**

### 2.4.4. Other Enhanced Distillation Techniques

To create the more energy-efficient distillation techniques, process intensification can be proven a very useful tool, *e.g.* in case of wall distillation column division, microwave enhanced separations, ultrasonic enhanced distillation. The main aim of dividing wall column (DWC) is to decrease the requirement of the number of columns for a multicomponent azeotropic mixture separation; many researchers have worked to design, control and optimize the column length and number. Although the applicability of the column length and number to separate the azeotropic mixtures has not been fully developed, the studies show that the implementation of this technique in extractive and azeotropic distillation reduce the energy consumption and equipment reduction (Dejanović et al., 2010, Delazar et al., 2012). Microwave enhanced separations are also in the progressive stage. Although most of the attention was given to extraction (Chemat et al., 2013, Meier et al., 2009), desorption (Chronopoulos et al., 2014, Therdthai et al., 2009) and drying (Mcloughlin et al., 2000, Feng et al., 2012), separation of azeotropic mixtures was also studied (Gao et al., 2013, Feng et al., 2013, Mahdi et al., 2014). But if the microwave radiation is applied on the azeotrope mixture, the azeotrope can be shifted. On the other hand the ultrasonic enhanced processes are also explored by some researchers (Abdul et al., 2011, Ripin et al., 2008). The studies revealed that if the sonification parameters are chosen wisely, the elimination of the azeotropic mixtures can be done. As a result, the azeotropic mixtures separation can be done in one column without any entrainer requirement. But, a large-scale ultrasonic assisted separation column was not achieved. Furthermore, the safety, operability and control of the system are still required to be studied. In conclusion, all the above discussed intensification processes are no doubt promising in nature, but it still requires some time for further research and development. Acosta-Esquijarosa et al. (2006) presented an efficient study for the dehydration of azeotropic mixture of acetonitrile + water through combined process. Firstly, they processed the azeotropic separation of acetonitrile from the binary mixture taking adequate extraction agent by crosscurrent liquid extraction process. After that the solvent rich phase obtained via liquid extraction process was processed by the batch distillation technique. Using

the commercial softwares Prosim Batch and Superpro Designer, validation of the feasibility of the proposed method had been done by simulation. Zerry et al. (2005) also attempted the hybrid pervaporation process combined with the batch distillation and obtained 40 Mol% feed concentration and complete the work with the reduction of operational cost as well as investment. A novel heat integration theory by using the hybrid distillation process with the pervaporation was developed by Gomez et al. (2008). They presented two membranes module designs. The results obtained by the simulation showed that the purity of product was reached up to 30% by using heat integration. With the development of the new process design the problems like decrease in temperature and concentration polarization phenomenon as well as an increase in the turbulence have been solved (Sangal et al., 2012, Sangal et al., 2014).
Main advantages and disadvantages of these processes are given in Table 2.4.

**Table 2.4. Advantages and Disadvantages of various Separation Processes**

| Separation Processes | Advantages | Disadvantages |
|---|---|---|
| **Liquid-Liquid Extraction** | 1. Simple operating System<br>2. Flexibility with physical properties as well as various parameters. | 1. Requirement of high dosage of solvent.<br>2. Low Selectivity.<br>3. Emulsions can be formed which is difficult to break. |
| **Membrane Processes** | 1. High selectivity and permeability.<br>2. Environmental friendly.<br>3. Flexible and easily scale-up. | 1. Low lifetime of membranes.<br>2. High cost of zeolite membranes.<br>3. Corrosion problems occur in PVA-iron oxide nanocomposite membranes. |
| **Pressure-Swing Distillation** | 1. No entrainer requires for separation.<br>2. Energy saving process via heat integration of the system. | 1. Complex automation.<br>2. Non - availability of azeotropic data at non-atmospheric pressures and data generation is very costly.<br>3. The separation of the azeotropic |

| | | |
|---|---|---|
| | | mixture is totally pressure dependent. |
| **Hybrid Processes (Pervaporation-Distillation)** | 1. Low energy consumption.<br>2. Low investment cost.<br>3. No waste has been produced. | 1. Lack of information.<br>2. Low permeate flow.<br>3. Scarcity of effective membranes. |
| **Extractive Distillation** | 1. Effective in separation of close boiling point azeotropes.<br>2. Extractant recycling rate is higher. | 1. High dosage of entrainer requires.<br>2. Typical VOCs pollutes the environment. |

## 2.5 Research Gaps

- Some typical solvents e.g. ethylene glycol and butyl acetate have been used for the dehydration of ACN + water mixtures. Recycling problem due to low boiling point, mixing problem with azeotropic mixture or high dose requirement are the drawbacks associated with these solvents. Thus, there should be novel solvents available for the separation processes that are more economical compatible, suitable and offer exceptional properties like, low or negligible vapor pressure, environmental compatibility, good thermal stability, water compatibility, biodegradability, wide liquid range and non-flammability.
- No study has been reported on separation of ACN + water mixture by using deep eutectic solvents (DESs) till date. Preparation of DESs is easy and cheap, and it shows almost all the properties required for a component to be used as entrainer like, low vapor pressure, water compatibility, biodegradability, wide liquid range and non-flammability. It is expected that DESs will solve many problems associated with previously reported solvents and salts.

## 2.6 Aims and Objectives

In view of the literature survey and the necessity of searching novel solvents which can separate acetonitrile + water mixture in much economical and eco-friendly manner, the following aims and objectives have been set for the present work:

1. To prepare the Deep eutectic solvents (DESs) using different raw materials, and characterize the prepared DESs for thermal stability, density, viscosity and water content of mixture.
2. To explore the separation ability of DESs with varying concentration on the acetonitrile + water system by measuring the vapor–liquid equilibrium (VLE) data for the system formed by acetonitrile, water, and DESs at atmospheric pressure.
3. Vapor–liquid equilibrium (VLE) data for the pseudo-binary mixtures of water + DESs and acetonitrile + DESs will be measured and fitted with the classical thermodynamic model to calculate the interaction parameters.
4. To correlate the experimental data with the classical thermodynamic models.

*Chapter-3*

# MATERIALS AND METHODS

## 3.0 GENERAL

This chapter describes the materials and method used in the separation of ACN + water mixture using novel solvents (Deep Eutectic Solvents) as entrainer by extractive distillation. Preparation of ACN + water azeotropic mixture, method and apparatus used for synthesis of deep eutectic solvents, experimental set-up for vapor–liquid equilibrium (VLE) studies, and analysis methods are explained in detail.

## 3.1 MATERIALS

### 3.1.1 Chemicals Used

The chemicals used were acetonitrile, glycolic acid, choline chloride, DL-malic acid, tetramethylammonium chloride, isopropyl alcohol, karl fischer reagent and double distilled water. Table 3.1 summarizes the list of chemicals, including their purity level and supplier. Acetonitrile (HP-LC grade) with a high purity of 99.8+%, tetramethylammonium chloride 98.0+%, and malic acid 98+% were supplied by Merck chemicals. Isopropyl alcohol with a purity of 99+% was purchased from Sigma-Aldrich, and glycolic acid (98+ %) was supplied by Spectrochem. Both ACN and isopropyl alcohol were used as procured without further purification. Choline chloride was provided by TCI Chemicals with a minimum purity of 98+%. Due to the hygroscopic nature of glycolic acid, malic acid, tetramethylammonium chloride and choline chloride, these were first dried for 24 hours in a vacuum oven before processing the DESs. The trace water content in these chemicals was analyzed using Karl Fischer titration analysis (type Esico 1760) and was observed to be less than 0.3 wt %.

### 3.2.1. Synthesis and Characterization of DESs

In this study, glycolic acid and DL-malic acid were used as hydrogen bond donor (HBD) and choline chloride and tetramethylammonium chloride as hydrogen bond acceptor (HBA) for synthesis of DESs. The DESs were prepared in the same manner as reported in the literature (Francisco et al., 2013). A Mettler Toledo electronic balance with a precision of ±0.0001 g was used.

**Table 3.1 Specifications of chemicals used**

| Name | CAS No. | Source | Purity(wt %) | Purification |
|---|---|---|---|---|
| Acetonitrile | 75-05-8 | Merck chemicals | 99.8+% | None |
| Glycolic acid | 79-14-1 | Spectrochem | 98+% | Vacuum drying |
| D-L malic acid | 6915-15-7 | Merck chemicals | 99+% | Vacuum drying |
| Choline chloride | 67-48-1 | TCI chemicals | 98+% | Vacuum drying |
| Tetramethylammonium chloride | 75-57-0 | Merck chemicals | 98+% | Vacuum drying |
| Karl Fischer reagent | 7446-09-5 | Merck chemicals | 99+% | None |
| Double distilled water | | Our laboratory | | |

For the synthesis of different DESs, a HBD and HBA were introduced into a closed 50 mL glass flask in predefined molar ratios, depending upon the type of DESs. Both were homogeneously mixed, and afterward, the mixture was heated using thermostatic oil bath and stirred till the melting of the mixture provided enough liquid. The schematic diagram of thermostatic oil bath is shown in Figure 3.1. The temperature of the oil bath was controlled at 70 °C (±0.1 °C) using a temperature controller (IKA ETS-D5). Once a colorless and transparent liquid formed, the heating was stopped and liquid was allowed to cool gradually to ambient temperature. To check the stability of the prepared DESs, it was kept at room temperature overnight. The water content in the prepared DESs was analyzed using the Karl Fischer titration method (Esico, 1760).

### 3.2.2. Instruments and Characterization Techniques

Prepared DES was analyzed for its moisture content, viscosity, density, thermal stability and hydrogen bond mechanism.

Density of the prepared DES was estimated by specific gravity bottle. Firstly the density of water was checked to conclude the error% and then density of the prepared DESs was checked. The viscosity of the prepared DESs was also measured by Brookfield DVII + Pro at 25°C.

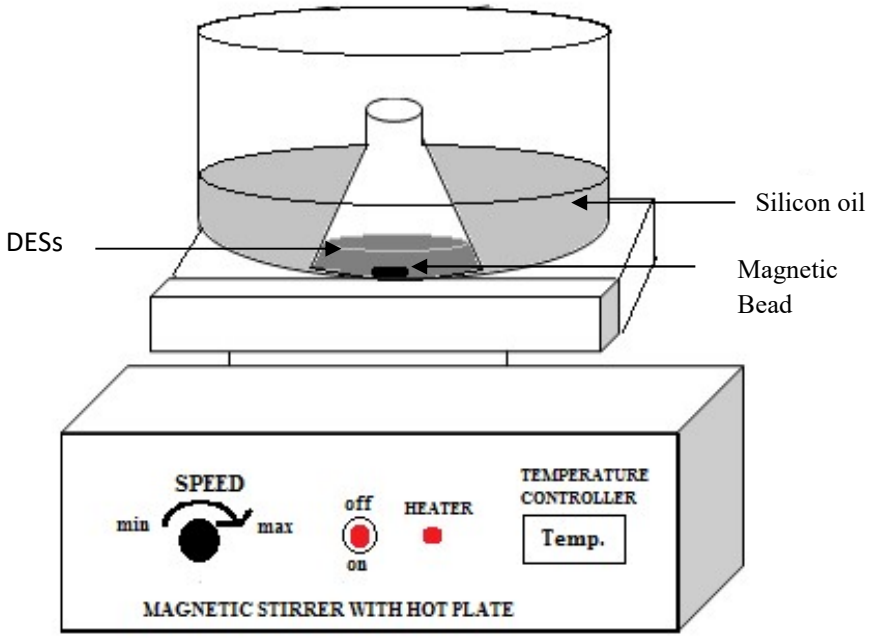


**Figure 3.1. Thermostatic Oil Bath with magnetic stirrer**

The thermal stability of prepared DES was evaluated by Thermogravimetric analysis (TGA) (PerkinElmer, STA6000). TGA was performed from 25ºC to 400ºC at 10ºC rise in temperature in nitrogen gas environment using 25mgof DES sample. Moreover, the characterization of the prepared DES was also carried out by FT-IR ((PerkinElmer) to determine the hydrogen bonding of the DES. The hydrogen bonding mechanism of the prepared DESs was confirmed by $^{1}$H NMR spectrometer. Bruker AVANCE Neo 500 MHz NMR spectrometer was operated at room temperature for the determination of $^{1}$H NMR spectra of the prepared DESs. The NMR sample has been prepared by dissolving 25mg of DES sample in 0.5ml of DMSO in 5 mm NMR tube. A homogenous mixture of DES and DMSO was prepared by vortex mixing and analyzed by NMR spectrometer. The spectra of different characterized DESs are presented in Chapter 4.

Improved Othmer type recirculation still was used to measure isobaric VLE data at atmospheric pressure. (Othmer et al., 1960, Kumar et al., 2010).

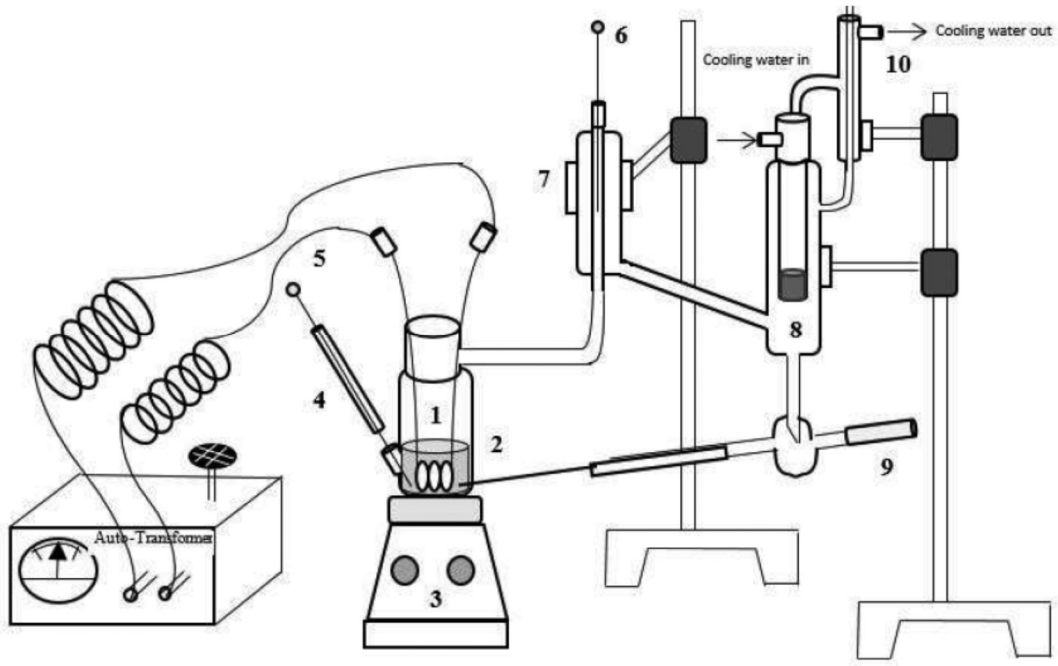


**Figure 3.2. Schematic Diagram of modified Othmer type recirculation still.**

### 3.3.1. Apparatus and Procedure for VLE Determination

Figure 3.2 represents the schematic diagram of modified Othmer type recirculation still used in the present study. The original Othmer recirculation still was modified by removing the drainage port and adding a widened loading port in the side of the still to avoid the clogging with salt and other compounds. A stirrer was also added under the still to assure uniform composition of the liquid within the body of the still. Moreover the constant volume condensate chamber was replaced with three condensers in series to increase the flexibility in operation by providing opportunity of controlling the holdup volume and sample size. The setup consists of a boiling still (1) of 150 mL capacity in which a nichrome wire heater (2) (glass-sealed) is provided to boil the mixture. A magnetic stirrer (3) (REMI Instruments-2MLH model, Bombay, India) was used to stir the still contents. The still has two side-angled openings: the left one (4) to draw the liquid phase sample and to accommodate a thermometer (5) and the right one to receive condensate recycle. Vapors generated in the still pass through

an air-cooled condenser (7) in which a thermometer (6) is incorporated. The uncondensed vapors and condensate move to the water-cooled condenser (8), and condensate flows down from this condenser to the condensate sample bulb (9) which is connected with a condensate sampling port. Almost all the vapor condenses in the water cooled recirculation condenser; if some uncondensed vapor is remaining, that undergoes condensation in another water-cooled condenser (10). An autotransformer was applied to supply the electricity to the nichrome wire heater (2). To measure the temperature at equilibrium, a precision and calibrated thermometer was used of 0.1 K uncertainty count.

### 3.3.2. Composition Analysis of Samples

The composition of the condensed vapor phase (ACN + water) at equilibrium was analyzed using a Bruker Gas chromatograph (SCION 456-GC) facilitated with FID (flame ionization detector) and TG-Bond Q column (30 m × 0.53 mm I.D., 20.0 µm film thickness) of Thermo Scientific. The detector temperature was set to 250 °C. Injections (1 µL) were performed in the split mode at a split ratio of 100:1 with an injector temperature of 200 °C. As carrier gas in Gas Chromatograph (GC), helium was used at a flow rate of 5.0 mL $min^{-1}$. The oven temperature was fixed at 180 °C. No presence of DES was observed in the vapor phase. The acetonitrile mole fractions in the liquid phase were determined using the same Gas Chromatograph method, while Karl Fischer moisture analysis (Esico model 1760) was used for determination of water content. While analyzing the liquid samples in Gas Chromatograph, a glass liner (Agilent Technologies) was used before the column. The glass liner is generally used to prevent any viscous liquid from entering the column; otherwise, it can damage the Gas Chromatograph column. DES was prevented from entering into the GC column by applying a clean glass liner after each gas chromatogram, and the same was found effective. In liquid samples, the mole fraction of DES was analyzed by applying the mass balance. A calibration, prepared from gravimetric standard solutions, was used to determine the equilibrium compositions of the samples (Figure 3.3). The uncertainty in the component mole fraction of the vapor and liquid phases was 0.003. The apparatus pressure was maintained at atmospheric pressure during the measurement process. The uncertainty calculation method is presented in Appendix 3.

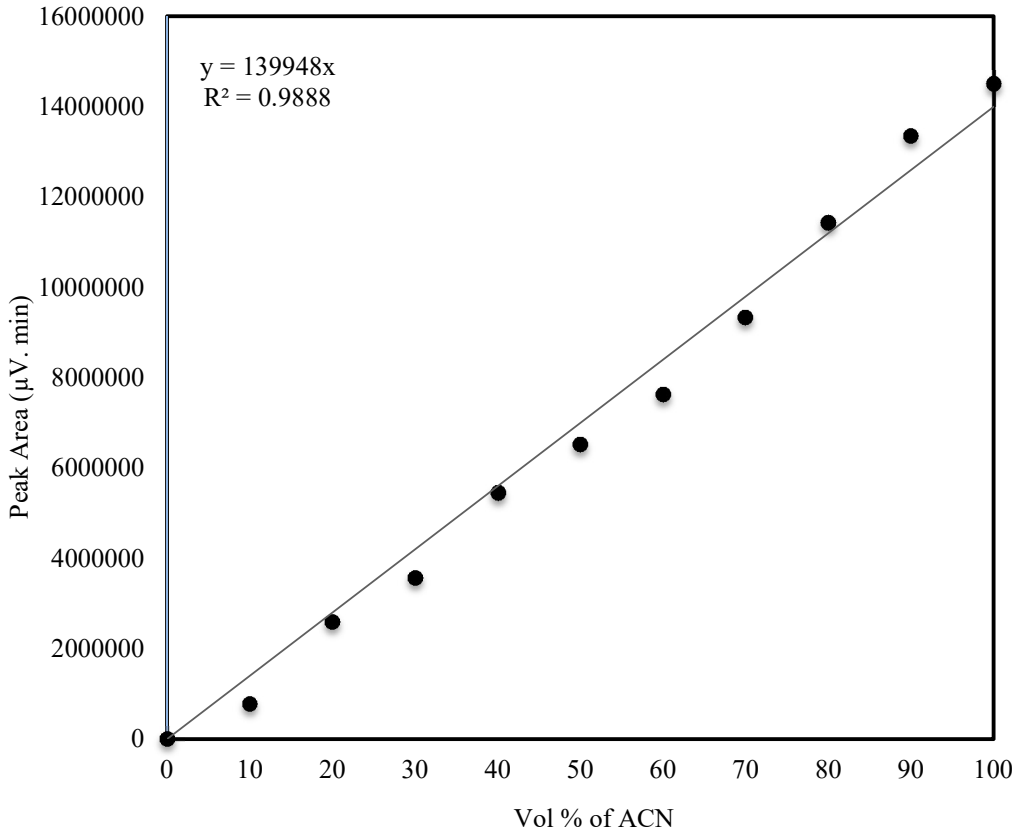


**Figure 3.3. Calibration Curve of ACN + water mixture**

### 3.4. Verification of the apparatus

In order to verify the reliability of the experimental setup and method used in the present work, the VLE data of the IPA and water binary system were measured at atmospheric pressure using the present setup, and the same was compared with literature data (Brunjes et al., 1943). Table 3.2 and Figure 3.4 represent the experimental T−x, y data obtained in this work. It can be observed that the measured VLE data of the IPA and water system in this work are in good agreement with the literature data, indicating that the VLE apparatus used in the work is reliable.

**Table 3.2. Experimental Isobaric VLE data for IPA (1) + water (2) system at atmospheric pressure (101.32 kPa)**

| S.No. | $T$ (K) | $x_1$ | $y_1$ |
|---|---|---|---|
| 1 | 373.0 | 0.000 | 0.000 |
| 2 | 369.2 | 0.011 | 0.132 |
| 3 | 368.0 | 0.015 | 0.187 |
| 4 | 365.4 | 0.022 | 0.259 |
| 5 | 363.9 | 0.027 | 0.305 |
| 6 | 361.8 | 0.032 | 0.352 |
| 7 | 358.9 | 0.046 | 0.428 |
| 8 | 356.7 | 0.076 | 0.482 |
| 9 | 355.9 | 0.119 | 0.507 |
| 10 | 355.5 | 0.135 | 0.519 |
| 11 | 354.8 | 0.260 | 0.541 |
| 12 | 354.0 | 0.369 | 0.561 |
| 13 | 353.7 | 0.477 | 0.582 |
| 14 | 353.6 | 0.558 | 0.623 |
| 15 | 353.5 | 0.667 | 0.681 |
| 16 | 353.7 | 0.762 | 0.732 |
| 17 | 353.8 | 0.840 | 0.800 |
| 18 | 354.1 | 0.865 | 0.829 |
| 19 | 354.9 | 0.952 | 0.938 |
| 20 | 355.6 | 1.000 | 1.000 |

Standard uncertainty $u(x)=u(y)=0.003$, $u(T)=0.1K$, $u\ (P)$ = 0.05kPa.

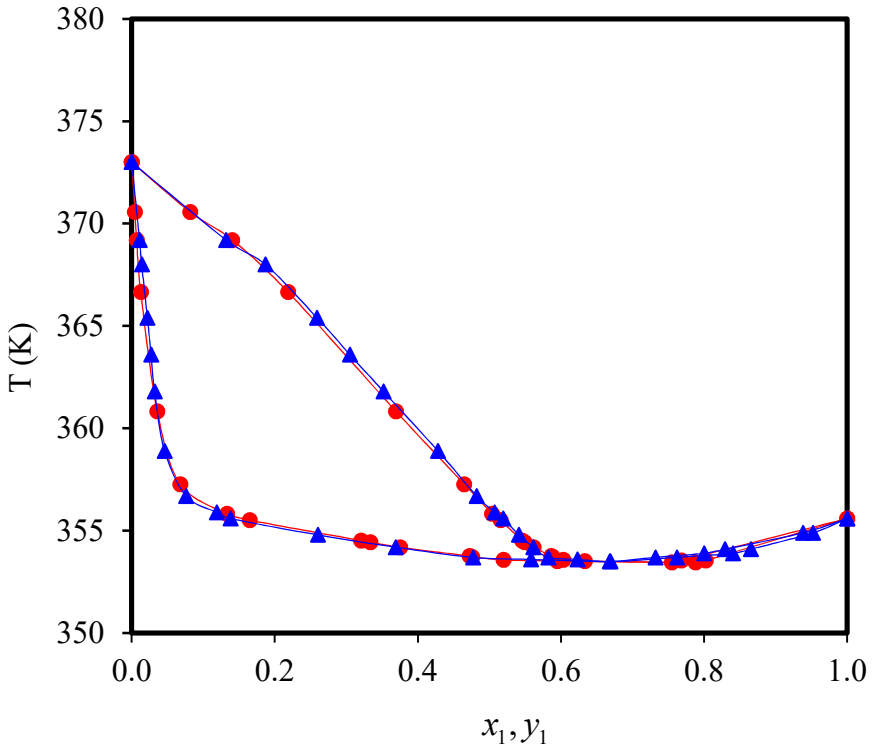


**Figure 3.4. Comparison of isobaric $T-x-y$ data for IPA (1) + water (2) system at atmospheric pressure, ▲:represents present work data; ●: represents data from literature** (Brunjes et al., 1943)

### 3.5. Correlation of VLE Data

By fugacity equality, the $\hat{f}^V$ and $\hat{f}^L$ of each component, $i$ in the vapor phase and liquid phase, should be equal at VLE (equation 3.1).

$$\hat{f}^V = \hat{f}^L \tag{3.1}$$

By applying the γ−φ approach, following equilibrium, equation 3.2, can be achieved

$$y_i \hat{\varphi}^V p = x_i \gamma_i p_i^s \varphi_i^s PE_i \tag{3.2}$$

where $\hat{f}^V$ and $\hat{f}^L$ are fugacity of component $i$ in the vapor and liquid phases respectively, $y_i$ the mole fraction of component $i$ in vapor phase, $\varphi_i^V$ the fugacity coefficient of component $i$

in vapor phase, $P$ the total system pressure, $x_i$ the mole fraction of component $i$ in liquid phases; $\gamma_i$ the activity coefficient of component $i$ in the liquid phase, $p_i^s$ the saturation vapor pressure of component $i$ at system temperature $T$, obtained from the Antoine equation and $\varphi_i^S$ the fugacity coefficient of saturated pure $i$ at the system temperature $T$. The Antoine constants were taken from the literature (Perry et al., 1934) and are listed in Table 3.3.

**Table 3.3. Antoine constants for ACN and water** (Perry et al., 1934)**)**

| Components | Antoine constants | | |
|---|---|---|---|
| | $A_1$ | $B_i$ | $C_i$ |
| ACN | 7.5305 | 1609.86 | 264.7 |
| Water | 8.07131 | 1730.63 | 233.426 |

Antoine equation: $\log p_i^{sat} = A_i - \frac{B_i}{T - 273 + C_i}$, units: $p(mmHg), T(K)$

The virial equation of state reduced at the second coefficient with Tsonopoulo's correlations was applied to calculate the fugacity coefficients (Tsonopoulos, 1974, Gjineci et al., 2016). Further, for Poynting effect (PE) estimation, DIPPR equations were used to calculate saturated liquid molar volumes and vapor pressures (Daubert et al., 1992).

$$PE_i = \exp\left[\frac{v_i^L\left(p - p_i^s\right)}{RT}\right]$$

(3.3)

Therefore, the activity coefficients can be given as equation 3.4.

$$\gamma_i = \frac{y_i\ \hat{\varphi}^V\ p}{x_i p_i^s\ \varphi_i^s\ PE_i} \quad (3.4)$$

The step by step methodology for calculation of second virial coefficient, fugacity coefficient and activity coefficient is given in Appendix 1.

The Poynting correction is close to unity when the difference $p_i$ - $p_i^{sat}$ is small, and this equation can thus be simplified to

$$y_i \hat{\varphi}_i^V p = x_i \gamma_i p_i^s \varphi_i^s$$

(3.5) Since DESs are nonvolatile component and found to be absent in the vapor phase, these systems can be simplified as pseudo-binary and pseudo-ternary, considering the DES as a single component (Rodriguez et al., 2015, Rodriguez et al., 2015).However, while calculating the activity coefficient of the ACN + water mixture in the liquid phase, the DES concentration was considered. Generally, to calculate the activity coefficient, $\gamma^{cal}$ of systems comprising DESs, the NRTL model is employed. (Rodriguez et al., 2015, Rodriguez et al., 2015, Peng et al., 2017).

Experimental activity coefficients for pseudo-binary systems of ACN + DES and water + DES were calculated using equation 3.5 and was fitted to the NRTL model. For the pseudo-ternary system ACN + water + DES, correlation was done on the solvent-free basis (Gjineci et al., 2016, Peng et al., 2017).

Regression analysis was performed using optimization techniques in the MATLAB® (version 9.3) program for the estimation of NRTL interaction parameters. Algorithm used was Nelder–Mead simplex search method (Lagariaset al., 1998) (*fmin search* function in MATLAB).

A relative least-squares error objective function (OF) was used to fit the experimental data (Kim et al., 2008).

$$OF = \sum_{i=1}^{n} \left[ \frac{\gamma_i^{\exp} - \gamma_i^{calc}}{\gamma_i^{\exp}} \right]^2$$

(3.6)

The OF was minimized in order to estimate the pseudo-binary and pseudo-ternary parameters for components in the ACN + water + DES system.

The relative volatility for ACN (1) + water (2) can be determined using equation 3.7.

$$\alpha_{12} = \frac{y_1 / x_1'}{y_2 / x_2'} \qquad (3.7)$$

# *Chapter – 4*

# RESULTS AND DISCUSSION

## 4.0 GENERAL

This chapter presents the detailed feasibility assessment of synthesized DESs (sugar based DESs and natural DESs) as entrainer, for separation of ACN + water azeotropic mixture via extractive distillation. It includes isobaric vapor–liquid equilibrium (VLE) studies for pseudo-binary systems (ACN + DES, water + DES) and pseudo-ternary systems (ACN + water + DES) at atmospheric pressure. Pseudo-ternary VLE studies were performed for different DES molar compositions; 5%, 10% and 15%. Further, correlation of experimental data for these systems was established using nonrandom two-liquid (NRTL) model. On the basis of characterization done for all types of DESs, the feasible hydrogen boding between different HBDs and HBAs were proposed and well optimized. The recoverability of used DESs was also investigated for its chemical stability during the process, to ensure its reuse.

## 4.1 Sugar Based DESs

In this section of study, glycolic acid which is also known as sugar based organic acid (Salusjärvi et al., 2019), was utilized for synthesis of DESs. Two different DESs were synthesized in predetermined molar ratios, using glycolic acid as a common hydrogen bond donor (HBD) and different hydrogen bond acceptors (HBAs) like, choline chloride & tetramethylammonium Chloride (TMAC). Performance of both DESs was evaluated for separation of ACN + water azeotropic mixture.

### 4.1.1 Glycolic acid + Choline chloride 3:1 DES (GC3:1)

Glycolic acid and choline chloride were mixed in 3:1 molar ratio and DES was synthesized following the procedure given in section 3.2.1 of chapter 3. The synthesized GC3:1 was characterized by different techniques for its physical, chemical and thermal properties. The separation ability of GC3:1 was evaluated by using its different dosage in ACN + water mixture.

#### 4.1.1.1 Characterization of Synthesized GC3:1

The thermal stability of synthesized GC3:1 was checked by Thermogravimetric analysis (PerkinElmer, STA6000) and is shown in Figure 4.1. TGA analysis was performed from

room temperature to 400 ˚C at atmospheric pressure. Results indicate that GC3:1 remains thermally stable in the working temperature range.

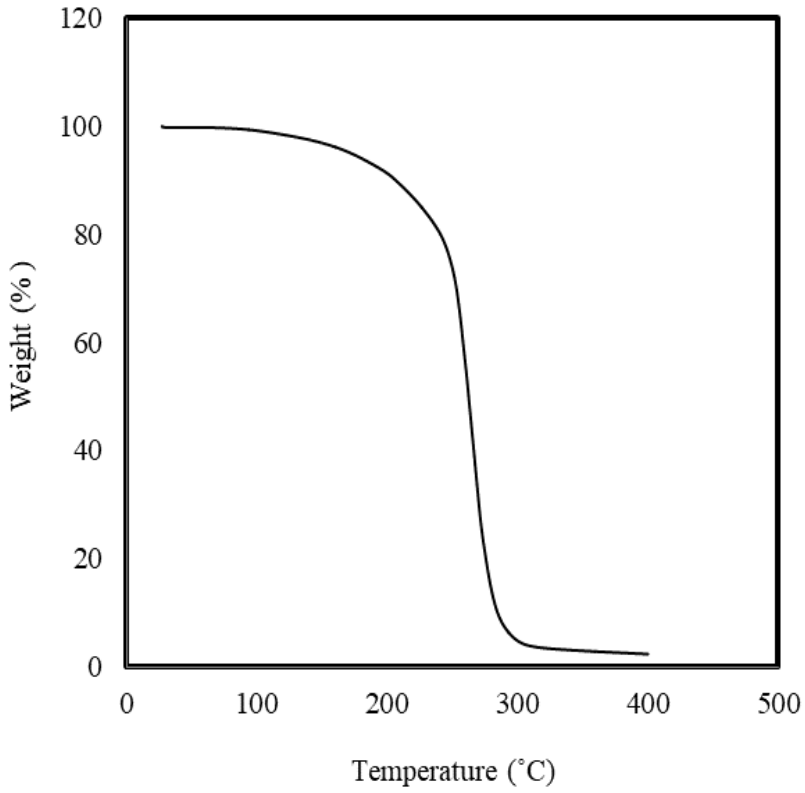


**Figure 4.1. TGA for GC3:1 from room temperature to 400 ˚C at atmospheric pressure**

To confirm the hydrogen boding among glycolic acid and choline chloride, Fourier transform infrared (FT-IR) (PerkinElmer) of synthesized GC3:1 was done and the spectra is shown in Figure 4.2. In the FT-IR spectra, at lower wavenumber, three bands with peaks at 1734, 1193, and 1083 $cm^{-1}$ were observed. This indicates the carbonyl group of glycolic acid and hydrogen bonding between the OH group of glycolic acid and $Cl^-$ of choline chloride, respectively. Near 3302 $cm^{-1}$, a broad band was also observed exhibiting an OH stretching region with the existence of extensive hydrogen bonds between OH of glycolic acid/choline chloride and $Cl^-$ of choline chloride (Perkins et al., 2014, Kaur et al., 2018). On the basis of this, the possible hydrogen bonding between glycolic acid and choline chloride is shown in

Figure 4.3, and the formula unit of prepared GC3:1 is $(C_5H_{14}NO)^+Cl^-\cdot 3\ (CH_2OH)-COOH$. Hydrogen bond formation between the glycolic acid and choline chloride decreases the freezing point of the mixture, which ultimately results in the formation of DES GC3:1. Proposed chemical structure of GC3:1 was also optimized by Gaussian 16 software and is illustrated in Figure 4.4.

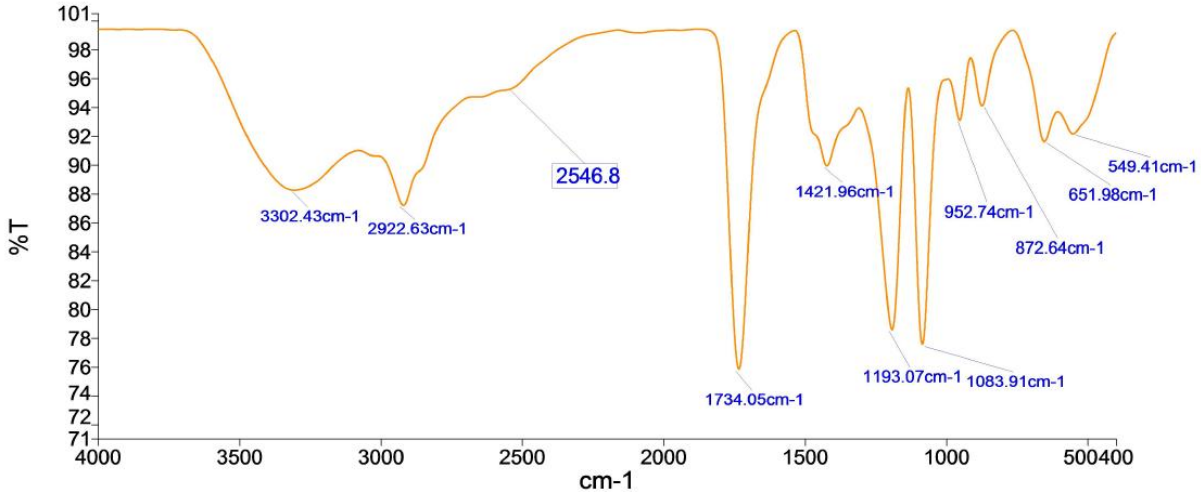


**Figure 4.2. FT-IR spectra for GC3:1**

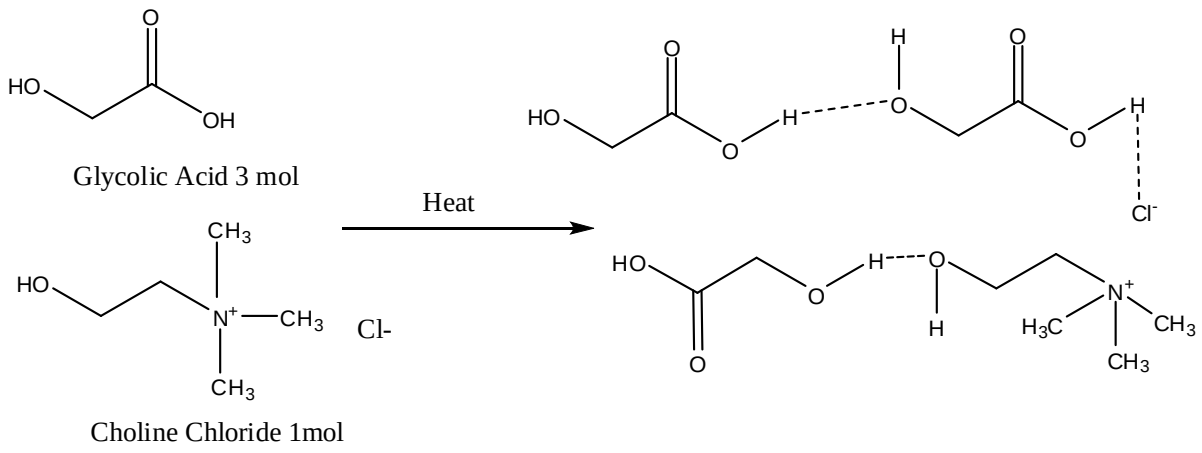


**Figure 4.3. Hydrogen bonding mechanism in Glycolic acid: Choline Chloride 3:1 (GC3:1)**

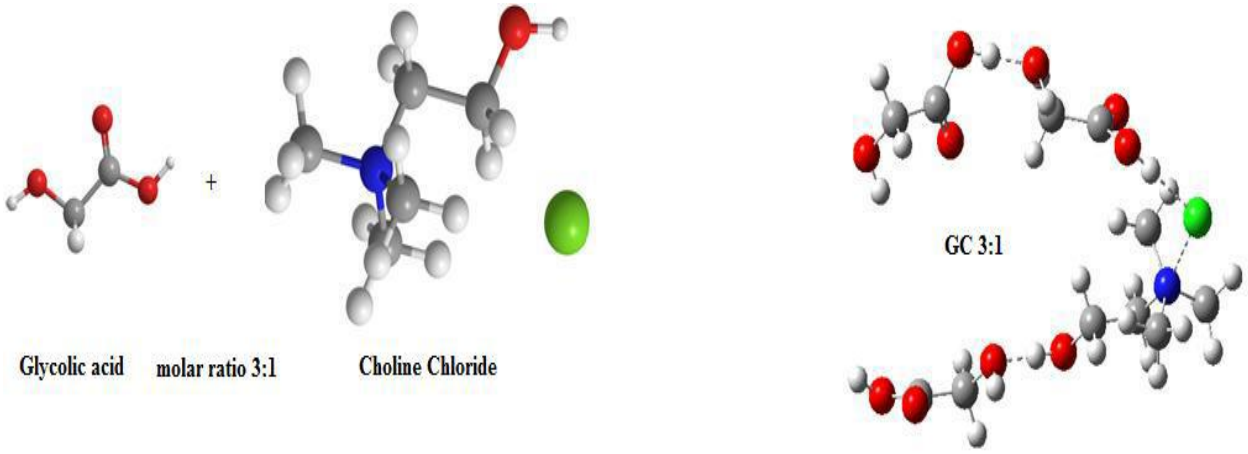


**Figure 4.4. Optimized Structure of GC3:1**

A Bruker AVANCE Neo 500 MHz NMR spectrometer was operated at room temperature for the determination of $^{1}H$ NMR spectra of the synthesized GC3:1. The GC3:1 sample has been prepared by dissolving 25 mg of the DES sample in 0.5 mL of DMSO in a 5 mm NMR tube. A homogeneous mixture of GC3:1 and DMSO has been prepared by vortex mixing. The $^{1}H$ NMR of the prepared NADES is shown in Figure 4.5. The structure of used GC3:1 has been determined by $^{1}H$ NMR spectra. Despite the dilution in DMSO, no effect has been seen on the molecular structure of GC3:1. Moreover, physical properties of GC3:1 like density, viscosity and moisture content were also determined using the methods described in chapter 3, and are listed in Table 4.1.

**Table 4.1. Physical Properties of GC3:1**

| **Properties** | **Value** |
|---|---|
| Density (ρ) | 1.265 g/cm$^3$ |
| Viscosity (μ) | 311.21 mPa/s |
| Moisture Content | 0.3 wt % |

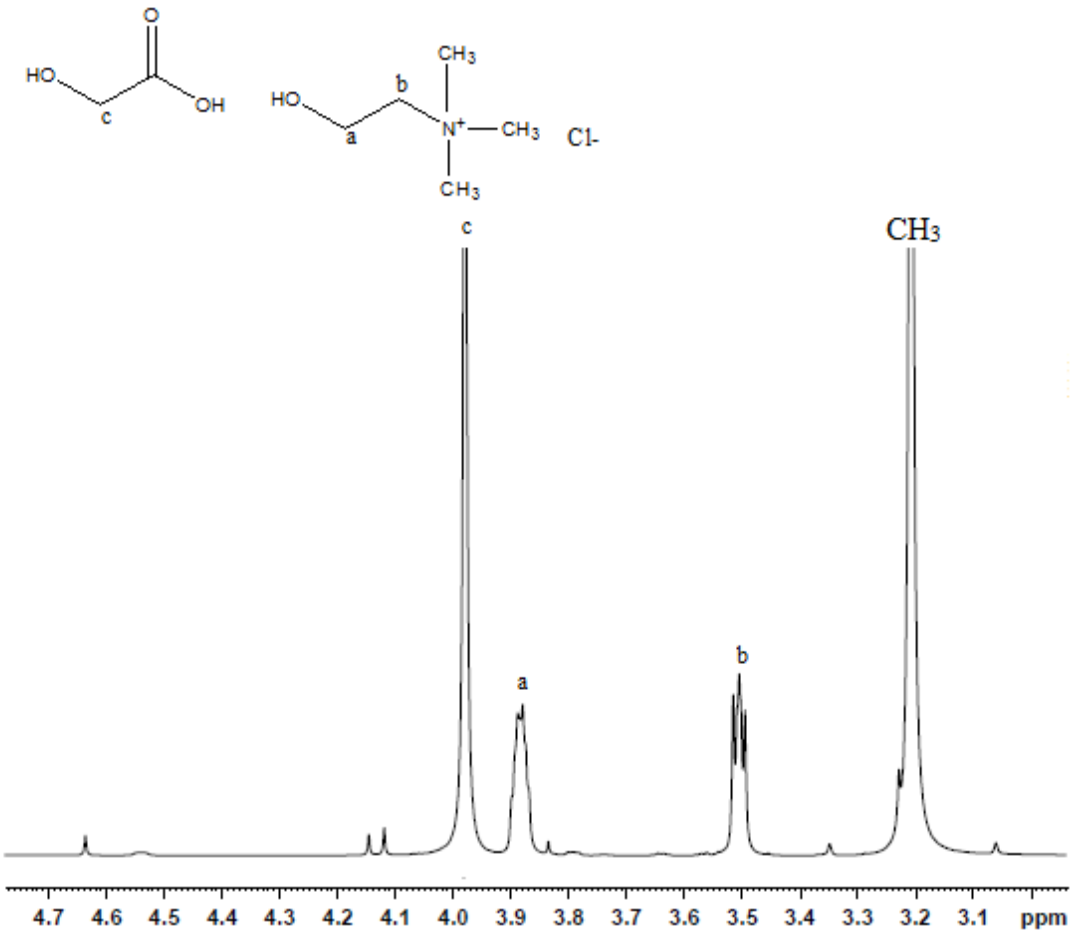


**Figure 4.5. $^{1}$H NMR spectra of the synthesized glycolic acid/cholinechloride 3:1 (GC3:1) DES**

### 4.1.1.2. Vapor–liquid equilibrium (VLE) measurements using GC3:1 as entrainer

To evaluate the effectiveness of GC3:1 as extractive agent, few preliminary experiments were performed. For this purpose, ACN + water mixture of azeotropic composition (67.4 mol% ACN) was prepared and experiments were conducted using various

GC3:1 concentration (0 to 15% mol/mol). The VLE data were recorded and relative volatility $\alpha_{12}$ were evaluated for these entrainer dosages and are given in Table 4.2. Figure 4.6 presents the influence of GC3:1 amount on $\alpha_{12}$ of ACN + water azeotropic mixture. It is evident from Figure 4.6, that by incorporating GC3:1, the relative volatility of ACN to water increases and this consequence is more apparent with increasing GC3:1 concentration. As it is visible from the above experiments that GC3:1 is capable in enhancing the $\alpha_{12}$, it may eliminate the ACN + water azeotrope. The plot of relative volatility versus GC3:1 concentration (Figure 4.6) shows that, at 15 mol % GC3:1 concentration, the relative volatility $\alpha_{12}$ was 4.51. This value is 4.5 times higher than the GC3:1-free system.

**Table 4.2. Effectiveness of GC3:1 concentration on relative volatility $\alpha_{12}$ ($x_1' \approx$ 0.674) of ACN (1) + water (2) system, Relative Volatilities $\alpha_{12}$ at atmospheric pressure (101.3 kPa): GC3:1= (0 to 15.0) mol%**

| Mol% of GC3:1 | Relative volatility $(\alpha_{12})$ |
|---|---|
| 0.0 | 1.06 |
| 2.0 | 1.20 |
| 3.3 | 1.25 |
| 5.0 | 1.32 |
| 6.8 | 1.78 |
| 10.4 | 2.69 |
| 15.0 | 4.51 |

Standard uncertainty $u(mole\ \%\ of\ GC(3:1)) = 0.1$, $u(\alpha) = 0.025$.

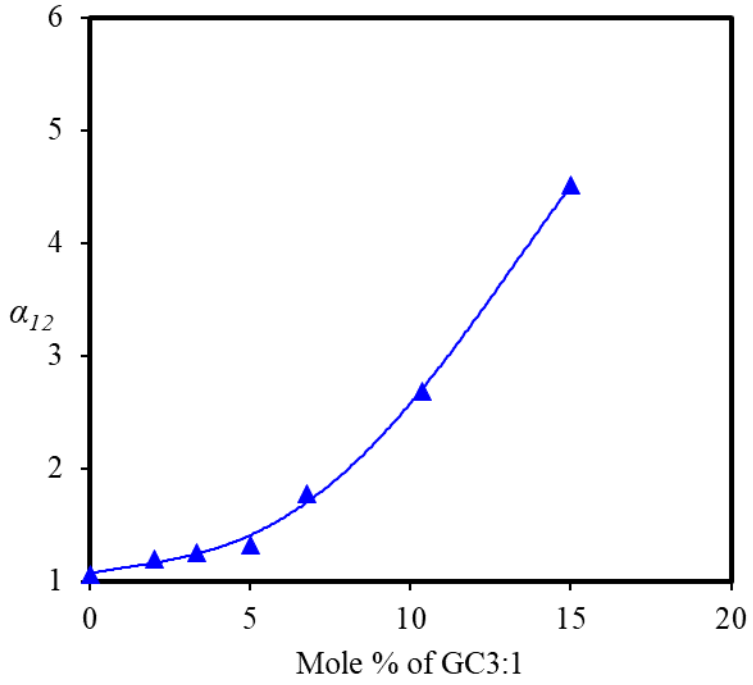


**Figure 4.6. Effect of GC3:1 concentration on the relative volatility $\alpha_{12}$ ($x_1' \approx$ 0.674) of the ACN (1) + water (2) system at 101.3 kPa**

The isobaric VLE data for the pseudo-binary systems of water (1) + GC3:1 (2) and ACN (1) + GC3:1 (2) were measured at 101.3 kPa and are presented in Table 4.3. Figure 4.7 (a), (b) represents the enhancement in normal boiling point $T_b$ of ACN and water respectively by addition of non-volatile component GC3:1. Boiling points of both were higher after addition of GC3:1. Further, experimental VLE data for both pseudo-binary systems (ACN + GC3:1 and water + GC3:1) were correlated with the NRTL model. The correlated results are plotted in Figure 4.7 and the deviation in equilibrium temperature and deviation in activity Coefficient are presented in Tables 4.3. The results represent a good correlation between experimental VLE data and predicted values by the NRTL model.

**Table 4.3. Experimental VLE data and correlated results of pseudo-binary systems (Water + GC3:1 and ACN + GC3:1), Activity Coefficient $\gamma_i$, deviation in activity Coefficient $\Delta\gamma_i$ and deviation in equilibrium temperature $\Delta T$ at 101.3 kPa**

| Water (1) + GC (3:1, mol/mol) (2) | | | | | | |
|---|---|---|---|---|---|---|
| **S. No.** | $T\,(K)$ | **Mole % of GC (3:1)** | $x_1$ | $\gamma_1^{\exp}$ | $\Delta\gamma_1^a$ | $\Delta T^b\,(K)$ |
| 1 | 373.1 | 0.00 | 1.000 | 1.000 | 0.0000 | -0.05 |
| 2 | 373.3 | 1.44 | 0.985 | 1.009 | 0.0093 | -0.26 |
| 3 | 373.5 | 2.99 | 0.969 | 1.018 | 0.0117 | -0.32 |
| 4 | 373.8 | 4.67 | 0.954 | 1.023 | 0.0101 | -0.28 |
| 5 | 374.2 | 6.49 | 0.936 | 1.027 | 0.0042 | -0.12 |
| 6 | 374.5 | 8.47 | 0.913 | 1.042 | 0.0109 | -0.30 |
| 7 | 374.9 | 10.63 | 0.893 | 1.050 | 0.0053 | -0.14 |
| 8 | 375.6 | 13.00 | 0.870 | 1.051 | 0.0021 | -0.06 |
| 9 | 376.5 | 15.61 | 0.844 | 1.050 | 0.0014 | -0.04 |
| 10 | 377.7 | 18.50 | 0.814 | 1.044 | 0.0058 | -0.16 |
| 11 | 379.3 | 21.72 | 0.784 | 1.025 | 0.0038 | -0.11 |
| 12 | 381.2 | 25.33 | 0.747 | 1.008 | 0.0091 | -0.27 |
| 13 | 383.7 | 29.39 | 0.706 | 0.980 | -0.0164 | 0.49 |
| 14 | 386.0 | 34.01 | 0.660 | 0.969 | -0.0260 | 0.80 |
| 15 | 388.0 | 39.30 | 0.608 | 0.984 | -0.0087 | 0.27 |
| ACN (1) + GC (3:1, mol/mol) (2) | | | | | | |
| S. No. | $T\,(K)$ | Mole % of GC (3:1) | $x_1$ | $\gamma_1^{\exp}$ | $\Delta\gamma_1^a$ | $\Delta T^b$ (K) |
| 1 | 354.7 | 0.00 | 1.000 | 1.000 | 0.0000 | 0.00 |
| 2 | 355.5 | 4.11 | 0.956 | 1.019 | 0.0126 | -0.41 |
| 3 | 356.7 | 8.30 | 0.916 | 1.025 | 0.0046 | -0.15 |
| 4 | 357.4 | 12.57 | 0.872 | 1.054 | 0.0117 | -0.37 |
| 5 | 358.3 | 16.92 | 0.830 | 1.077 | 0.0103 | -0.32 |
| 6 | 359.4 | 21.35 | 0.784 | 1.103 | 0.0064 | -0.19 |
| 7 | 360.7 | 25.87 | 0.740 | 1.124 | -0.0023 | 0.07 |
| 8 | 362.1 | 30.48 | 0.694 | 1.150 | -0.0078 | 0.23 |
| 9 | 363.7 | 35.19 | 0.647 | 1.177 | -0.0120 | 0.35 |

| | | | | | | |
|---|---|---|---|---|---|---|
| 10 | 365.2 | 39.99 | 0.601 | 1.212 | -0.0050 | 0.14 |
| 11 | 366.8 | 44.88 | 0.550 | 1.263 | 0.0167 | -0.46 |
| 12 | 369.9 | 49.88 | 0.501 | 1.269 | -0.0030 | 0.08 |
| 13 | 373.2 | 54.99 | 0.452 | 1.281 | -0.0132 | 0.37 |
| 14 | 376.5 | 60.20 | 0.398 | 1.328 | 0.0126 | -0.35 |

Standard uncertainty:
$u(x_1)=0.003$, $u(mole\ \%\ of\ GC(3:1))=0.1$, $u(T)=0.1K$, $u(P)=0.05kPa$, [a] $\Delta\gamma_1 = \gamma_1^{exp} - \gamma_1^{cal}$, [b] $\Delta T = T^{exp} - T^{cal}$, Superscripts "exp" and "*cal*" represents to calculated and experimental values respectively.

The isobaric VLE data for the pseudo-ternary system of ACN (1) + water (2) + GC3:1 (3) at different entrainer contents (5, 10, and 15 mol %) were experimentally measured at 101.3 kPa. Experimental data are reported in Table 4.4, where $x_1$ and $x_1^{'}$ are the mole fractions of ACN in liquid phase and the mole fraction of ACN in liquid phase expressed on GC3:1 free basis respectively, $y_1$ is the mole fraction of ACN in the vapor phase and $T$ is the equilibrium temperature. The T−x, y diagrams are plotted in Figure 4.8 to explore the salting-out effect triggered by GC3:1 at 5, 10, and 15 mol %, respectively. Nonvolatile entrainer addition (GC3:1) increases the system equilibrium temperature. The more DES, GC3:1, addition in the system, the higher the equilibrium temperature is established.

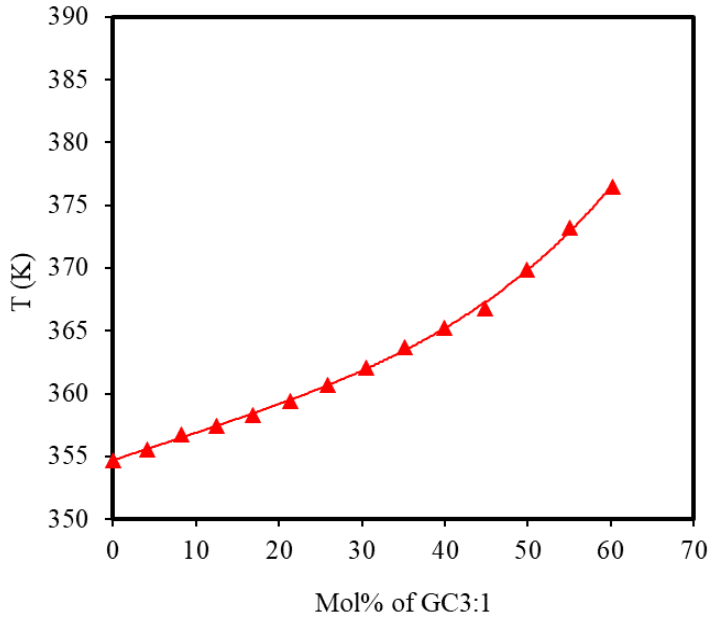


**(a)**

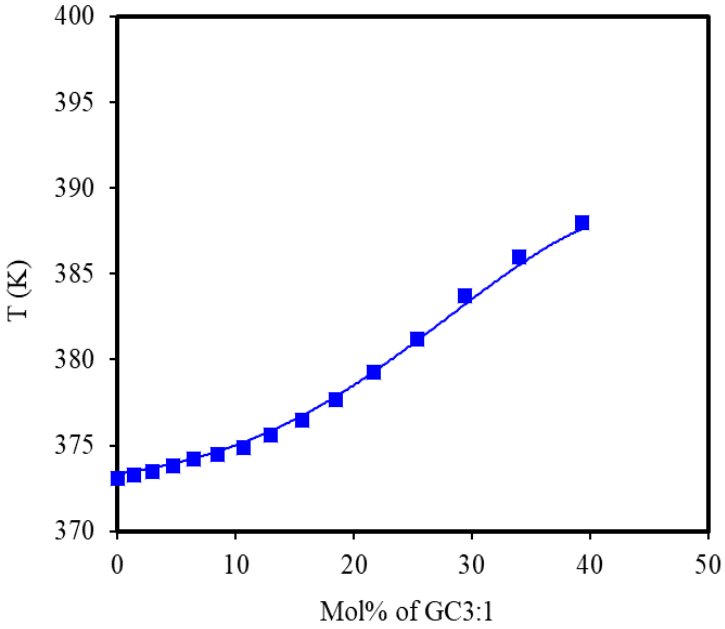


**(b)**

**Figure 4.7 (a), (b): Effect of GC3:1on the normal boiling point of ACN and water at 101.3 kPa. Experimental data for ACN (▲) and water (■) and solid lines, calculations based on NRTL model**

**Table 4.4. Experimental Isobaric VLE data for ACN (1) + water (2) + GC3:1 (3) system, experimental Activity Coefficient $\gamma_i^{exp}$ and Relative Volatilities $\alpha_{12}$ at 101.3 kPa. Presence of GC3: 1 was not observed in the vapor phase**

| S. No. | $T$ (K) | $x_1^{'}$ | $x_1$ | $x_2$ | $y_1$ | $\gamma_1^{exp}$ | $\gamma_2^{exp}$ | $\alpha_{12}$ |
|---|---|---|---|---|---|---|---|---|
| **Glycolic acid/ChCl 3:1= 5 mol%** | | | | | | | | |
| 1 | 356.0 | 1.000 | | | 1.000 | | | |
| 2 | 356.5 | 0.893 | 0.849 | 0.102 | 0.919 | 1.023 | 1.492 | 1.36 |
| 3 | 357.1 | 0.873 | 0.829 | 0.121 | 0.896 | 1.003 | 1.577 | 1.25 |
| 4 | 358.2 | 0.813 | 0.774 | 0.178 | 0.865 | 1.003 | 1.336 | 1.46 |
| 5 | 359.0 | 0.723 | 0.687 | 0.263 | 0.815 | 1.039 | 1.193 | 1.69 |
| 6 | 359.2 | 0.662 | 0.629 | 0.321 | 0.800 | 1.108 | 1.049 | 2.04 |
| 7 | 361.0 | 0.533 | 0.506 | 0.444 | 0.728 | 1.187 | 0.963 | 2.35 |
| 8 | 362.1 | 0.433 | 0.412 | 0.538 | 0.657 | 1.276 | 0.959 | 2.51 |
| 9 | 363.5 | 0.412 | 0.391 | 0.559 | 0.639 | 1.251 | 0.923 | 2.53 |
| 10 | 364.3 | 0.329 | 0.313 | 0.638 | 0.563 | 1.346 | 0.949 | 2.62 |
| 11 | 366.4 | 0.222 | 0.211 | 0.741 | 0.490 | 1.636 | 0.882 | 3.37 |
| 12 | 367.0 | 0.211 | 0.200 | 0.750 | 0.466 | 1.609 | 0.892 | 3.26 |
| 13 | 368.6 | 0.187 | 0.178 | 0.773 | 0.436 | 1.621 | 0.861 | 3.36 |
| 14 | 369.1 | 0.162 | 0.154 | 0.797 | 0.381 | 1.612 | 0.899 | 3.18 |
| 15 | 371.5 | 0.132 | 0.125 | 0.825 | 0.339 | 1.646 | 0.851 | 3.37 |
| 16 | 372.0 | 0.122 | 0.116 | 0.835 | 0.320 | 1.656 | 0.848 | 3.39 |
| 17 | 372.5 | 0.119 | 0.113 | 0.837 | 0.312 | 1.634 | 0.841 | 3.36 |
| 18 | 373.0 | 0.102 | 0.096 | 0.854 | 0.301 | 1.823 | 0.823 | 3.81 |
| 19 | 373.9 | 0.100 | 0.095 | 0.854 | 0.251 | 1.507 | 0.854 | 3.02 |
| 20 | 374.2 | 0.0876 | 0.083 | 0.867 | 0.233 | 1.581 | 0.852 | 3.16 |
| 21 | 374.8 | 0.000 | | | 0.000 | | | |
| **Glycolic acid/ChCl 3:1= 10 mol%** | | | | | | | | |
| 1 | 357.0 | 1.000 | | | 1.000 | | | |
| 2 | 357.6 | 0.912 | 0.822 | 0.079 | 0.965 | 1.074 | 0.795 | 2.65 |
| 3 | 357.6 | 0.870 | 0.784 | 0.117 | 0.947 | 1.104 | 0.820 | 2.64 |
| 4 | 358.4 | 0.821 | 0.739 | 0.161 | 0.926 | 1.119 | 0.801 | 2.72 |
| 5 | 359.1 | 0.765 | 0.689 | 0.212 | 0.901 | 1.143 | 0.789 | 2.80 |
| 6 | 359.3 | 0.693 | 0.624 | 0.276 | 0.883 | 1.230 | 0.711 | 3.34 |
| 7 | 361.7 | 0.569 | 0.512 | 0.388 | 0.812 | 1.283 | 0.742 | 3.27 |
| 8 | 362.5 | 0.496 | 0.446 | 0.454 | 0.784 | 1.387 | 0.706 | 3.69 |
| 9 | 364.0 | 0.433 | 0.390 | 0.510 | 0.734 | 1.423 | 0.730 | 3.61 |
| 10 | 364.9 | 0.390 | 0.351 | 0.550 | 0.713 | 1.494 | 0.706 | 3.89 |

| | | | | | | | | |
|---|---|---|---|---|---|---|---|---|
| 11 | 366.3 | 0.354 | 0.319 | 0.581 | 0.680 | 1.508 | 0.707 | 3.88 |
| 12 | 366.9 | 0.327 | 0.294 | 0.605 | 0.638 | 1.507 | 0.752 | 3.63 |
| 13 | 367.8 | 0.294 | 0.264 | 0.635 | 0.609 | 1.558 | 0.748 | 3.74 |
| 14 | 371.0 | 0.214 | 0.192 | 0.708 | 0.512 | 1.645 | 0.745 | 3.86 |
| 15 | 372.0 | 0.200 | 0.180 | 0.720 | 0.508 | 1.663 | 0.727 | 3.97 |
| 16 | 372.8 | 0.182 | 0.164 | 0.735 | 0.452 | 1.620 | 0.754 | 3.70 |
| 17 | 373.5 | 0.165 | 0.149 | 0.751 | 0.442 | 1.644 | 0.756 | 3.73 |
| 18 | 374.0 | 0.158 | 0.142 | 0.758 | 0.428 | 1.632 | 0.758 | 3.68 |
| 19 | 374.1 | 0.138 | 0.124 | 0.776 | 0.385 | 1.753 | 0.767 | 3.90 |
| 20 | 374.2 | 0.119 | 0.107 | 0.792 | 0.341 | 1.904 | 0.777 | 4.18 |
| 21 | 374.8 | 0.088 | 0.079 | 0.822 | 0.261 | 2.098 | 0.805 | 4.42 |
| 22 | 375.5 | 0.000 | | | 0.000 | | | |
| **Glycolic acid/ChCl 3:1= 15 mol%** | | | | | | | | |
| 1 | 358.3 | 1.000 | | | 1.000 | | | |
| 2 | 358.3 | 0.932 | 0.792 | 0.058 | 0.985 | 1.113 | 0.453 | 4.79 |
| 3 | 358.5 | 0.867 | 0.737 | 0.113 | 0.967 | 1.167 | 0.505 | 4.50 |
| 4 | 358.7 | 0.824 | 0.700 | 0.150 | 0.949 | 1.199 | 0.584 | 3.99 |
| 5 | 359.2 | 0.765 | 0.650 | 0.200 | 0.926 | 1.241 | 0.623 | 3.85 |
| 6 | 359.4 | 0.702 | 0.597 | 0.253 | 0.912 | 1.324 | 0.581 | 4.40 |
| 7 | 364.3 | 0.456 | 0.388 | 0.463 | 0.812 | 1.565 | 0.564 | 5.14 |
| 8 | 368.3 | 0.312 | 0.265 | 0.584 | 0.703 | 1.768 | 0.606 | 5.22 |
| 9 | 370.4 | 0.271 | 0.230 | 0.619 | 0.643 | 1.755 | 0.637 | 4.84 |
| 10 | 370.9 | 0.267 | 0.227 | 0.624 | 0.641 | 1.746 | 0.624 | 4.90 |
| 11 | 371.1 | 0.234 | 0.199 | 0.652 | 0.605 | 1.871 | 0.653 | 5.01 |
| 12 | 372.1 | 0.221 | 0.188 | 0.663 | 0.581 | 1.849 | 0.657 | 4.88 |
| 13 | 373.2 | 0.199 | 0.169 | 0.681 | 0.552 | 1.900 | 0.656 | 4.98 |
| 14 | 373.8 | 0.187 | 0.159 | 0.691 | 0.533 | 1.909 | 0.661 | 4.94 |
| 15 | 374.0 | 0.176 | 0.150 | 0.700 | 0.526 | 1.990 | 0.657 | 5.17 |
| 16 | 374.5 | 0.154 | 0.132 | 0.718 | 0.471 | 1.997 | 0.702 | 4.84 |
| 17 | 374.8 | 0.143 | 0.122 | 0.728 | 0.433 | 1.976 | 0.734 | 4.57 |
| 18 | 375.6 | 0.101 | 0.086 | 0.764 | 0.310 | 1.958 | 0.827 | 3.99 |
| 19 | 376.1 | 0.068 | 0.057 | 0.794 | 0.231 | 2.155 | 0.873 | 4.15 |
| 20 | 376.6 | 0.000 | | | 0.000 | | | |

Standard uncertainty $u(x_1)=u(x_1')=u(y)=0.003, u(T)=0.1K, u(mole\ \%\ of\ GC(3:1))=0.1,$ $u(\alpha)=0.025$.

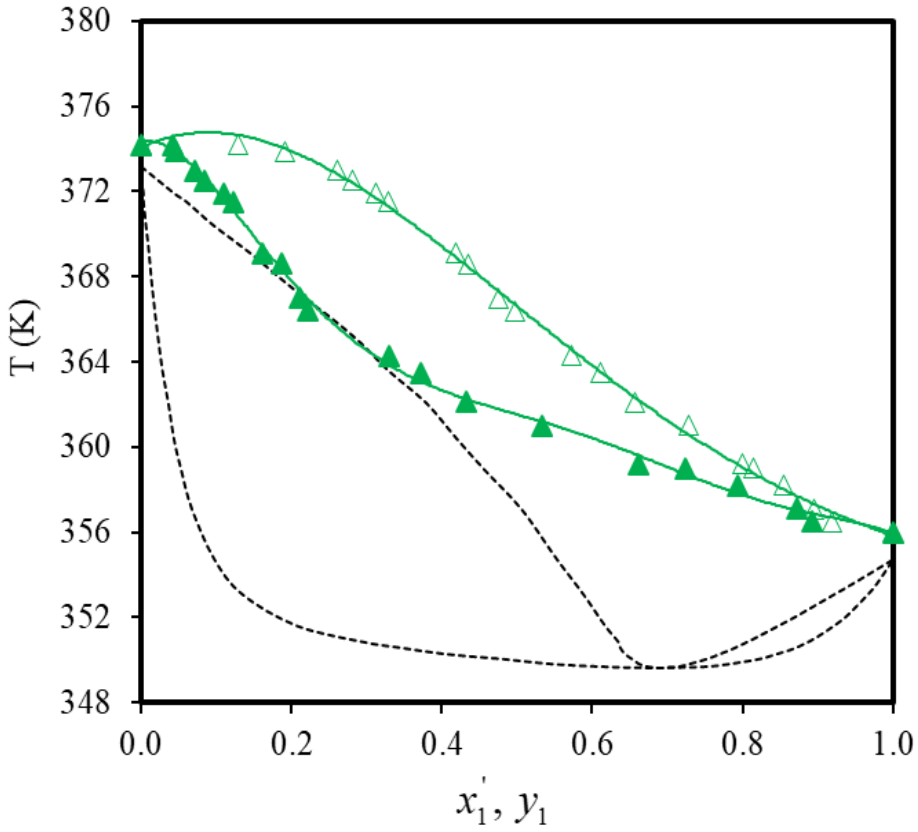


**Figure 4.8 (a): Temperature−composition diagram for the acetonitrile (1) + water (2) + GC3:1 (3) system at 101.3 kPa with GC3:1= 5 mol%. $x_1'$ vs T (▲) and $y_1$ vs T (Δ), --- GC3:1= 0 %.**

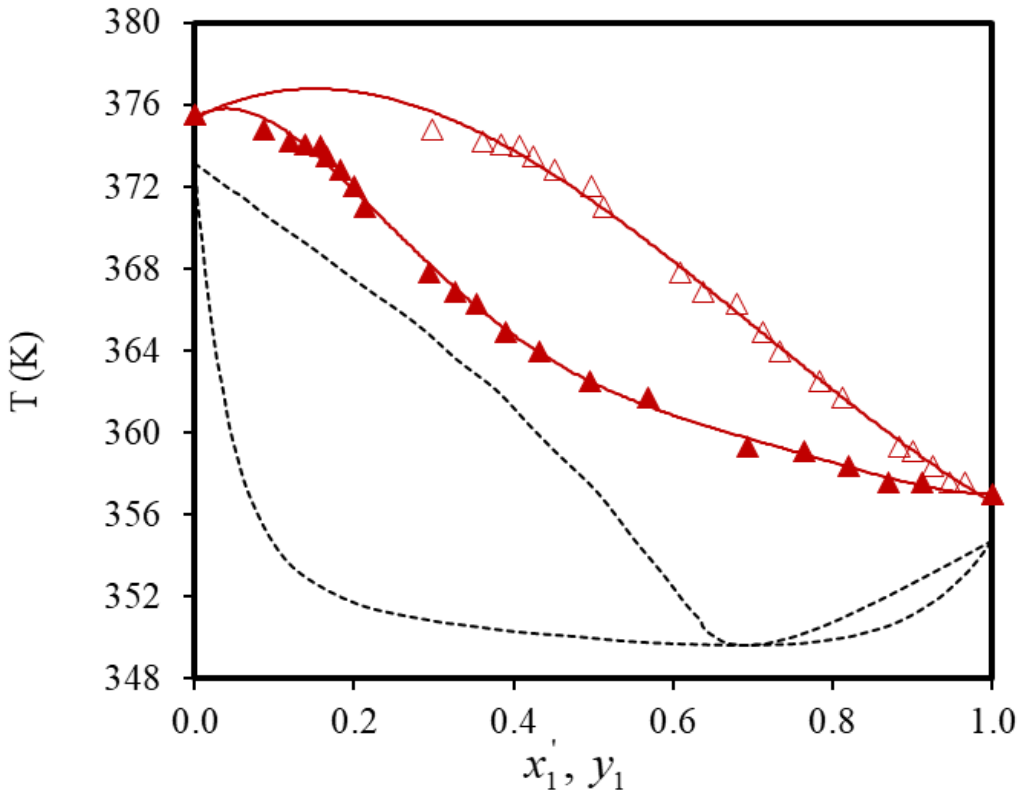


**Figure 4.8. (b): Temperature−composition diagram for the acetonitrile (1) + water (2) + GC (3:1) (3) system at 101.3 kPa with GC3:1= 10 mol%. $x_1'$ vs T (▲) and $y_1$ vs T (Δ), --- GC3:1= 0%.**

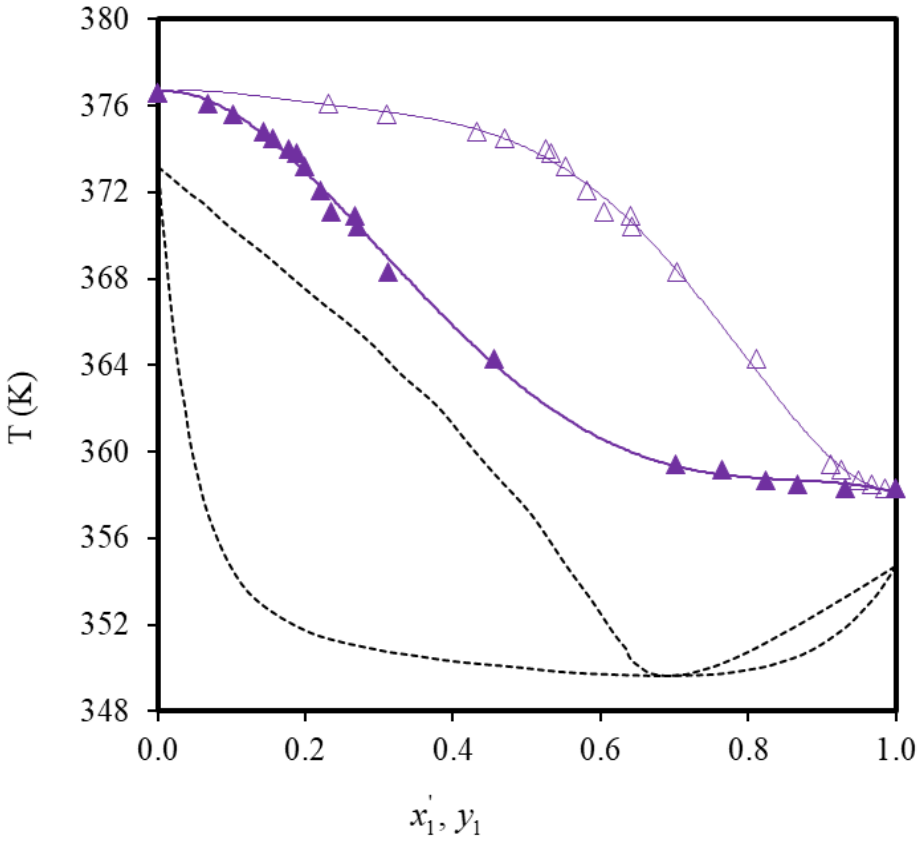


**Figure 4.8. (c): Temperature−composition diagram for the acetonitrile (1) + water (2) + GC (3:1) (3) system at 101.3 kPa with GC3:1= 15 mol%. $x_1'$ vs T (▲) and $y_1$ vs T (Δ), --- GC3:1= 0%**

The x−y diagrams for the above experimental conditions are also represented by Figure 4.9. At the azeotropic point, the relative volatility for the ACN + water system is unity, and to destroy the azeotrope, the relative volatility should be greater than 1. We can see from Table 4.4 that GC3:1 is fairly effective to increase the relative volatility of the ACN + water system to greater than 1 in the entire concentration range. The azeotrope of the ACN + water binary mixture disappears at the lowest GC3:1 content (5 mol %).

Pseudo-ternary VLE data for ACN + water + GC3:1 system was also fitted to the NRTL model. Due to DES possessing a high viscosity, the NRTL model parameters calculated from pseudo-binary systems cannot be applied for accurate prediction of the VLE behavior of Pseudo-ternary (ACN + water + GC3:1) system (Rodriguez et al., 2015, Rodriguez et al., 2015). Therefore, the NRTL model was used directly for correlation of ternary system VLE data, and the estimated results of average difference in equilibrium temperature and ACN mole fraction in vapor phase are presented in Table 4.5 and shown in Figure 4.9. The estimated values of average difference in equilibrium temperature and ACN mole fraction in vapor phase were found to be 0.009 and 0.42 K, respectively. This indicates that the NRTL model can be used for prediction of VLE data for GC3:1 containing system.

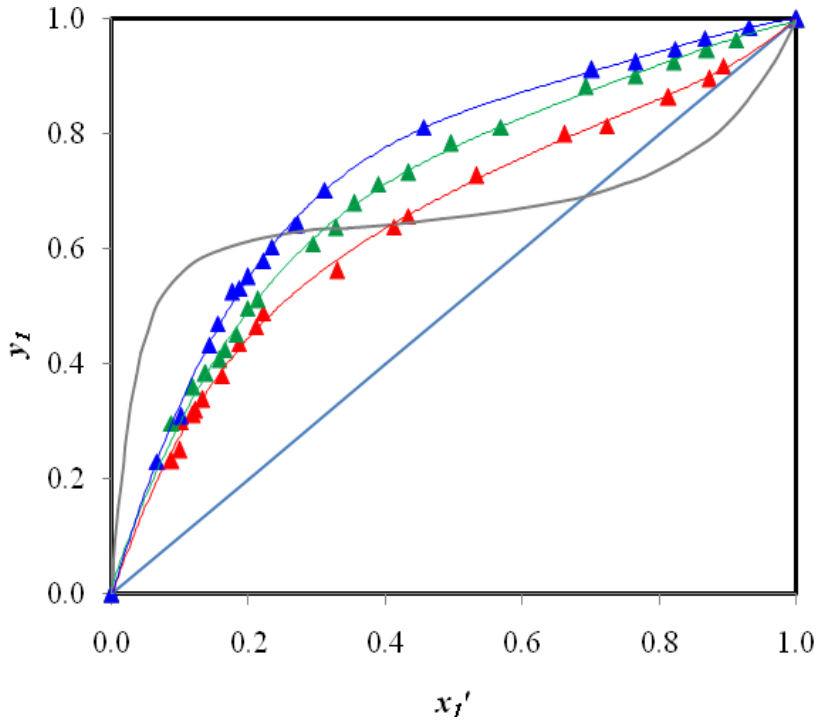


**Figure 4.9. Experimental and calculated VLE data for ACN (1) + water (2) + GC3:1 (3) pseudo-ternary system at 101.3 kPa. For GC3:1= 5 mol% (▲), for GC3:1= 10 mol% (▲), for GC3:1= 15 mol% (▲), and solid lines, calculations based on the NRTL model**

**Table 4.5. The parameters and correlation deviations of NRTL model for GC3:1 containing systems at 101.3 kPa**

| Systems | $\Delta g_{12}$ | $\Delta g_{21}$ | $\alpha$ | $DT(K)$ | $dT(K)$ | $Dy_1$ | $dy_1$ |
|---|---|---|---|---|---|---|---|
| ACN (1) + GC3:1 (2) | 7382.1 | -3247.6 | 0.3 | 0.25 | 0.46 | | |
| Water (1) + GC3:1 (2) | -930.9 | 835.4 | 0.3 | 0.24 | 0.79 | | |
| ACN (1) + water (2) + GC3:1 (3) | 3587 | -542.3 | 0.3 | 0.42 | 0.98 | 0.0093 | 0.016 |

$\Delta g_{12} = (g_{12}-g_{22})$; $\Delta g_{21} = (g_{21}-g_{11})$

$$DT = (1/n)\sum_{k=1}^{n}\left|T^{\exp} - T^{cal}\right|_k$$

$$dT = \max\left(\left|T^{\exp} - T^{cal}\right|\right)$$

$$Dy_1 = (1/n)\sum_{k=1}^{n}\left|y_1^{\exp} - y_1^{cal}\right|_k$$

$$dy_1 = \max\left(\left|y_1^{\exp} - y_1^{cal}\right|\right)$$

#### 4.1.1.3 Recoverability Test of GC3:1

In order to evaluate the recoverability of the used GC3:1 as an entrainer, an aqueous solution of about 5% (mol/mol) was prepared for GC3:1, and in a subsequent process, it underwent boiling for 2 h in a rota evaporator. After each run, the entrainer was recovered by evaporating the water in a vessel and was reused for the subsequent run. Recovered GC3:1 was vacuum-dried, and the FT-IR spectrum was then obtained. The FT-IR spectrum of recovered GC3:1 is given in Figure 4.10. While comparing the spectra of freshly prepared and recovered GC3:1, no significant change is observed. Hence recovered GC3:1 can be reused for distillation as its chemical properties are stable.

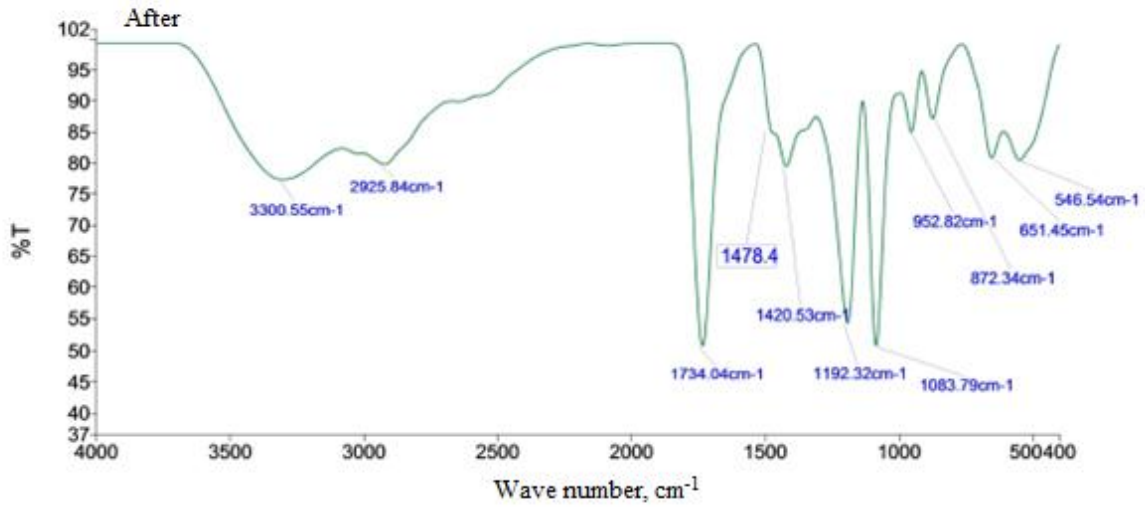


**Figure 4.10. Typical FTIR spectrum of GC3:1 after use**

### 4.1.2 Glycolic Acid and Tetramethylammonium Chloride 3:1 (GTM3:1)

Ammonium-based deep eutectic solvent, GTM3:1 (glycolic acid–TMAC in 3:1 molar ratio) was synthesized and investigated for its effectiveness as entrainer for separation of ACN + water azeotropic mixture via extractive distillation.

#### 4.1.2.1 Characterization of Synthesized GTM3:1

Prior to its application, synthesized GTM3:1 was characterized by different analytical techniques. Thermo gravimetric analysis of GTM3:1 was performed to verify its thermal stability using PerkinElmer, STA6000 TGA analyzer (Figure 4.11). Good thermal stability of GTM3:1 enables its use as entrainer for extractive distillation of ACN + water mixture.

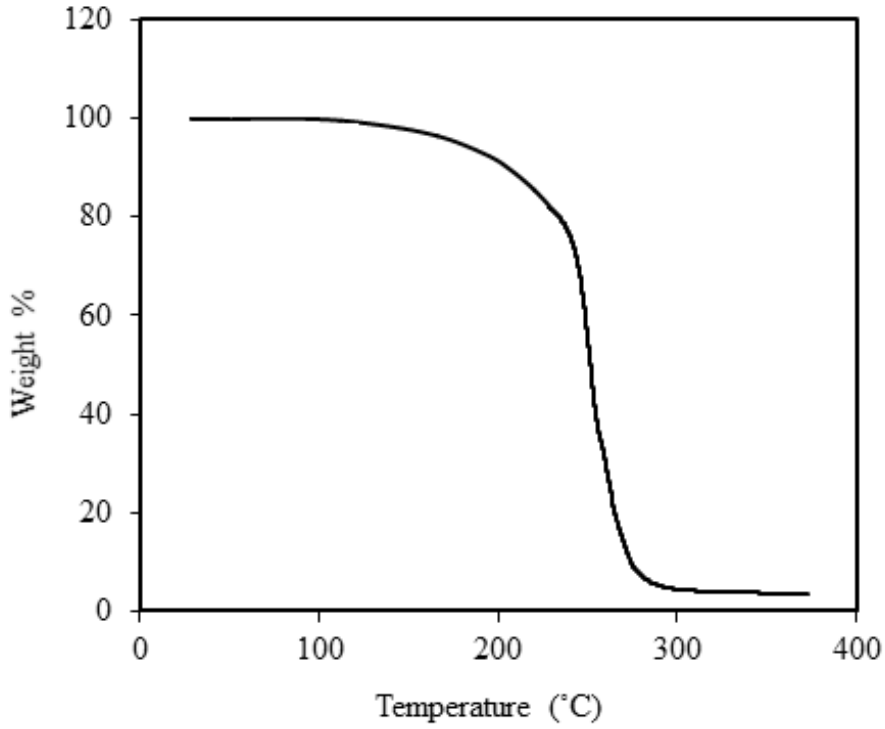


**Figure 4.11. TGA for GTM3:1 from room temperature to 400 ˚C at atmospheric pressure**

FT-IR analysis (PerkinElmer) of prepared GTM3:1 was also conducted, and its spectra are represented in Figure 4.12. In the FT-IR spectra, a sharp and high intensity peak at 1731 $cm^{-1}$ with comparatively narrower band at 1194 and 1085 $cm^{-1}$ can be observed at the lower wave number side of the FT-IR spectra. The peak at 1731 $cm^{-1}$ can be allocated to the free carbonyl group stretching of glycolic acid. The C-N stretching in the Tetramethylammonium chloride (TMAC) and hydrogen bond between OH group and $Cl^-$ of glycolic acid and TMAC, respectively, is represented by the peaks at 1194-1085 $cm^{-1}$. A broad band in the middle of 3100-3700 $cm^{-1}$, with peak at 3303 $cm^{-1}$ demonstrates the existence of both free and hydrogen bonded OH groups of glycolic acid–glycolic acid molecules. Because of formation of hydrogen bond between the glycolic acid and TMAC, freezing point of the mixture decreases which results the formation of DES.

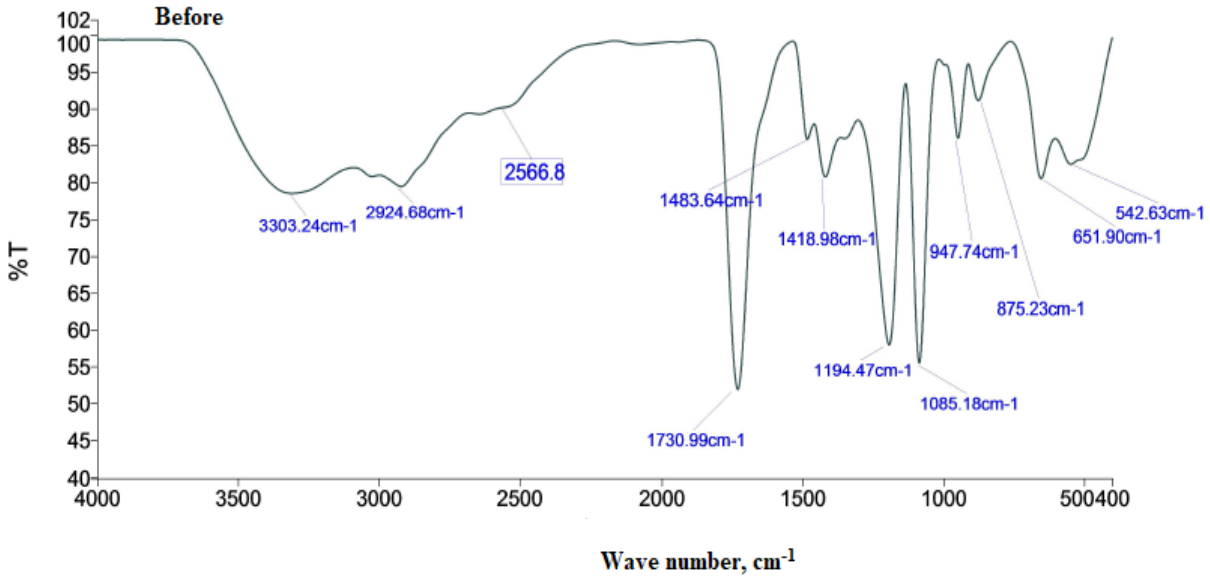


**Figure 4.12. Typical FT-IR spectra for GTM3:1**

The hydrogen bonding between glycolic acid and TMAC was proposed based on this study and is shown in Figure 4.13. The formula unit of synthesized GTM3:1 is $(C_4H_{12}NO)^+$ $Cl^-$ .3($CH_2OH$).COOH. The optimized structure studied by Gaussian 16 software is presented in Figure 4.14. $^1H$ NMR spectra of GTM3:1 was also determined and is given in Figure 4.15.

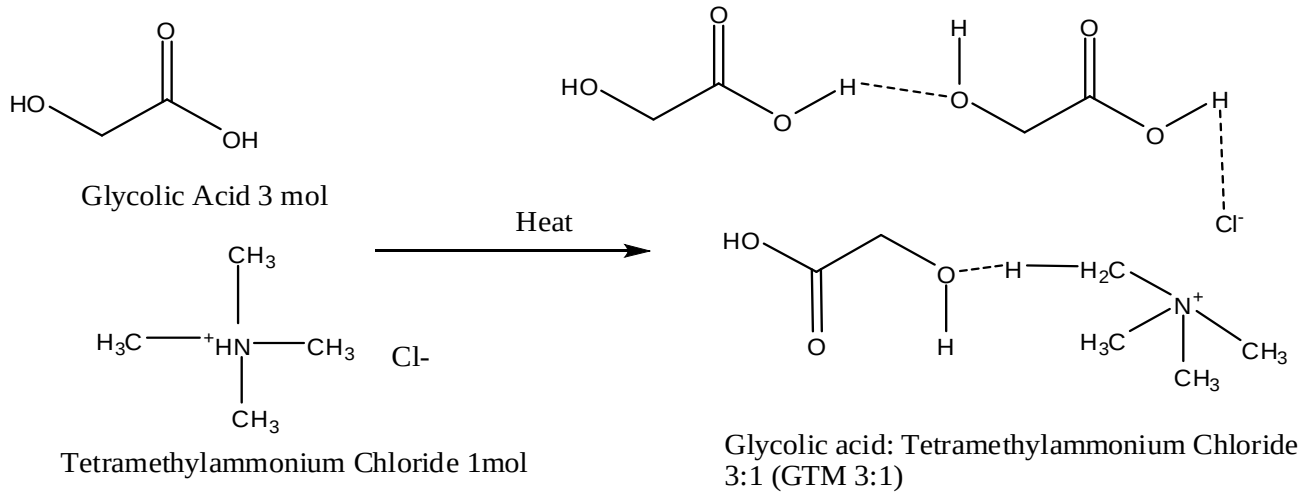


**Figure 4.13. Hydrogen Bonding Mechanism of GTM3:1**

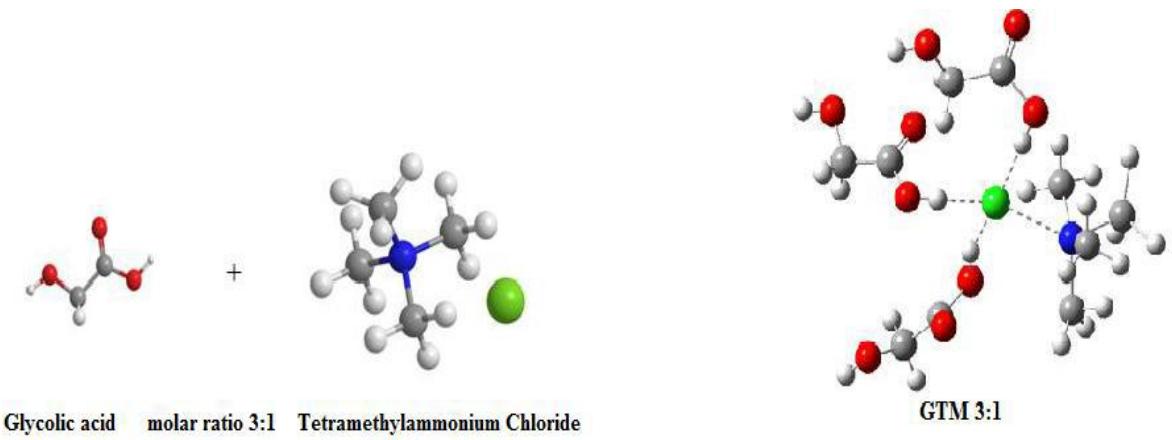


**Figure 4.14. Optimized Structure of GTM3:1**

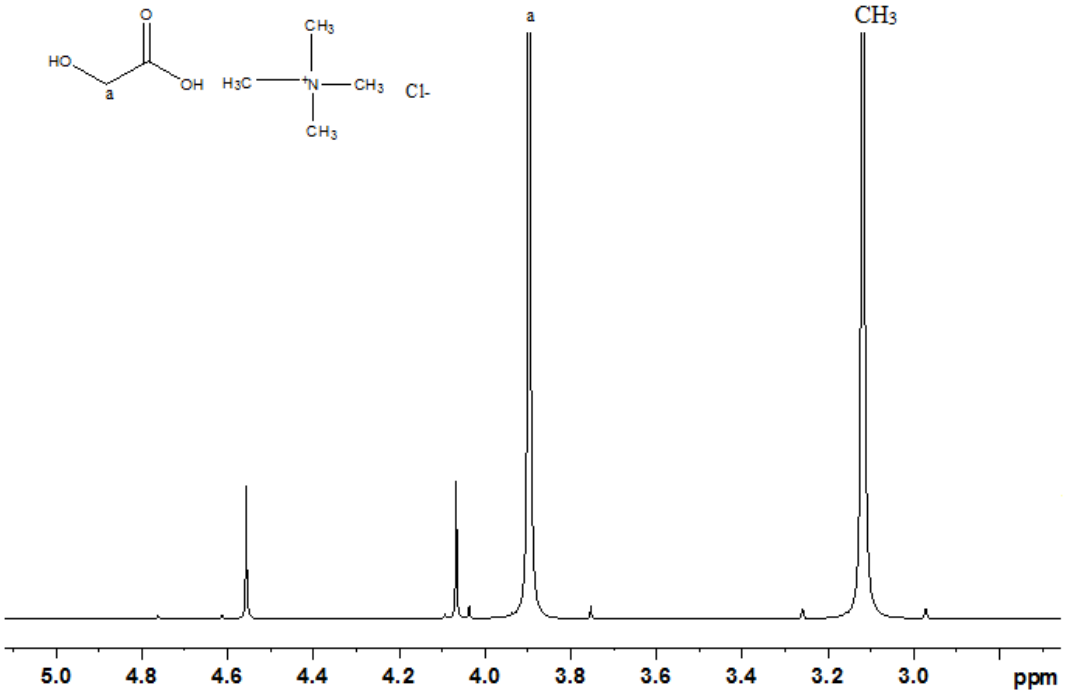


**Figure 4.15. $^{1}$H NMR spectra of GTM3:1**

GTM3:1 was also characterized for its physical properties (viscosity, moisture content, and density) following the method given in section 3.2.2 of chapter 3 and same are reported in Table 4.6.

**Table 4.6. Physical Properties of GTM3:1**

| **Properties** | **Value** |
|---|---|
| Density (ρ) | 1.281 g/cm$^3$ |
| Viscosity (μ) | 387.54 mPa/s |
| Moisture Content | 0.34 wt% |

**4.1.2.2. Vapor–liquid equilibrium (VLE) measurements using GTM3:1 as entrainer**

The ability of GTM3:1 to increase the relative volatility $\alpha_{12}$ of azeotropic mixture of ACN + water has been studied. For this purpose, experiments were performed in near azeotrope composition ($x_1' \approx 0.674$) of ACN + water mixture in the presence of GTM3:1 and relative volatilities were evaluated. Results for different molar compositions of GTM3:1 (0 to17.7 mol%) are presented in Table 4.7 and are depicted in Figure 4.16. The relative volatility of ACN to water enhances with the concentration of GTM3:1 in the liquid phase. The more GTM3:1, the greater the relative volatility of ACN to water, which means, the easier the separation. At 17.7 mol% of GTM3:1, the value of $\alpha_{12}$ were 5.31, which are 5.31 times than for the GTM3:1 free system.

**Table 4.7. Effect of GTM3:1 concentration on relative volatility $\alpha_{12}$ ($x_1' \approx 0.674$) of ACN (1) + water (2) system, Relative volatilities $\alpha_{12}$ at atmospheric pressure (101.3 kPa):GTM3:1= (0 to 17.7) mol%**

| Mol% of GTM3:1 | Relative volatility $(\alpha_{12})$ |
|---|---|
| 0.0 | 1.06 |
| 2.0 | 1.26 |
| 3.3 | 1.47 |
| 6.7 | 1.87 |
| 10.2 | 2.68 |
| 13.9 | 3.99 |
| 17.7 | 5.31 |

Standard uncertainty $u(mole\ \%\ of\ GTM(3:1)) = 0.1$, $u(\alpha) = 0.025$.

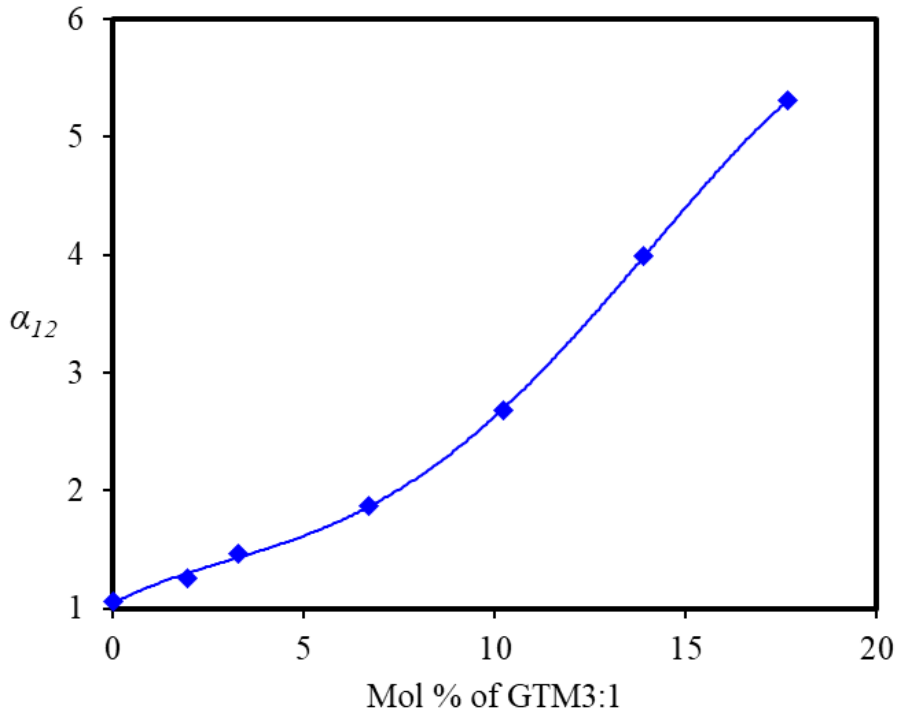


**Figure 4.16. Effect of GTM3:1 concentration on the relative volatility $\alpha_{12}$ ($x_1' \approx$ 0.674) of the ACN (1) + water (2) system at 101.3 kPa**

The isobaric VLE data for pseudo-binary systems of ACN (1) + GTM3:1(2) and water (1) + GTM3:1(2) were measured at 101.3 kPa and the experimental data are given in Table 4.8. The increment in boiling point $T_b$ of ACN and water due to inclusion of non-volatile GTM3:1 is represented in Figure 4.17. Boiling points of ACN and water both were higher after addition of GTM3:1.

**Table 4.8. Experimental VLE data and correlated results of pseudo-binary systems (Water + GTM3:1 and ACN + GTM3:1), Activity Coefficient $\gamma_i$, deviation in activity Coefficient $\Delta\gamma_i$ and deviation in equilibrium temperature $\Delta T$ at 101.3 kPa**

| **Water (1) + GTM (3:1, mol/mol) (2)** | | | | | | |
|---|---|---|---|---|---|---|
| **S.No.** | $T\,(K)$ | **Mole % of GTM (3:1)** | $x_1$ | $\gamma_1^{\exp}$ | $\Delta\gamma_1^a$ | $\Delta T^b\,(K)$ |
| 1 | 373.1 | 0.00 | 1.000 | 1.002 | 0.002 | 0.003 |
| 2 | 373.3 | 1.42 | 0.987 | 1.007 | 0.008 | -0.174 |
| 3 | 373.7 | 2.95 | 0.970 | 1.010 | 0.014 | -0.346 |
| 4 | 374.2 | 4.60 | 0.954 | 1.008 | 0.018 | -0.453 |
| 5 | 374.9 | 6.39 | 0.934 | 1.004 | 0.023 | -0.617 |
| 6 | 376.1 | 8.35 | 0.918 | 0.979 | 0.008 | -0.182 |
| 7 | 377.4 | 10.48 | 0.892 | 0.963 | 0.010 | -0.242 |
| 8 | 378.7 | 12.83 | 0.870 | 0.943 | 0.008 | -0.186 |
| 9 | 380.2 | 15.41 | 0.845 | 0.922 | 0.009 | -0.223 |
| 10 | 382.2 | 18.27 | 0.817 | 0.890 | 0.003 | -0.056 |
| 11 | 384.5 | 21.46 | 0.787 | 0.855 | -0.002 | 0.118 |
| 12 | 387.6 | 25.03 | 0.753 | 0.807 | -0.017 | 0.670 |
| 13 | 390.9 | 29.07 | 0.707 | 0.772 | -0.005 | 0.245 |
| 14 | 394.5 | 33.66 | 0.665 | 0.730 | -0.005 | 0.274 |
| 15 | 398.8 | 38.93 | 0.612 | 0.693 | 0.009 | -0.366 |
| **ACN (1) + GTM (3:1, mol/mol) (2)** | | | | | | |
| **S.No.** | $T\,(K)$ | **Mole % of GTM (3:1)** | $x_1$ | $\gamma_1^{\exp}$ | $\Delta\gamma_1^a$ | $\Delta T^b$ **(K)** |
| 1 | 354.7 | 0.00 | 1.000 | 0.999 | -0.001 | 0.070 |
| 2 | 355.5 | 4.05 | 0.959 | 1.016 | 0.013 | -0.374 |
| 3 | 356.5 | 8.18 | 0.916 | 1.031 | 0.022 | -0.645 |
| 4 | 357.8 | 12.40 | 0.878 | 1.034 | 0.016 | -0.450 |
| 5 | 359.2 | 16.70 | 0.833 | 1.045 | 0.013 | -0.380 |
| 6 | 360.8 | 21.09 | 0.787 | 1.054 | 0.008 | -0.205 |
| 7 | 362.6 | 25.58 | 0.745 | 1.056 | -0.005 | 0.199 |
| 8 | 364.5 | 30.16 | 0.696 | 1.068 | -0.008 | 0.321 |

| | | | | | | |
|---|---|---|---|---|---|---|
| 9 | 366.5 | 34.84 | 0.651 | 1.078 | -0.014 | 0.506 |
| 10 | 368.6 | 39.62 | 0.606 | 1.090 | -0.017 | 0.582 |
| 11 | 370.7 | 44.50 | 0.553 | 1.124 | 0.001 | 0.010 |
| 12 | 372.9 | 49.50 | 0.505 | 1.157 | 0.021 | -0.605 |
| 13 | 376.2 | 54.60 | 0.457 | 1.162 | 0.013 | -0.364 |
| 14 | 381.4 | 59.83 | 0.401 | 1.149 | -0.012 | 0.440 |

Standard uncertainty $u(x_1)=0.003, u(T)=0.1K, u(mole\ \%\ of\ GTM(3:1))=0.1,$ $u(P)=0.05kPa.$, [a] $\Delta\gamma_1 = \gamma_1^{\exp} - \gamma_1^{cal}$, [b] $\Delta T = T^{\exp} - T^{cal}$

VLE Measurements were made for ACN (1) + water (2) + GTM3:1 (3) pseudo-ternary system at atmospheric pressure, by keeping the DES concentration fix for every group of experimentation. The isobaric VLE data for different DES mole percent (5%, 10%, and 15%) are given in Table 4.9. Where $T$ is the equilibrium temperature, $x_1$ is the mole fraction of ACN in liquid phase, $x_1'$ is the mole fraction of ACN in liquid phase expressed on GTM3:1 free basis and $y_1$ is the mole fraction of ACN in the vapor phase. To describe the salting-out effect caused by addition of GTM3:1, the $T-x,y$ data are depicted in Figures 4.18 (a), (b) and (c) for 5, 10 and 15 mol% concentrations respectively. The equilibrium temperature of system increases, due to the addition of the GTM3:1.

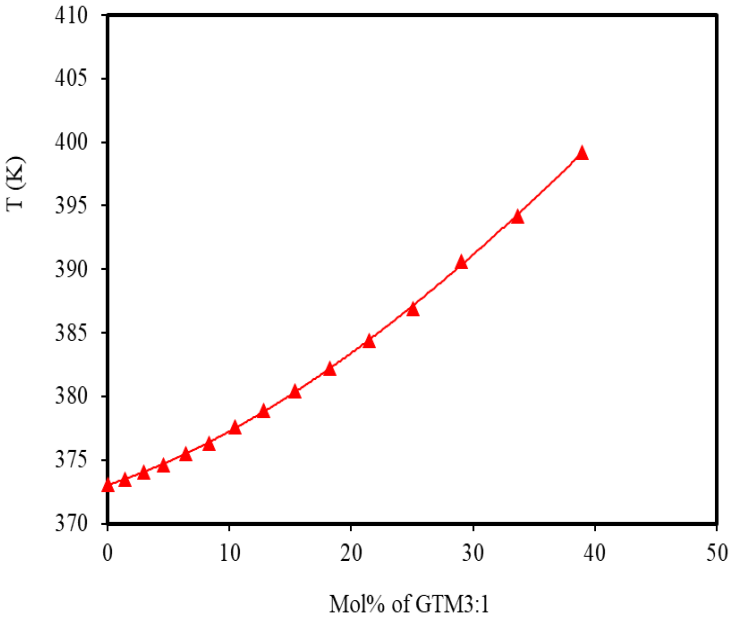


**(a)**

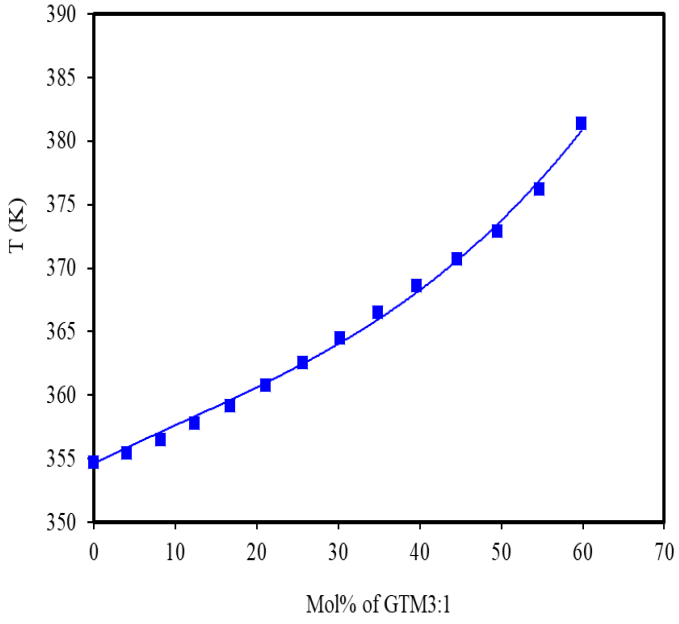


**(b)**

**Figure 4.17 (a), (b): Effect of GTM3:1on the normal boiling point of ACN and water at 101.3 kPa. Experimental data for ACN (▲) and water (■) and solid lines, calculations based on NRTL model**

**Table 4.9. Experimental Isobaric VLE data for ACN (1) + water (2) + GTM3:1 (3) system, experimental Activity Coefficient $\gamma_1^{exp}$ and Relative Volatilities $\alpha_{12}$ at 101.3 kPa. Presence of GTM3: 1 was not detected in the vapor phase**

| S.No. | *T* (K) | $x_1^{'}$ | $x_1$ | $x_2$ | $y_1$ | $\gamma_1^{exp}$ | $\gamma_2^{exp}$ | $\alpha_{12}$ |
|---|---|---|---|---|---|---|---|---|
| **Glycolic acid/TMAC 3:1= 5 mol%** | | | | | | | | |
| 1 | 357.3 | 1.000 | | | 1.000 | | | |
| 2 | 357.3 | 0.901 | 0.856 | 0.094 | 0.951 | 1.025 | 0.946 | 2.13 |
| 3 | 357.4 | 0.842 | 0.800 | 0.150 | 0.914 | 1.051 | 1.036 | 1.99 |
| 4 | 357.5 | 0.806 | 0.765 | 0.185 | 0.876 | 1.050 | 1.210 | 1.70 |
| 5 | 357.9 | 0.757 | 0.720 | 0.231 | 0.849 | 1.069 | 1.158 | 1.80 |
| 6 | 358.3 | 0.709 | 0.675 | 0.277 | 0.828 | 1.098 | 1.083 | 1.98 |
| 7 | 358.4 | 0.689 | 0.655 | 0.296 | 0.812 | 1.106 | 1.104 | 1.95 |
| 8 | 359.6 | 0.658 | 0.625 | 0.325 | 0.782 | 1.077 | 1.114 | 1.86 |
| 9 | 360.1 | 0.601 | 0.571 | 0.379 | 0.755 | 1.121 | 1.052 | 2.05 |
| 10 | 361.2 | 0.543 | 0.515 | 0.434 | 0.717 | 1.143 | 1.016 | 2.14 |
| 11 | 363.8 | 0.413 | 0.392 | 0.557 | 0.647 | 1.253 | 0.895 | 2.60 |
| 12 | 365.3 | 0.392 | 0.372 | 0.576 | 0.624 | 1.221 | 0.871 | 2.57 |
| 13 | 365.9 | 0.347 | 0.330 | 0.620 | 0.599 | 1.298 | 0.844 | 2.81 |
| 14 | 367.3 | 0.316 | 0.300 | 0.650 | 0.580 | 1.326 | 0.800 | 2.99 |
| 15 | 368.2 | 0.291 | 0.277 | 0.674 | 0.563 | 1.361 | 0.776 | 3.14 |
| 16 | 369.6 | 0.267 | 0.253 | 0.697 | 0.558 | 1.416 | 0.721 | 3.47 |
| 17 | 370.5 | 0.248 | 0.236 | 0.715 | 0.530 | 1.408 | 0.723 | 3.42 |
| 18 | 372.1 | 0.202 | 0.192 | 0.758 | 0.484 | 1.511 | 0.706 | 3.71 |
| 19 | 374.2 | 0.177 | 0.168 | 0.783 | 0.453 | 1.521 | 0.673 | 3.86 |
| 20 | 376.4 | 0.138 | 0.131 | 0.820 | 0.387 | 1.569 | 0.666 | 3.95 |
| 21 | 377.2 | 0.110 | 0.105 | 0.846 | 0.340 | 1.690 | 0.677 | 4.16 |
| 22 | 378.3 | 0.086 | 0.082 | 0.868 | 0.285 | 1.759 | 0.687 | 4.23 |
| 23 | 379.8 | 0.000 | | | 0.000 | | | |
| **Glycolic acid/TMAC 3:1= 10 mol%** | | | | | | | | |
| 1 | 359.2 | 1.000 | | | 1.000 | | | |
| 2 | 359.2 | 0.879 | 0.791 | 0.109 | 0.977 | 1.076 | 0.356 | 5.85 |
| 3 | 359.3 | 0.838 | 0.755 | 0.146 | 0.943 | 1.085 | 0.655 | 3.20 |
| 4 | 359.4 | 0.829 | 0.754 | 0.156 | 0.932 | 1.070 | 0.729 | 2.83 |
| 5 | 359.9 | 0.786 | 0.707 | 0.193 | 0.908 | 1.095 | 0.782 | 2.69 |
| 6 | 360.2 | 0.754 | 0.679 | 0.221 | 0.893 | 1.112 | 0.783 | 2.72 |
| 7 | 361.1 | 0.738 | 0.664 | 0.236 | 0.883 | 1.094 | 0.777 | 2.68 |
| 8 | 361.9 | 0.713 | 0.644 | 0.259 | 0.872 | 1.089 | 0.748 | 2.75 |

| | | | | | | | | |
|---|---|---|---|---|---|---|---|---|
| 9 | 362.4 | 0.671 | 0.605 | 0.296 | 0.853 | 1.117 | 0.740 | 2.84 |
| 10 | 364.1 | 0.627 | 0.567 | 0.337 | 0.821 | 1.091 | 0.741 | 2.73 |
| 11 | 365.7 | 0.559 | 0.503 | 0.397 | 0.803 | 1.147 | 0.652 | 3.22 |
| 12 | 368.7 | 0.465 | 0.419 | 0.481 | 0.734 | 1.156 | 0.649 | 3.18 |
| 13 | 370.2 | 0.419 | 0.378 | 0.524 | 0.711 | 1.189 | 0.614 | 3.41 |
| 14 | 372.3 | 0.329 | 0.297 | 0.606 | 0.651 | 1.304 | 0.593 | 3.80 |
| 15 | 373.1 | 0.286 | 0.257 | 0.643 | 0.623 | 1.409 | 0.588 | 4.13 |
| 16 | 375.4 | 0.230 | 0.207 | 0.693 | 0.580 | 1.529 | 0.560 | 4.62 |
| 17 | 375.8 | 0.217 | 0.195 | 0.705 | 0.562 | 1.554 | 0.565 | 4.63 |
| 18 | 376.2 | 0.195 | 0.176 | 0.725 | 0.539 | 1.641 | 0.571 | 4.83 |
| 19 | 377.2 | 0.175 | 0.159 | 0.751 | 0.493 | 1.610 | 0.585 | 4.58 |
| 20 | 378.1 | 0.140 | 0.126 | 0.774 | 0.431 | 1.735 | 0.617 | 4.65 |
| 21 | 378.9 | 0.097 | 0.087 | 0.815 | 0.350 | 1.989 | 0.651 | 5.02 |
| 22 | 380.4 | 0.045 | 0.041 | 0.860 | 0.185 | 2.185 | 0.735 | 4.83 |
| 23 | 381.4 | 0.000 | | | 0.000 | | | |
| **Glycolic acid/TMAC 3:1= 15 mol%** | | | | | | | | |
| 1 | 361.1 | 1.000 | | | 1.000 | | | |
| 2 | 361.1 | 0.856 | 0.728 | 0.122 | 0.989 | 1.119 | 0.141 | 15.12 |
| 3 | 361.9 | 0.829 | 0.705 | 0.146 | 0.977 | 1.113 | 0.240 | 8.76 |
| 4 | 362.5 | 0.811 | 0.690 | 0.161 | 0.973 | 1.113 | 0.249 | 8.40 |
| 5 | 363.4 | 0.781 | 0.665 | 0.187 | 0.969 | 1.119 | 0.238 | 8.77 |
| 6 | 363.9 | 0.759 | 0.645 | 0.205 | 0.962 | 1.130 | 0.261 | 8.04 |
| 7 | 364.7 | 0.705 | 0.599 | 0.251 | 0.927 | 1.145 | 0.397 | 5.31 |
| 8 | 366.3 | 0.654 | 0.555 | 0.294 | 0.903 | 1.149 | 0.424 | 4.93 |
| 9 | 367.2 | 0.618 | 0.527 | 0.326 | 0.876 | 1.144 | 0.473 | 4.37 |
| 10 | 368.1 | 0.572 | 0.486 | 0.364 | 0.858 | 1.184 | 0.469 | 4.52 |
| 11 | 369.3 | 0.511 | 0.434 | 0.416 | 0.819 | 1.222 | 0.501 | 4.33 |
| 12 | 371.2 | 0.449 | 0.382 | 0.469 | 0.782 | 1.257 | 0.499 | 4.40 |
| 13 | 372.0 | 0.413 | 0.351 | 0.500 | 0.759 | 1.297 | 0.503 | 4.48 |
| 14 | 372.8 | 0.387 | 0.329 | 0.522 | 0.746 | 1.330 | 0.493 | 4.65 |
| 15 | 374.9 | 0.289 | 0.246 | 0.604 | 0.677 | 1.527 | 0.502 | 5.16 |
| 16 | 376.1 | 0.220 | 0.187 | 0.662 | 0.591 | 1.696 | 0.556 | 5.12 |
| 17 | 376.8 | 0.195 | 0.166 | 0.686 | 0.553 | 1.750 | 0.573 | 5.11 |
| 18 | 377.9 | 0.168 | 0.143 | 0.707 | 0.524 | 1.873 | 0.569 | 5.45 |
| 19 | 379.4 | 0.112 | 0.095 | 0.757 | 0.413 | 2.121 | 0.623 | 5.58 |
| 20 | 381.1 | 0.071 | 0.060 | 0.790 | 0.305 | 2.366 | 0.666 | 5.74 |
| 21 | 382.7 | 0.037 | 0.031 | 0.820 | 0.189 | 2.693 | 0.709 | 6.07 |
| 22 | 383.4 | 0.000 | | | 0.000 | | | |

Standard uncertainty $u(x_1) = u(x_1') = u(y) = 0.003, u(T) = 0.1K, u(\textit{mole \% of GTM}\ (3:1)) = 0.1$, $u(\alpha) = 0.025$.

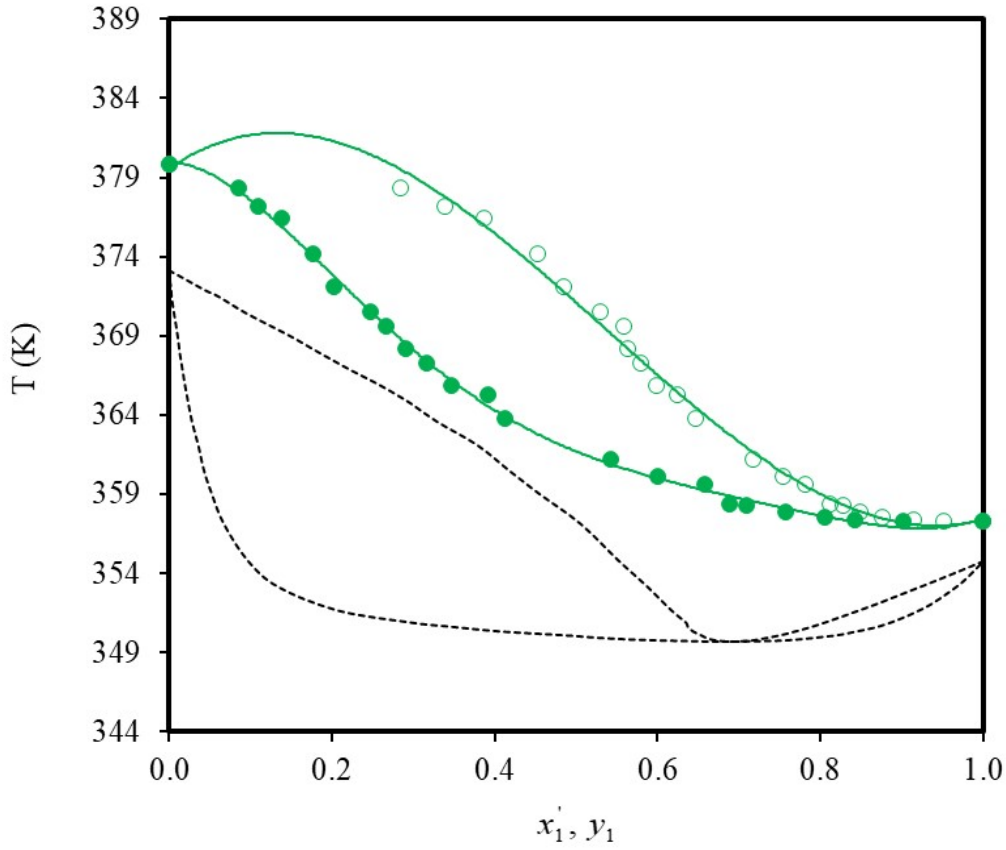


**Figure 4.18. (a)Temperature−composition diagram for the acetonitrile (1) + water (2) + GTM3:1 (3) system at 101.3 kPa with GTM3:1= 5 mol%. $x_1'$ vs T (●) and $y_1$ vs T (○), --- GTM3:1= 0 %.**

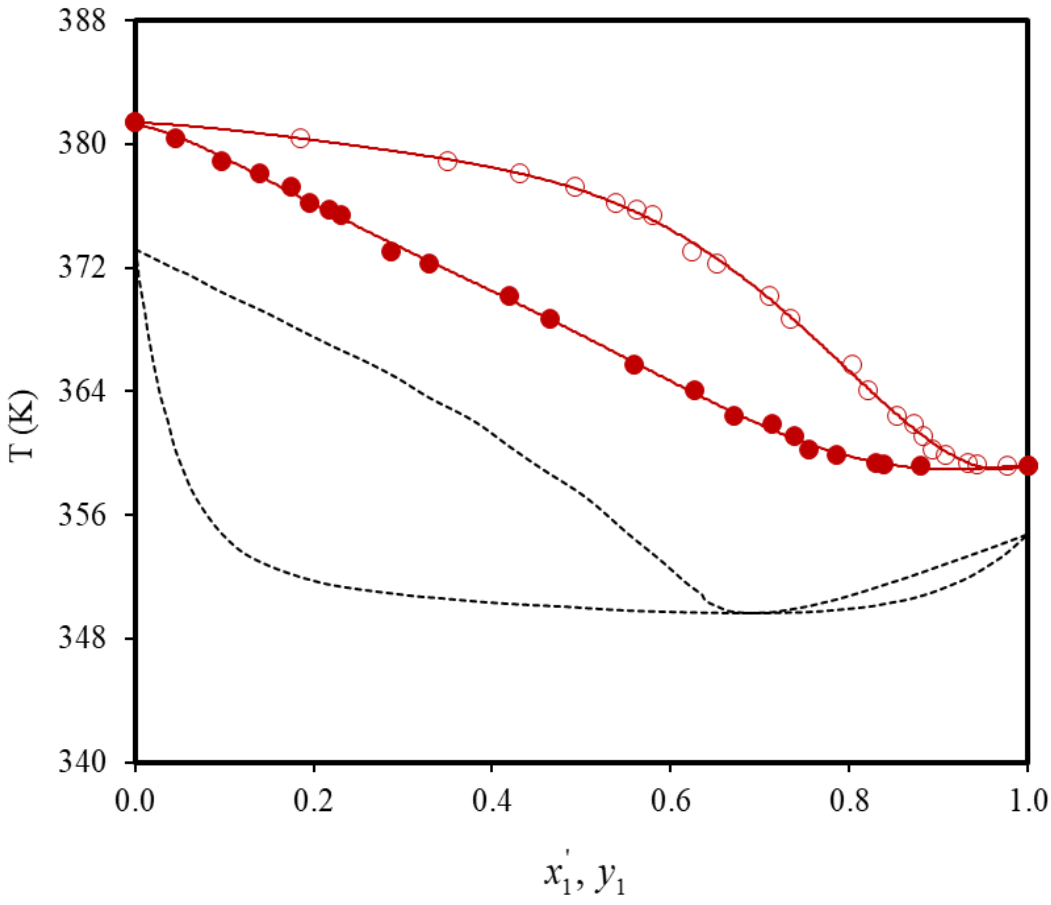


**Figure 4.18. (b) Temperature−composition diagram for the acetonitrile (1) + water (2) + GTM3:1 (3) system at 101.3 kPa withGTM3:1= 10 mol%.** $x_1'$ **vs T (●) and** $y_1$ **vs T (○), --- GTM3:1= 0%**

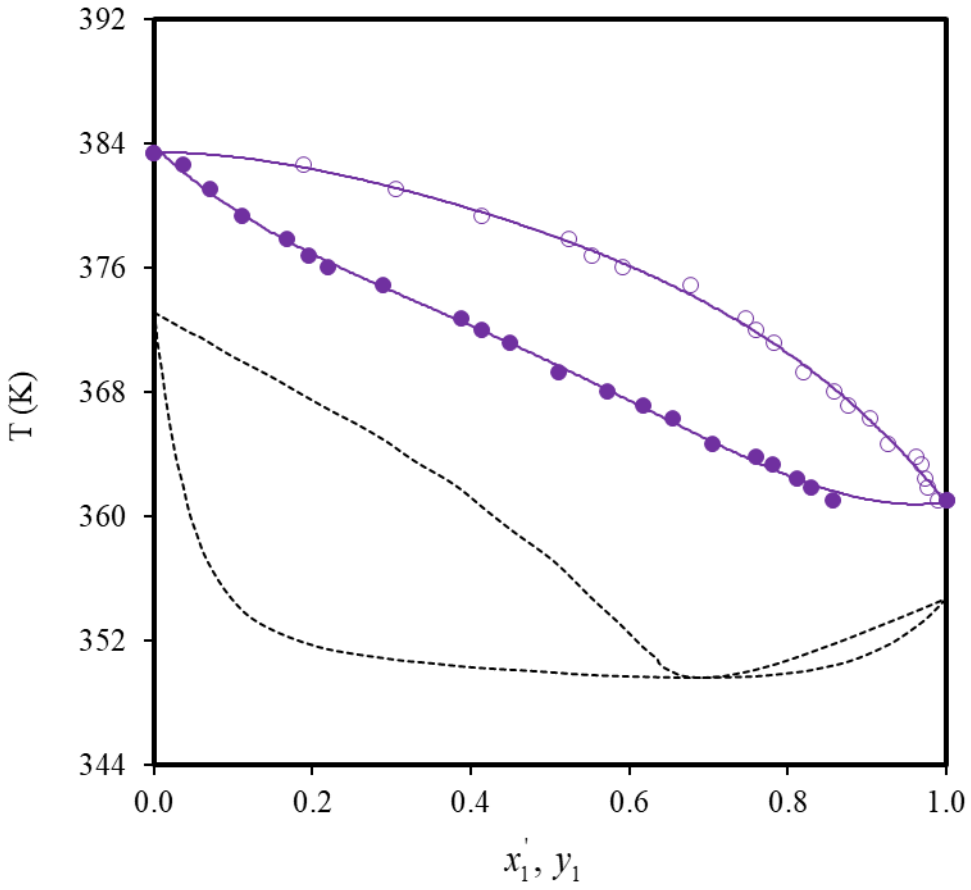


**Figure 4.18. (c) Temperature−composition diagram for the acetonitrile (1) + water (2) + GTM 3:1 (3) system at 101.3 kPa with GTM 3:1= 15 mol%.** $x_1^{'}$ **vs T (●) and** $y_1$ **vs T (○), ---- GTM3:1= 0%**

The $x-y$ diagram for different GTM3:1 molar concentration is also represented by Figure 4.19. From the figure, it is clear that GTM3:1 creates the good salting-out effect on the azeotropic mixture of ACN (1) + water (2). The addition of a small quantity of GTM3:1 produces considerable effect, due to this the ACN concentration in vapor phase increase consistently. We can see from Table 4.9 that GTM3:1 effectively improves the relative volatility of acetonitrile to water and it is greater than unity in the whole concentration range.

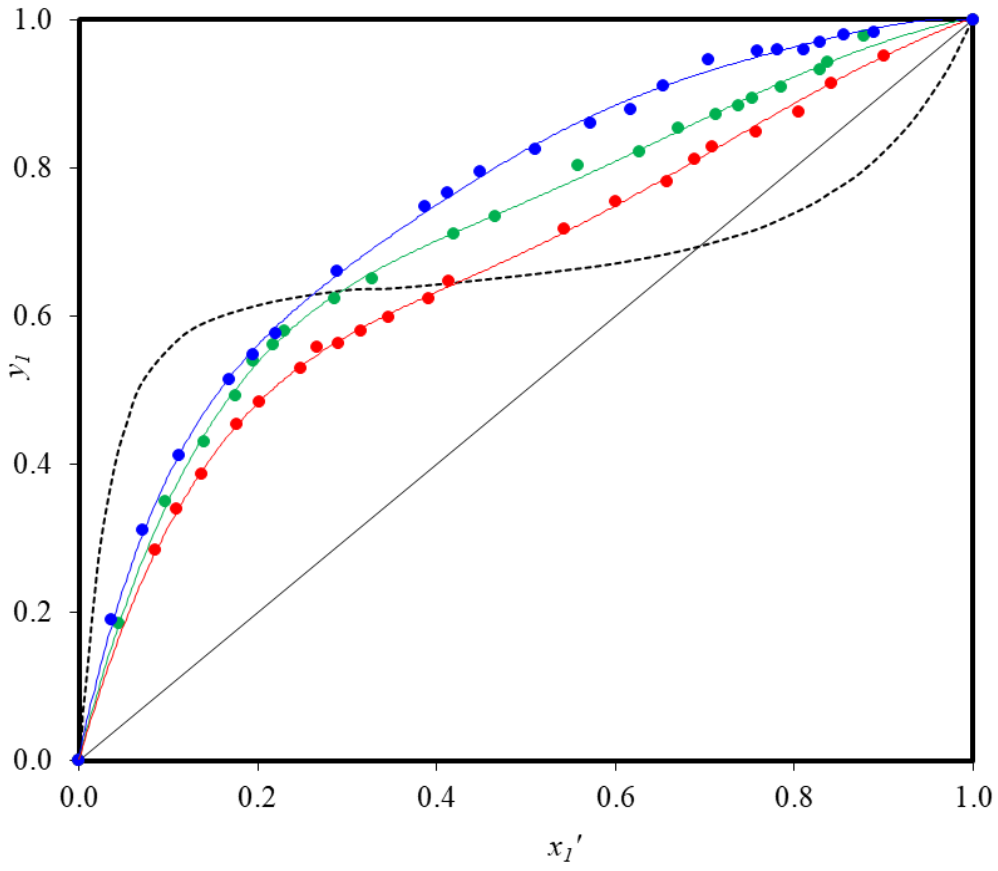


**Figure 4.19. Experimental and calculated VLE data for ACN (1) + water (2) + GTM3:1 (3) pseudo-ternary system at 101.3 kPa. For GTM= 5 mol% (●), for GTM= 10 mol% (●), for GTM= 15 mol% (●), --- GTM3:1= 0% and solid lines, calculations based on the NRTL model**

#### 4.1.2.3. Comparison of GTM3:1 with other Entrainers

The performance of an entrainer in extractive distillation process can be evaluated from the enhancement in relative volatility of the system. The proposed DES (GTM3:1) was compared with typical conventional entrainers (Zang et al., 2013, Cui et al., 2007, Zhou et al., 2009, Acosta et al., 2006) and previously used ILs (Fang et al., 2013, Fang et al., 2015) for its performance. DMSO (Zang et al., 2013) (molar mass= 62.07 g/mol) presented high relative volatility values (≈10) for the ACN + water system but at very high entrainer dosage only; 40 and 60 mol% (≈ 55.2 and 73.5 mass% respectively at azeotropic composition). At 20 mol% concentration it could not break the azeotrope. On the other hand, GTM3:1 (molar mass= 84.44 g/mol) at 5 mol% (≈ 11.7 mass% at azeotropic composition) concentration was found sufficient enough to break the azeotrope completely. Out of all the used ILs (Fang et al., 2013, Fang et al., 2015),, only 1-butyl-3- methylimidazolium dibutyl phosphate ([Bmim][DBP]) and 1-butyl-3-methylimidazolium chloride ([Bmim][Cl]) were found effective to break the ACN + water azeotrope and the separation ability of [Bmim][Cl] was found better than [Bmim][DBP]. [Bmim][Cl] (molar mass= 174.68 g/mol) was best performing at 30 mass% (≈ 7.6 mol% at azeotropic composition). By comparing the performance of [Bmim][Cl] with GTM3:1, it was observed that even at the highest [Bmim][Cl] dose the relative volatility for ACN + water system was low as compared to GTM3:1. Mixing problem and high dose requirement of ethylene glycol (Cui et al., 2007, Zhou et al., 2009) and recycling problem of butyl acetate (Acosta et al., 2006) due to its low boiling point make these inconvenient to be used as entrainer for acetonitrile dehydration. As compared to conventional entrainers and ILs, amount of GTM3:1 requirement is low for separation of ACN + water azeotropic mixture. Moreover, easy and low cost preparation, less toxicity and more biodegradable components than ILs are additional advantages of using GTM3:1 as entrainer.

The results of correlation of the average deviation in vapor mole fraction and temperature for both the pseudo-binary systems are listed in Tables 4.8 and 4.10, and are represented in Figure 4.17. Results indicate that good correlation between predicted values and experimental data were obtained by using NRTL model.

The Pseudo-ternary VLE data for ACN + water + GTM3:1 system was also correlated by using NRTL model. Since, DESs have high viscosity, for binary subsystems (containing DES) NRTL parameters cannot be applied to predict the ternary system's VLE behavior under identical conditions. Hence, the NRTL model was employed for correlating the ternary systems directly. The results of data correlation (binary interaction parameters for NRTL model and the difference in vapor mole fraction and temperature) are presented in Table 4.10, and graphical representations are shown in Figure 4.19. Figure shows that the calculated results agree well with the experimental data. The average absolute differences for the equilibrium temperature and vapor phase ACN mole fraction were 0.45 K and 0.0068 respectively. Figure 4.19 reveals that the NRTL model correlated the experimental data quite well in the presence of GTM3:1.

**Table 4.10. The parameters and correlation deviations of NRTL model for GTM3:1 containing systems at 101.3 kPa**

| Systems | $\Delta g_{12}$ | $\Delta g_{21}$ | $\alpha$ | $DT(K)$ | $dT(K)$ | $Dy_1$ | $dy_1$ |
|---|---|---|---|---|---|---|---|
| ACN (1) + GTM3:1 (2) | 5567.9 | -2786.3 | 0.3 | 0.37 | 0.64 | | |
| Water (1) + GTM3:1 (2) | 1833.7 | -5778.6 | 0.3 | 0.28 | 0.67 | | |
| ACN (1)+water(2) +GTM3:1(3) | -973.6 | 3123.2 | 0.3 | 0.45 | 0.74 | 0.0068 | 0.015 |

$\Delta g_{12}=(g_{12}-g_{22})$; $\Delta g_{21}=(g_{21}-g_{11})$

$$DT=(1/n)\sum_{k=1}^{n}\left|T^{\exp}-T^{cal}\right|_k$$

$$dT=\max\left(\left|T^{\exp}-T^{cal}\right|\right)$$

$$Dy_1=(1/n)\sum_{k=1}^{n}\left|y_1^{\exp}-y_1^{cal}\right|_k$$

$$dy_1=\max\left(\left|y_1^{\exp}-y_1^{cal}\right|\right)$$

### 4.1.2.3. Recoverability Test of GTM3:1

The recoverability of the used GTM3:1 was studied by boiling the content of vessel in rota evaporator for 2 h. Recovered GTM3:1 was vacuum dried before its reuse. After every individual run, the GTM3:1 was retrieved and reused for the successive runs till five cycles. Recovered GTM3:1 was then characterized using FT-IR and its spectra is given in Figure 4.20. When this spectra is compared with the freshly prepared GTM3:1 spectra in Figure 4.12, no remarkable change was found. Hence, due to stable chemical properties of recovered GTM3:1, it can be reused as entrainer for distillation.

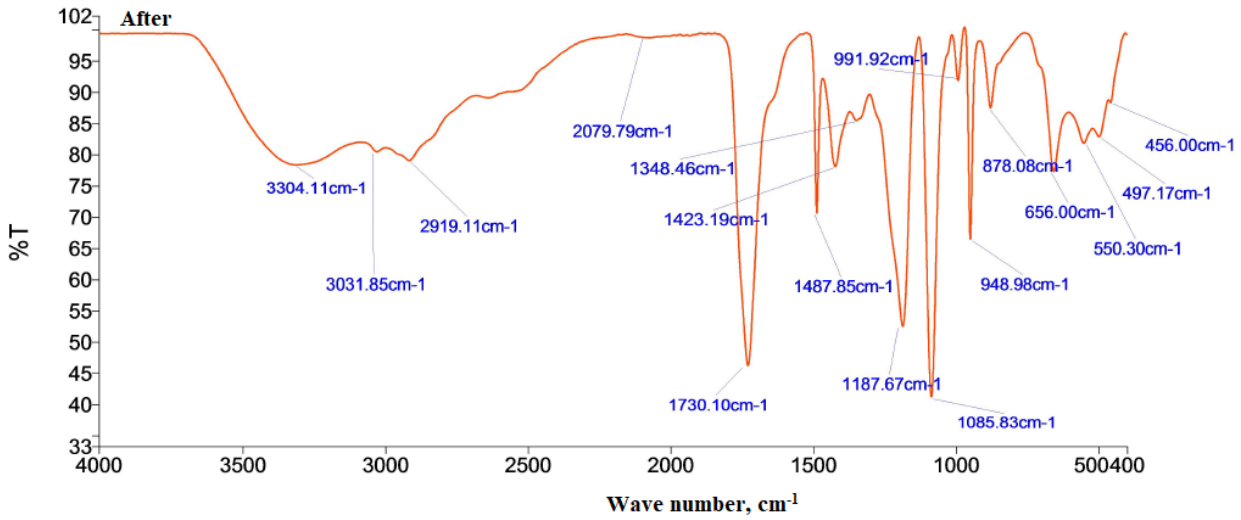


**Figure 4.20. Typical FTIR spectrum of GTM3:1 after use**

While comparing the performance of of both sugar based DESs, the separation ability of GTM3:1 was found better than GC3:1. In GC3:1 choline chloride is used as HBA which consists a hydroxyl group which is electron withdrawing in nature. Due to this nature, the chances of formation of hydrogen bonding with water is very low. On the other hand, in GTM3:1, tetramethylammonium chloride is used as HBA, which consists four methyl groups

that are electron donating in nature. Therefore, strong hydrogen bond between water and DES results better separation of ACN + water mixture.

## 4.2 NATURAL DEEP EUTECTIC SOLVENTS (NADESs)

Natural deep eutectic solvents (NADESs) are promising green solvents and are commonly known as replacement of ILs, because of resemblance of its properties with ILs. These are made up of two (or even more) non-toxic and biodegradable chemical compounds, mainly a HBD and a HBA and that leads toward the evolution of NADES (Samarov et al., 2017). By virtue of a strong intermolecular hydrogen-bonding effect among these compounds, the newly formed mixture is having very low melting temperature than individual components. Most NADESs shows no reactivity with water and there are multiple numbers of possible natural primary metabolites and their compositions which can produce NADEs. The uncommon intermolecular adjustment in a NADES matrix cause exceptional solubilizing and stabilizing properties. These properties make them qualified to be used as an entrainer for extractive distillation. In this section of study, DL-malic acid which is derived from naturally occurring compounds, was considered as HBD and choline chloride, TMAC were used as HBAs for synthesis of different NADESs.

### 4.2.1 DL-Malic acid + choline chloride 1:1 NADES (MC1:1)

NADES was prepared employing DL-malic acid as hydrogen bond donor (HBD) and choline chloride as hydrogen bond acceptor (HBA) in 1:1 molar ratio (MC1:1) with a molar mass of 136.85 g/g mol. The preparation of MC1:1 was completed by pursuing the same method as described in Chapter 3.

#### 4.2.1.1 Characterization of Synthesized MC1:1

Prepared MC1:1 NADES was characterized for thermal stability and moisture content using TGA analyser (PerkinElmer, STA6000) and Karl–Fischer titration (Esico 1760), respectively. Result of thermogravimetric analysis is presented in Figure 4.21.

To confirm the hydrogen boding among DL-malic acid and choline chloride FT-IR (PerkinElmer) analysis was performed. Further, $^{1}$H NMR was also performed to confirm the purity of Prepared MC1:1. The FTIR spectra of MC1:1 before its use is shown in Figure 4.22 and $^{1}$H NMR spectra is represented in Figure 4.23. In the FTIR spectrum of the fresh MC1:1,

strong band near 1723 $cm^{-1}$ with other weaker band near 1173 $cm^{-1}$ can be seen. The band near 1723 $cm^{-1}$ shows the presence of hydrogen bonding between O = C–OH of DL-malic acid and 'N' of choline chloride (O = C–OH------N) (Acosta et al., 2006, Rodriguez et al., 2015).

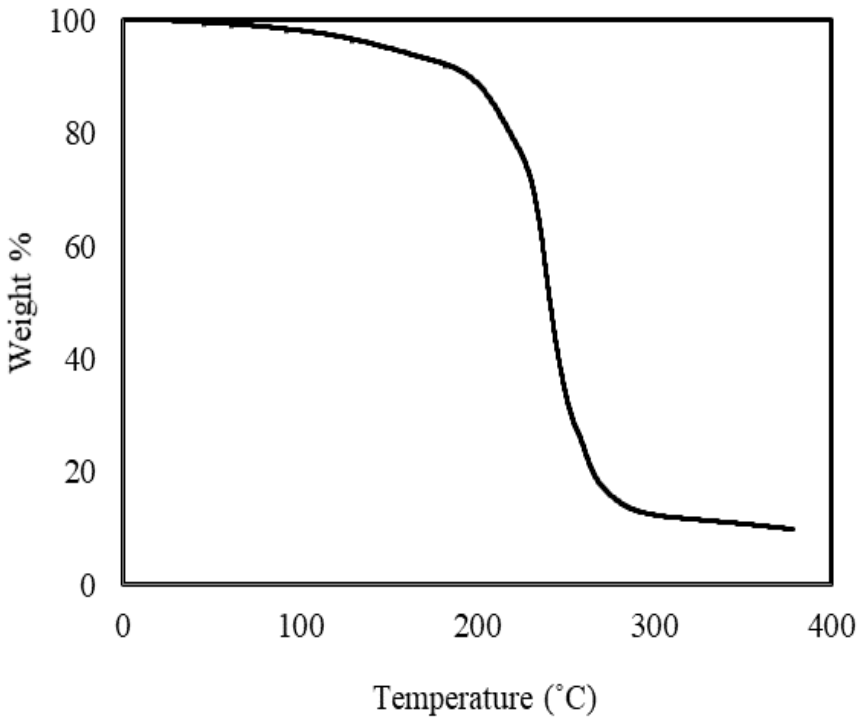


**Figure 4.21. TGA Plot of MC1:1**

Further, the C–N stretching in choline chloride is assigned to the peak at 1173 $cm^{-1}$ and stretching vibration of carbonyl group (CO) appeared at 950 $cm^{-1}$. In OH stretching region, broad band near 2943 $cm^{-1}$ indicates the formation of additional more hydrogen bonds between DL-malic acid and choline chloride in the form of OH (DL-malic acid)$\cdots Cl^{-}$, OH (choline)$\cdots Cl^{-}$, and DL-malic acid–DL-malic acid hydrogen bonds (Abbott et al., 2007, Xin et al., 2017). Based on the above study, the feasible hydrogen boding among DL-malic acid and choline chloride is represented in Figure 4.24. The optimized structure using Gaussian 16 software is also illustrated in Figure 4.25.

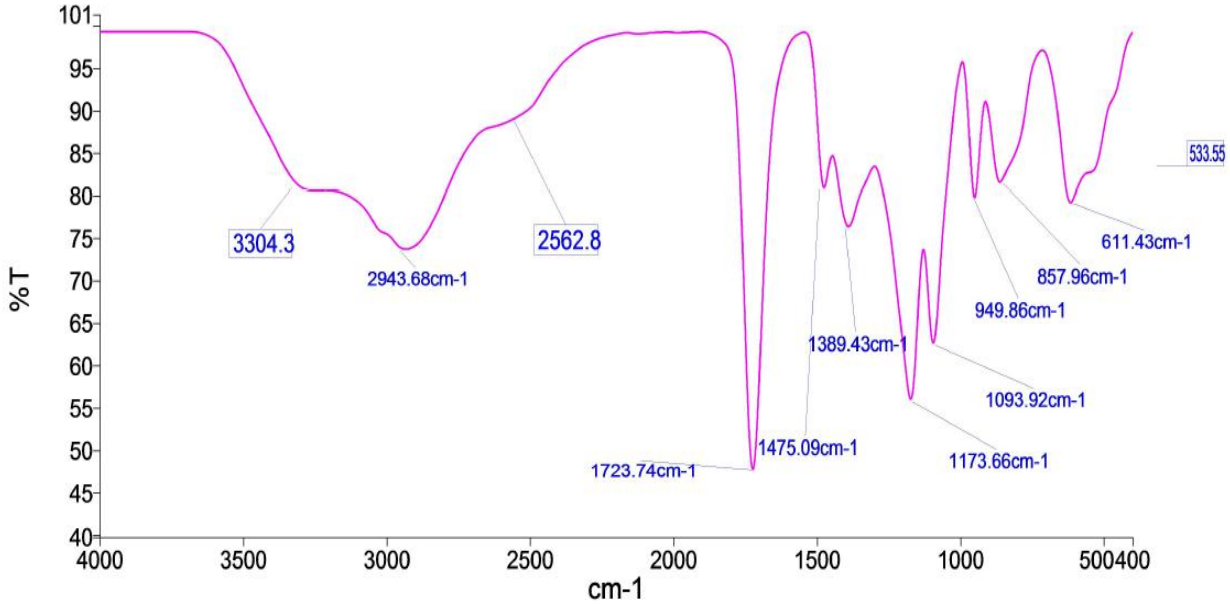


**Figure 4.22. FT-IR Spectrum of MC1:1**

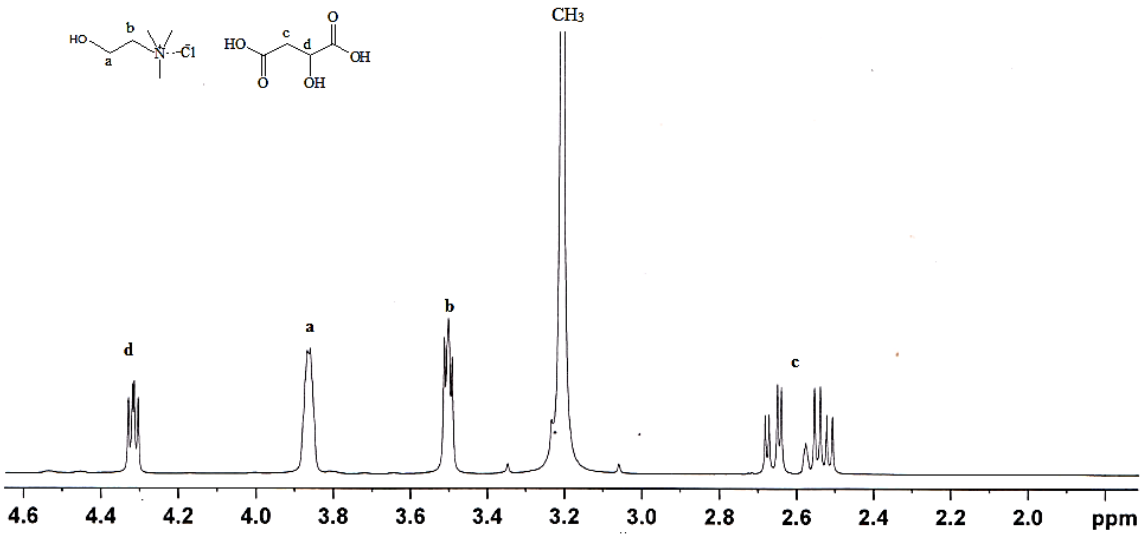


**Figure 4.23. $H^1$ NMR spectra of prepared Malic acid Choline chloride 1:1 (MC1:1) NADES**

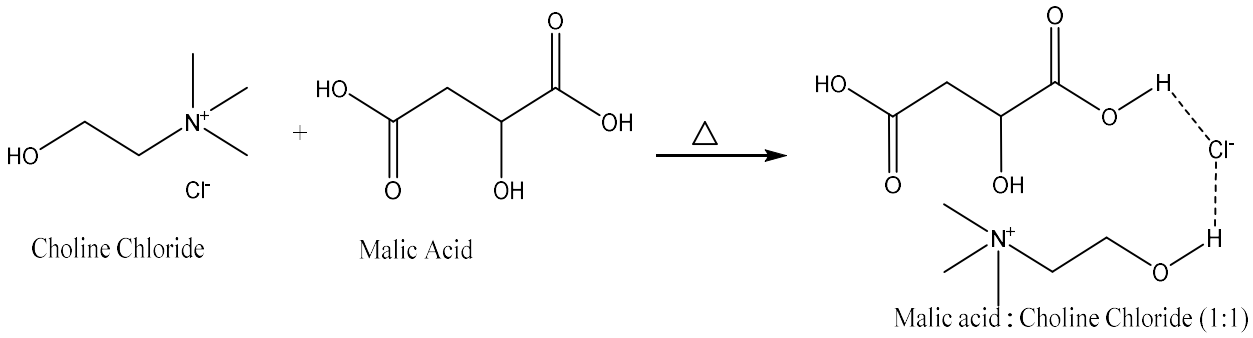


**Figure 4.24. Hydrogen Bonding Mechanism in Malic acid Choline Chloride 1:1 (MC1:1)**

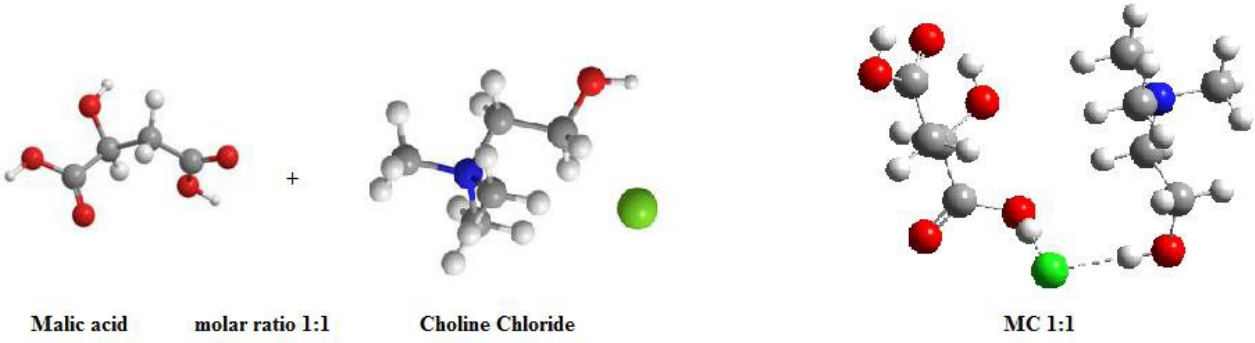


**Figure 4.25. Optimised structure of MC1:1**

The physical properties of MC1:1 were also evaluated and are given in Table 4.11. The viscosity of DESs attributes to the extensive hydrogen bonding present between its HBD and HBA, which restricts the mobility of the ions present in the DES components. Due to this, the viscosity of dicarboxylic acid based DES, MC1:1 was found more than the DESs containing monocarboxylic acid (GC3:1 and GTM3:1).

**Table 4.11. Physical Properties of MC1:1**

| **Properties** | **Value** |
|---|---|
| Density (ρ) | 1.335 g/cm$^3$ |
| Viscosity (μ) | 33145.3 mPa/s |
| Moisture Content | 0.3 wt% |

#### 4.2.1.2 Vapor–liquid equilibrium (VLE) measurements using MC1:1 as entrainer

The variation in the relative volatility $\alpha_{12}$ of the ACN + water mixture (close-to-azeotrope composition, $x_1^{'}$ = 0.674) by varying the MC1:1 concentration in the range 0−20 mol % was studied and is presented in Table 4.12. The plot of relative volatility versus MC1:1 concentration (Figure 4.26) shows that, at 20 mol% MC1:1 concentration, the relative volatility $\alpha_{12}$ was 3.98. This value is 3.98 times that in the MC1:1-free system.

**Table 4.12. Effect of MC1:1 concentration on relative volatility $\alpha_{12}$ ($x_1^{'}$≈ 0.674) of ACN (1) + water (2) system, Relative volatilities $\alpha_{12}$ at atmospheric pressure (101.3 kPa): MC1:1= (0 to 20) mol%**

| **Mol% of MC1:1** | **Relative volatility $(\alpha_{12})$** |
|---|---|
| 0 | 1.06 |
| 2 | 1.24 |
| 5 | 1.55 |
| 7 | 1.72 |
| 10 | 2.10 |
| 12 | 2.49 |
| 15 | 3.08 |
| 20 | 3.97 |

Standard uncertainty *u (mol% of MC (1:1))* = 0.1, $u(\alpha) = 0.025$.

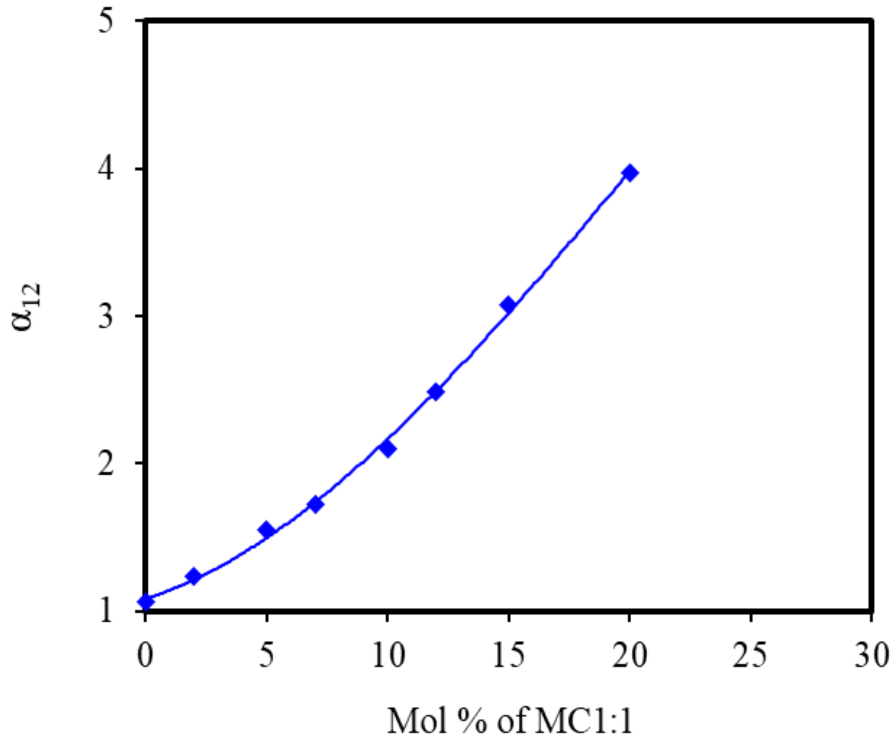


**Figure 4.26. Effect of MC1:1 concentration on relative volatility $\alpha_{12}$ ($x_1' \approx 0.674$) of ACN (1) + water (2) system at 101.3 kPa**

VLE data at isobaric condition (101.3 kPa) were estimated for pseudo-binary mixtures [water (1) + MC1:1 (2)] and [ACN (1) + MC1:1 (2)]. The experimental VLE data and activity coefficients for water + MC1:1 and ACN + MC1:1 are listed in Table 4.13. Further, because of the incorporation of nonvolatile constituent MC1:1 in pure ACN and water, boiling point ($T_b$) enhancement occurred in both and is shown in Figure 4.27 (a), (b), respectively. As it is visible from the figures, boiling point enhances by introducing MC1:1 and this effect is more for higher dosage.

**Table 4.13. Experimental VLE data and correlated results of pseudo-binary systems (Water + MC1:1 and ACN + MC1:1), Activity Coefficient $\gamma_i$, deviation in activity Coefficient $\Delta\gamma_i$ and deviation in equilibrium temperature $\Delta T$ at 101.3 kPa**

| Water (1) + MC1:1 (mol/mol) (2) | | | | | | |
|---|---|---|---|---|---|---|
| S. No. | $T(K)$ | Mole % of MC (1:1) | $x_1$ | $\gamma_1^{exp}$ | $\Delta\gamma_1^a$ | $\Delta T^b$ $(K)$ |
| 1 | 373.1 | 0.00 | 1.000 | 1.002 | 0.0017 | 0.00 |
| 2 | 373.4 | 0.92 | 0.990 | 1.001 | 0.0012 | -0.02 |
| 3 | 373.6 | 1.92 | 0.981 | 1.002 | 0.0027 | 0.03 |
| 4 | 374.0 | 3.01 | 0.969 | 1.000 | 0.0014 | -0.01 |
| 5 | 374.6 | 4.21 | 0.957 | 0.991 | -0.0060 | -0.22 |
| 6 | 375.7 | 5.53 | 0.944 | 0.984 | -0.0112 | -0.37 |
| 7 | 376.3 | 7.00 | 0.928 | 0.980 | -0.0119 | -0.39 |
| 8 | 376.9 | 8.64 | 0.914 | 0.978 | -0.0105 | -0.35 |
| 9 | 377.4 | 10.49 | 0.895 | 0.970 | -0.0128 | -0.42 |
| 10 | 378.0 | 12.57 | 0.873 | 0.964 | -0.0120 | -0.40 |
| 11 | 378.7 | 14.95 | 0.851 | 0.965 | -0.0034 | -0.15 |
| 12 | 379.9 | 17.68 | 0.823 | 0.956 | -0.0007 | -0.07 |
| 13 | 381.5 | 20.86 | 0.791 | 0.942 | -0.0016 | -0.10 |
| 14 | 383.4 | 24.60 | 0.753 | 0.927 | 0.0013 | -0.01 |
| 15 | 385.6 | 29.08 | 0.709 | 0.914 | 0.0100 | 0.28 |
| ACN (1) + MC1:1 (mol/mol) (2) | | | | | | |
| S. No. | $T(K)$ | Mole % of MC (1:1) | $x_1$ | $\gamma_1^{exp}$ | $\Delta\gamma_1^a$ | $\Delta T^b$(K) |
| 1 | 354.7 | 0.00 | 1.000 | 0.999 | -0.0006 | 0.07 |
| 2 | 355.6 | 2.64 | 0.972 | 0.999 | -0.0017 | 0.11 |
| 3 | 356.8 | 5.42 | 0.945 | 0.990 | -0.0118 | 0.44 |
| 4 | 357.6 | 8.34 | 0.915 | 0.998 | -0.0071 | 0.28 |
| 5 | 358.5 | 11.42 | 0.886 | 1.003 | -0.0052 | 0.22 |
| 6 | 359.3 | 14.67 | 0.853 | 1.017 | 0.0030 | -0.05 |
| 7 | 360.5 | 18.10 | 0.818 | 1.023 | 0.0029 | -0.05 |
| 8 | 361.6 | 21.73 | 0.781 | 1.037 | 0.0093 | -0.25 |
| 9 | 363.1 | 25.58 | 0.743 | 1.043 | 0.0064 | -0.16 |
| 10 | 364.9 | 29.67 | 0.703 | 1.045 | -0.0005 | 0.07 |

| | | | | | | |
|---|---|---|---|---|---|---|
| 11 | 366.9 | 34.02 | 0.660 | 1.051 | -0.0051 | 0.22 |
| 12 | 369.1 | 38.66 | 0.613 | 1.061 | -0.0079 | 0.31 |
| 13 | 371.5 | 43.62 | 0.563 | 1.079 | -0.0025 | 0.13 |
| 14 | 374.3 | 48.92 | 0.510 | 1.102 | 0.0063 | -0.16 |

Standard uncertainty u *($x_1$) = 0.003, u(T) = 0.1 K, u (mol% of MC (1:1))=* 0.1, $u(P) = 0.05\,kPa.$ [a] $\Delta\gamma_1 = \gamma_1^{\exp} - \gamma_1^{cal}$, [b] $\Delta T = T^{\exp} - T^{cal}$

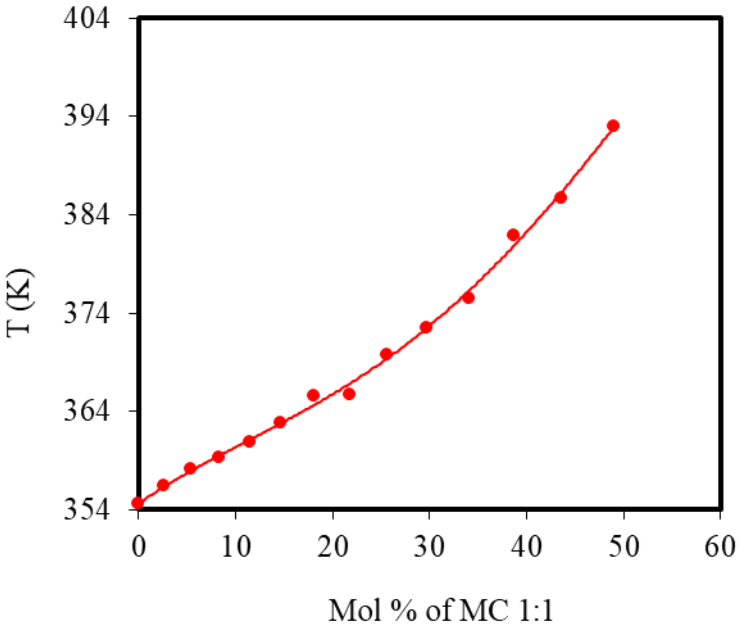


**(a)**

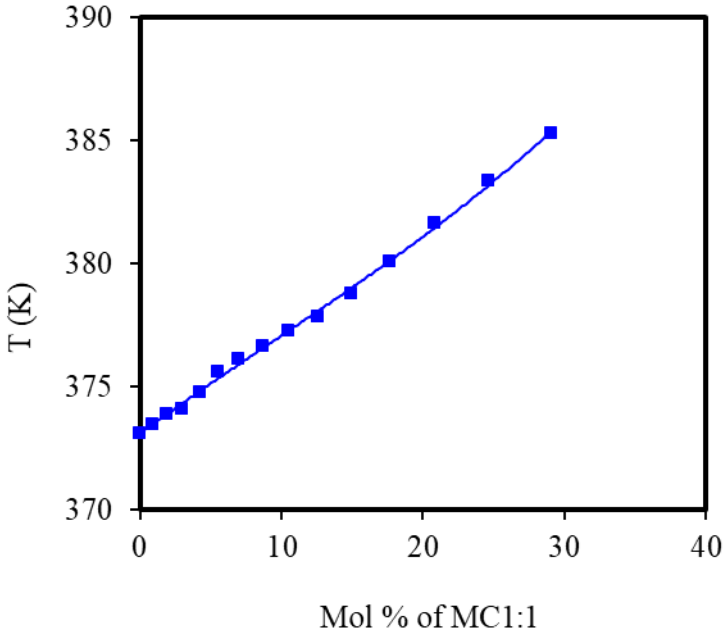


**(b)**

**Figure 4.27 (a), (b): Effect of MC1:1 on the normal boiling point of water and ACN at 101.3 kPa. Experimental data for ACN (●) and water (■); and solid lines, calculations based on NRTL model.**

The VLE data for pseudo-ternary system of ACN (1) + water (2) + MC1:1 (3) were measured experimentally at 101.3 kPa for different MC1:1 molar fraction (0.05, 0.10 and 0.15). The experimental data are listed in Table 4.14, where $x_1^{'}$ represents the mole fraction of ACN in liquid phase expressed on MC1:1 free basis, $x_1$ and $x_2$ represents the molar fractions of ACN and water in liquid phase, respectively. $y_1$ denotes the molar fraction of ACN in the vapor phase and $T$ denotes the equilibrium temperature.

Figure 4.28 represents the $T$−composition diagram to represent the salting out impact generated due to MC1:1 at different molar fractions (0.05, 0.10 and 0.15). At the same time, MC1:1-free $T - x, y$ diagram was also given to conveniently compare each other. It is visible from the figure that, equilibrium temperature enhances with the increasing MC1:1 concentration in liquid phase, which suggests the interactions between the MC1:1 and mixture becomes stronger as a result it becomes uneasy for the mixture to vaporize.

The equilibrium diagram for these experiments is also depicted in Figure 4.29. The azotropic point for the ACN + water mixture was eliminated at the minimum MC1:1 dose 5 mol% but it could not work below this concentration. It can be seen from Figure 4.29 that in low ACN concentration region, the experimental *x'-y* curve using MC1:1 is lying under the *x-y* curve of the (ACN + water) system. This effect can be attributed to the lower activity coefficient value of water ($\gamma_{water}$) obtained for the (water + MC1:1) binary system. Contrarily, for higher ACN concentrations, including the azeotropic region, it was found that MC1:1 is able to increase the ACN relative volatilities. This trend should be related with the activity coefficients of the ACN + MC1:1 binary mixture ($\gamma_{ACN}$). Due to different interactions of MC1:1 with ACN and water, strong salt-out effect was observed at higher MC1:1 dosage. From Table 4.14 it can be seen that MC1:1 is quite effective in increasing the relative volatility of ACN + water system and it was >1 in the entire concentration range.

**Table 4.14. Experimental Isobaric VLE data for ACN (1) + water (2) + MC1:1 (3) system, experimental Activity Coefficient $\gamma_i^{exp}$ and Relative Volatilities $\alpha_{12}$ at 101.3 kPa**

| S. No. | $T$ (K) | $x_1^{'}$ | $x_1$ | $x_2$ | $y_1$ | $\gamma_1^{exp}$ | $\gamma_2^{exp}$ | $\alpha_{12}$ |
|---|---|---|---|---|---|---|---|---|
| **Malic acid/Choline Chloride1:1= 5 mol%** | | | | | | | | |
| 1 | 356.4 | 1.000 | | | 1.000 | | | |
| 2 | 356.7 | 0.940 | 0.795 | 0.155 | 0.949 | 1.122 | 0.610 | 1.20 |
| 3 | 356.8 | 0.897 | 0.776 | 0.174 | 0.915 | 1.105 | 0.904 | 1.24 |
| 4 | 357.0 | 0.815 | 0.722 | 0.228 | 0.861 | 1.110 | 1.122 | 1.40 |
| 5 | 357.5 | 0.737 | 0.673 | 0.278 | 0.810 | 1.104 | 1.230 | 1.52 |
| 6 | 358.3 | 0.665 | 0.633 | 0.317 | 0.768 | 1.085 | 1.271 | 1.66 |
| 7 | 359.4 | 0.627 | 0.597 | 0.354 | 0.753 | 1.093 | 1.165 | 1.81 |
| 8 | 360.2 | 0.580 | 0.550 | 0.399 | 0.719 | 1.104 | 1.143 | 1.85 |
| 9 | 361.2 | 0.559 | 0.531 | 0.419 | 0.718 | 1.108 | 1.051 | 2.00 |
| 10 | 361.9 | 0.524 | 0.498 | 0.451 | 0.693 | 1.119 | 1.032 | 2.05 |
| 11 | 363.1 | 0.466 | 0.462 | 0.487 | 0.647 | 1.087 | 1.050 | 2.10 |
| 12 | 364.4 | 0.427 | 0.415 | 0.535 | 0.620 | 1.116 | 0.983 | 2.19 |
| 13 | 365.1 | 0.403 | 0.391 | 0.559 | 0.598 | 1.119 | 0.966 | 2.21 |
| 14 | 366.0 | 0.365 | 0.347 | 0.602 | 0.563 | 1.157 | 0.943 | 2.24 |
| 15 | 367.6 | 0.311 | 0.295 | 0.656 | 0.506 | 1.167 | 0.922 | 2.28 |
| 16 | 369.1 | 0.284 | 0.269 | 0.681 | 0.487 | 1.178 | 0.873 | 2.40 |
| 17 | 370.2 | 0.265 | 0.252 | 0.699 | 0.472 | 1.182 | 0.841 | 2.47 |
| 18 | 371.3 | 0.216 | 0.205 | 0.745 | 0.400 | 1.195 | 0.861 | 2.42 |
| 19 | 371.9 | 0.184 | 0.170 | 0.780 | 0.348 | 1.230 | 0.875 | 2.37 |
| 20 | 372.7 | 0.148 | 0.140 | 0.809 | 0.288 | 1.212 | 0.895 | 2.34 |
| 21 | 373.6 | 0.112 | 0.106 | 0.844 | 0.226 | 1.221 | 0.903 | 2.32 |
| 22 | 374.6 | 0.075 | 0.072 | 0.878 | 0.158 | 1.231 | 0.910 | 2.30 |
| 23 | 375.3 | 0.000 | | | 0.000 | | | |
| **Malic acid/Choline chloride 1:1= 10 mol%** | | | | | | | | |
| 1 | 357.8 | 1.000 | | | 1.000 | | | |
| 2 | 357.9 | 0.887 | 0.799 | 0.101 | 0.932 | 1.057 | 1.198 | 1.73 |
| 3 | 358.2 | 0.859 | 0.774 | 0.126 | 0.902 | 1.047 | 1.362 | 1.50 |
| 4 | 358.4 | 0.831 | 0.749 | 0.152 | 0.896 | 1.067 | 1.193 | 1.74 |
| 5 | 358.8 | 0.789 | 0.710 | 0.190 | 0.868 | 1.078 | 1.188 | 1.76 |
| 6 | 359.4 | 0.735 | 0.662 | 0.238 | 0.845 | 1.106 | 1.086 | 1.97 |
| 7 | 359.9 | 0.702 | 0.631 | 0.269 | 0.831 | 1.123 | 1.029 | 2.10 |
| 8 | 360.5 | 0.641 | 0.578 | 0.324 | 0.780 | 1.131 | 1.086 | 1.99 |
| 9 | 361.1 | 0.601 | 0.542 | 0.359 | 0.749 | 1.138 | 1.092 | 1.98 |
| 10 | 361.8 | 0.578 | 0.522 | 0.381 | 0.737 | 1.138 | 1.051 | 2.05 |

| | | | | | | | | |
|---|---|---|---|---|---|---|---|---|
| 11 | 362.9 | 0.524 | 0.472 | 0.428 | 0.698 | 1.155 | 1.029 | 2.10 |
| 12 | 364.1 | 0.474 | 0.427 | 0.473 | 0.662 | 1.167 | 0.998 | 2.17 |
| 13 | 365.6 | 0.429 | 0.386 | 0.515 | 0.632 | 1.179 | 0.944 | 2.29 |
| 14 | 367.0 | 0.397 | 0.359 | 0.545 | 0.614 | 1.184 | 0.887 | 2.41 |
| 15 | 367.6 | 0.376 | 0.339 | 0.561 | 0.594 | 1.195 | 0.884 | 2.43 |
| 16 | 369.1 | 0.316 | 0.285 | 0.615 | 0.532 | 1.218 | 0.881 | 2.46 |
| 17 | 370.2 | 0.264 | 0.238 | 0.663 | 0.466 | 1.237 | 0.895 | 2.43 |
| 18 | 371.3 | 0.237 | 0.213 | 0.688 | 0.435 | 1.250 | 0.878 | 2.49 |
| 19 | 372.3 | 0.219 | 0.199 | 0.711 | 0.416 | 1.246 | 0.846 | 2.55 |
| 20 | 373.1 | 0.179 | 0.161 | 0.739 | 0.355 | 1.282 | 0.874 | 2.52 |
| 21 | 374.1 | 0.150 | 0.135 | 0.766 | 0.309 | 1.295 | 0.872 | 2.54 |
| 22 | 375.4 | 0.109 | 0.098 | 0.802 | 0.239 | 1.324 | 0.877 | 2.55 |
| 23 | 376.6 | 0.000 | | | 0.000 | | | |
| **Malic acid/Choline chloride1:1= 15 mol%** | | | | | | | | |
| 1 | 359.1 | 1.000 | | | 1.000 | | | |
| 2 | 359.3 | 0.928 | 0.789 | 0.061 | 0.968 | 1.066 | 0.883 | 2.33 |
| 3 | 359.4 | 0.896 | 0.762 | 0.089 | 0.950 | 1.080 | 0.933 | 2.23 |
| 4 | 359.7 | 0.847 | 0.720 | 0.130 | 0.932 | 1.110 | 0.871 | 2.45 |
| 5 | 360.0 | 0.824 | 0.701 | 0.150 | 0.919 | 1.115 | 0.878 | 2.44 |
| 6 | 360.5 | 0.725 | 0.618 | 0.234 | 0.854 | 1.157 | 1.001 | 2.21 |
| 7 | 361.3 | 0.667 | 0.567 | 0.283 | 0.818 | 1.181 | 0.998 | 2.25 |
| 8 | 361.9 | 0.607 | 0.516 | 0.334 | 0.780 | 1.215 | 0.999 | 2.30 |
| 9 | 362.9 | 0.561 | 0.476 | 0.373 | 0.753 | 1.234 | 0.968 | 2.39 |
| 10 | 364.1 | 0.524 | 0.446 | 0.406 | 0.736 | 1.243 | 0.907 | 2.54 |
| 11 | 365.2 | 0.486 | 0.413 | 0.437 | 0.714 | 1.260 | 0.876 | 2.64 |
| 12 | 366.5 | 0.421 | 0.358 | 0.491 | 0.660 | 1.296 | 0.882 | 2.67 |
| 13 | 367.7 | 0.375 | 0.319 | 0.532 | 0.624 | 1.326 | 0.863 | 2.76 |
| 14 | 368.8 | 0.335 | 0.285 | 0.565 | 0.584 | 1.347 | 0.863 | 2.78 |
| 15 | 370.1 | 0.302 | 0.257 | 0.594 | 0.561 | 1.386 | 0.824 | 2.96 |
| 16 | 371.3 | 0.286 | 0.243 | 0.607 | 0.549 | 1.383 | 0.794 | 3.04 |
| 17 | 372.4 | 0.257 | 0.219 | 0.631 | 0.520 | 1.413 | 0.780 | 3.13 |
| 18 | 373.4 | 0.232 | 0.198 | 0.654 | 0.491 | 1.436 | 0.770 | 3.20 |
| 19 | 374.1 | 0.196 | 0.167 | 0.682 | 0.445 | 1.513 | 0.786 | 3.29 |
| 20 | 374.9 | 0.167 | 0.143 | 0.709 | 0.399 | 1.551 | 0.795 | 3.31 |
| 21 | 376.0 | 0.149 | 0.126 | 0.724 | 0.370 | 1.576 | 0.786 | 3.37 |
| 22 | 376.7 | 0.128 | 0.109 | 0.742 | 0.334 | 1.610 | 0.792 | 3.40 |
| | 378.7 | 0.000 | | | 0.000 | | | |

Standard uncertainty $u(x_1) = u(x_1') = u(y) = 0.003$, $u(T) = 0.1$ K, $u$ (mol% of MC (1:1) =0.1, $x_1'$ *is mole fraction of ACN in liquid phase expressed on MC1:1 free basis*

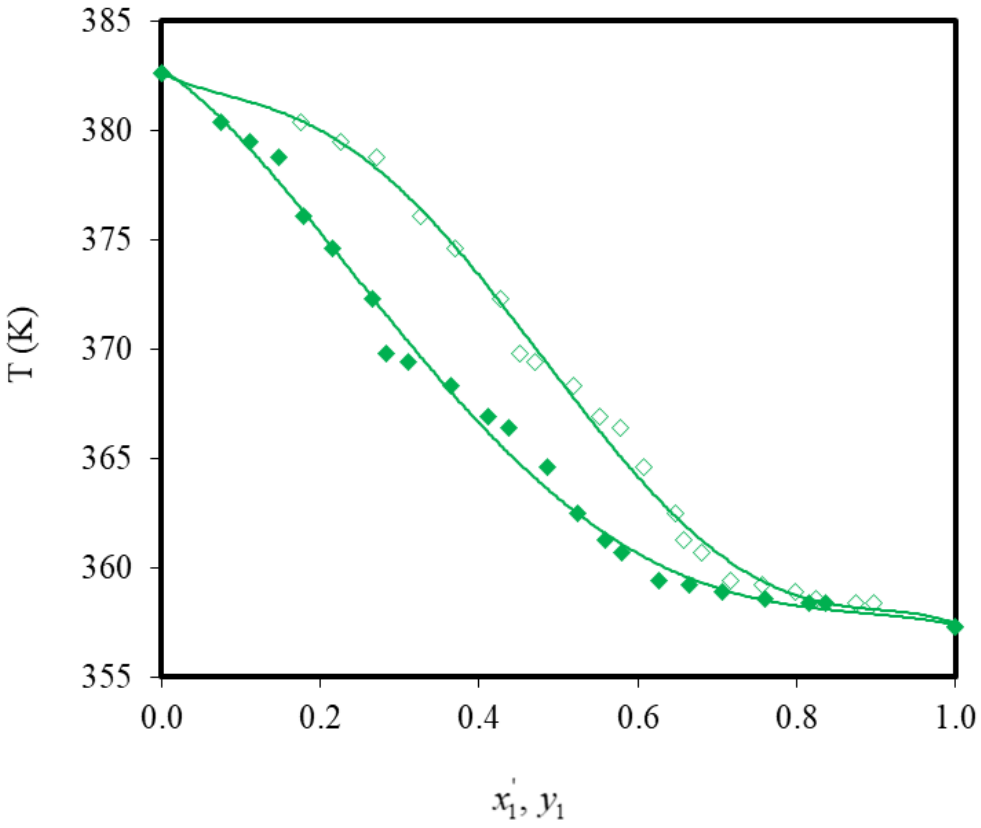


**Figure 4.28 (a) Temperature−composition diagram for the acetonitrile (1) + water (2) + MC1:1 (3) system at 101.3 kPa with MC1:1= 5 mol%. $x_1'$ vs T (♦) and $y_1$ vs T (◊), --- MC1:1= 0%**

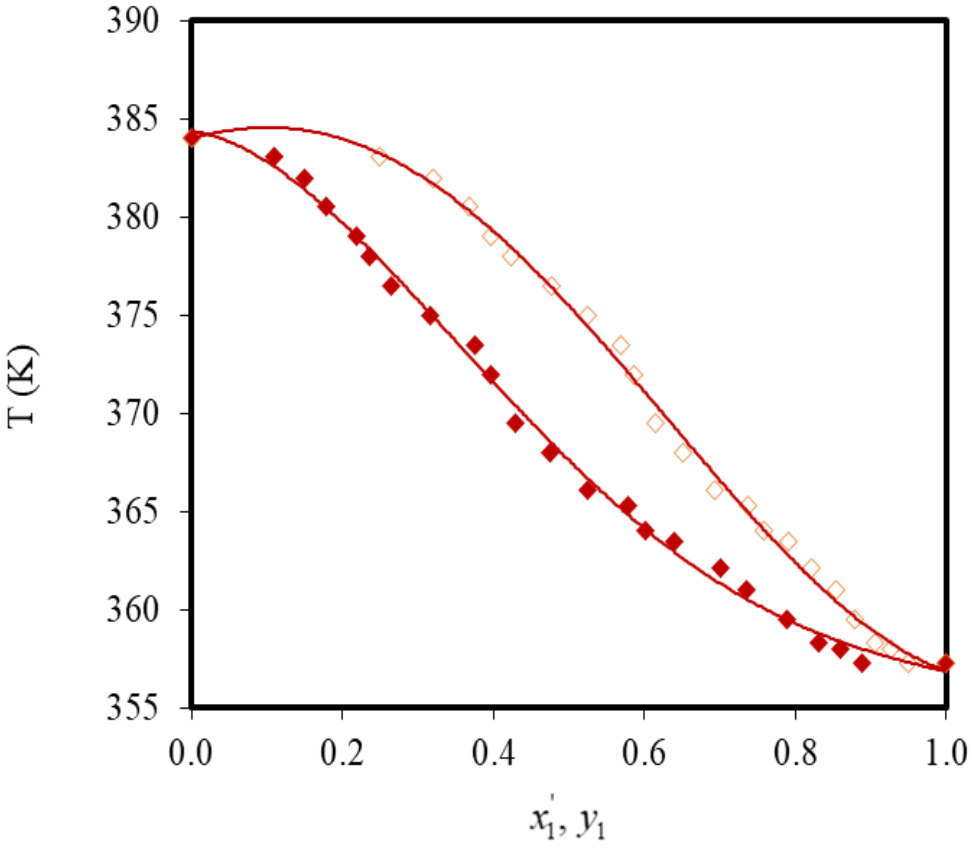


**Figure 4.28. (b) Temperature−composition diagram for the acetonitrile (1) + water (2) + MC:1 (3) system at 101.3 kPa with MC:1= 10 mol%.** $x_1'$ **vs T (♦) and** $y_1$ **vs T (◊), --- MC1:1= 0%**

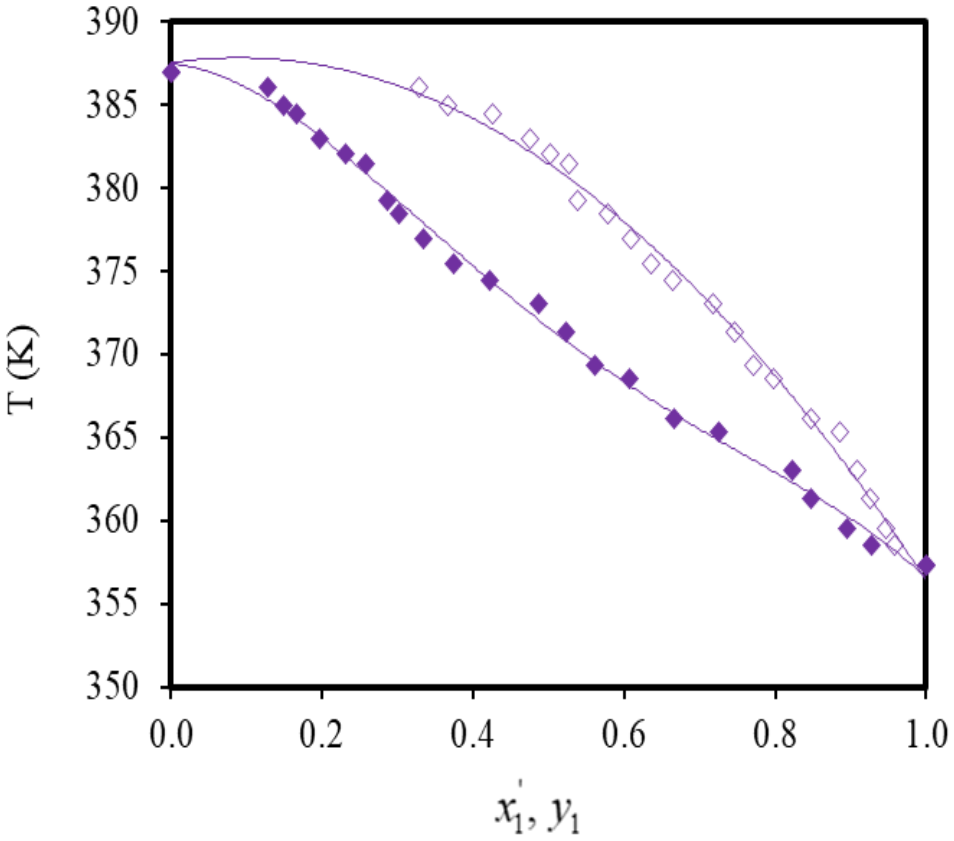


**Figure 4.28. (c) Temperature−composition diagram for the acetonitrile (1) + water (2) + MC:1 (3) system at 101.3 kPa with MC:1= 15 mol%.** $x_1'$ **vs T (♦) and** $y_1$ **vs T (◊), --- MC1:1= 0%**

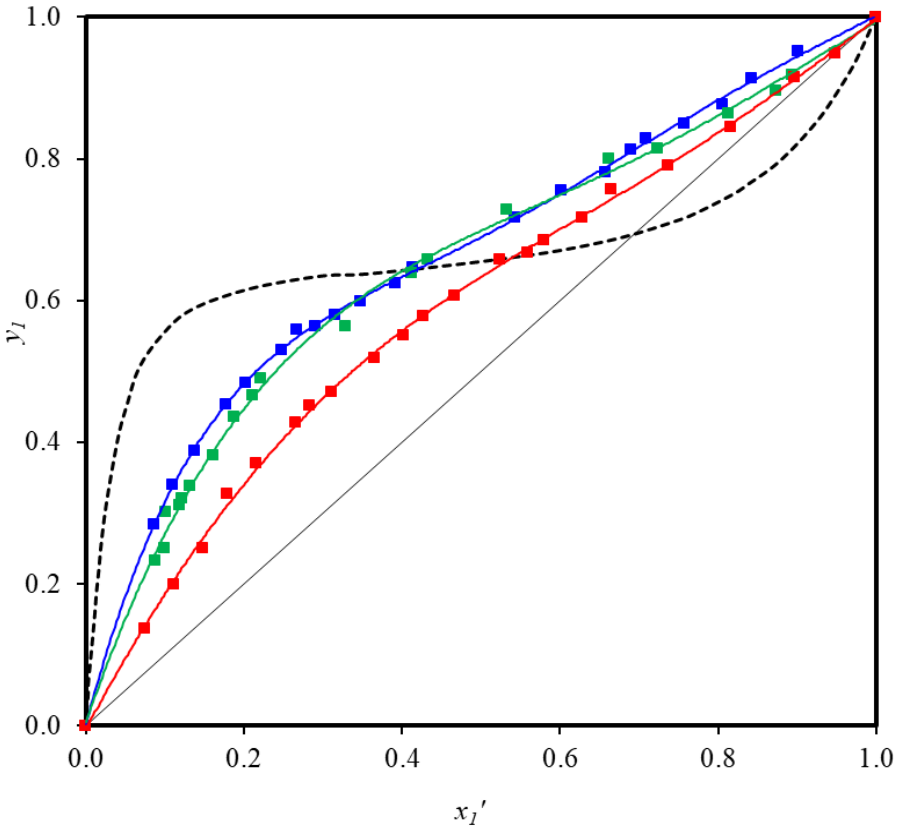


**Figure 4.29. Experimental and calculated VLE data for ACN (1) + water (2) + MC1:1 (3) pseudo-ternary system at 101.3 kPa. For MC1:1= 5 mol% (♦), for MC1:1= 10 mol% (♦), for MC1:1= 15 mol% (♦), --- MC1:1= 0% and solid lines, calculations based on the NRTL model**

While correlating the experimental VLE data with the predicted values using NRTL model, results illustrate that, predicted values from NRTL model provided good correlation with the experimental data as shown in Figure 4.29. The values of the binary interaction parameters and the average difference in $T$ and $y_i$ in ternary system are given in Table 4.15. The average absolute differences for the equilibrium temperature and ACN mole fraction in the vapor phase are 0.15 K and 0.0023 respectively.

**Table 4.15. The parameters and correlation deviations of NRTL model for MC1:1 containing systems at 101.3 kPa**

| Systems | $\Delta g_{12}$ | $\Delta g_{21}$ | $\alpha$ | $DT(K)$ | $dT(K)$ | $Dy_1$ | $dy_1$ |
|---|---|---|---|---|---|---|---|
| ACN(1) + MC1:1(2) | 3702.6 | -2010.8 | 0.3 | 0.18 | 0.44 | | |
| Water(1) + MC1:1(2) | 4493.8 | -4899.9 | 0.3 | 0.19 | 0.42 | | |
| ACN(1) + water(2) + MC1:1(3) | 1858.8 | -998.9 | 0.3 | 0.15 | 0.56 | 0.0023 | 0.0108 |

$$\Delta g_{12}=(g_{12}-g_{22});\ \Delta g_{21}=(g_{21}-g_{11})$$

$$DT=(1/n)\sum_{k=1}^{n}\left|T^{\exp}-T^{cal}\right|_k$$

$$dT=\max\left(\left|T^{\exp}-T^{cal}\right|\right)$$

$$Dy_1=(1/n)\sum_{k=1}^{n}\left|y_1^{\exp}-y_1^{cal}\right|_k$$

$$dy_1=\max\left(\left|y_1^{\exp}-y_1^{cal}\right|\right)$$

### 4.2.1.3 Recoverability test of MC1:1

In order to evaluate the recoverability of the used MC1:1, water present in it was evaporated in rota evaporator after each run. Further retrieved MC1:1 was vacuum dried before its reuse. This process was repeated for the successive runs till five cycles and performance (in terms of purity of products) did not drop below 5% in all cases. Further recovered MC1:1 after fifth cycle was characterized by FT-IR and its spectra is given in Figure 4.30. Although no notable change was observed in the spectra of recovered MC1:1, but the drop in performance of recovered NADES can be related with the possible esterification of the malic acid at the time of recovery (Rodriguez et al., 2019).

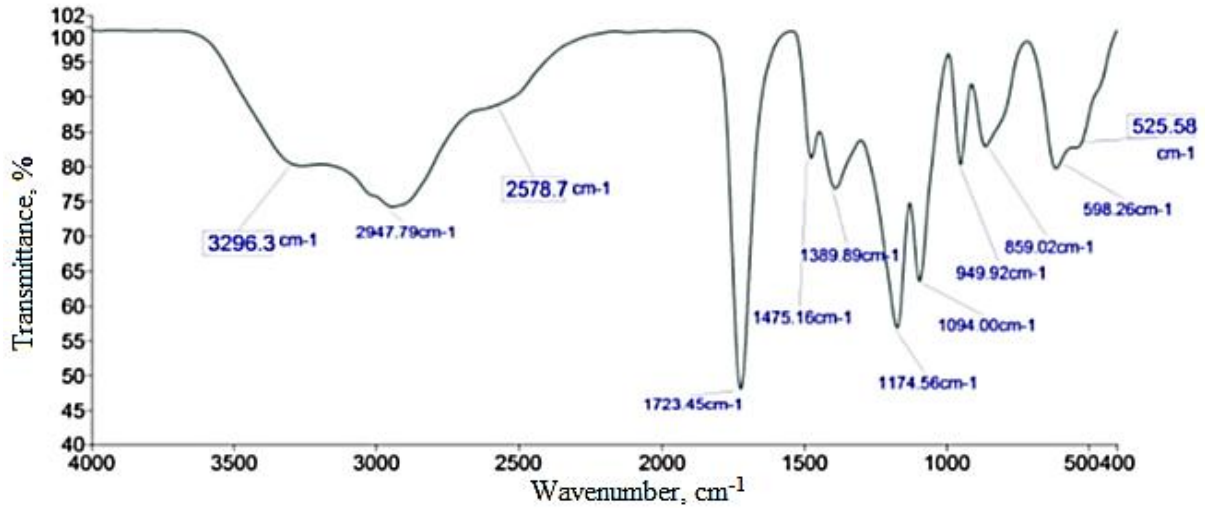


**Figure 4.30. FT-IR spectrum of MC1:1 after use**

### 4.2.2 Malic acid + tetramethylammonium chloride 1:1 NADES (MTM1:1)

In this section of study, another NADES was synthesized using DL-malic acid as HBD and tetramethylammonium chloride (TMAC) as HBA in 1:1 molar ratio (MTM1:1). Further, it was characterized for different properties and evaluated for its ability to break the ACN + water azeotrope.

#### 4.2.2.1 Characterization of Synthesized MTM1:1

Synthesized MTM1:1 was characterized to evaluate its thermal stability during the distillation operation. TGA was performed at atmospheric pressure in the temperature range of room temperature to 400˚C. As shown in Figure 4.31, till near 200˚C MTM1:1 was found thermally stable, which proves its good thermally stable during the distillation process.

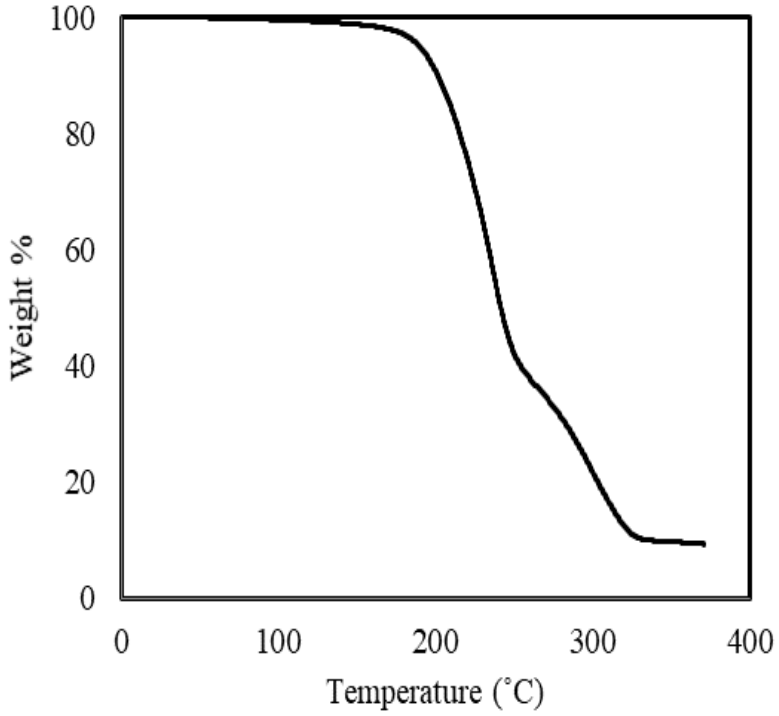


**Figure 4.31. TGA plot of MTM1:1**

Further, FTIR analysis of freshly prepared MTM1:1 was done and the spectra is shown in Figure 4.32. In the FTIR spectrum of the fresh MTM1:1, broader band with high intensity peak at 1724 $cm^{-1}$ with other broader band and high peak near 1169 $cm^{-1}$ can be observed. The band near 1724 $cm^{-1}$ can be assigned to the existence of hydrogen bond between − OH of DL-Malic acid and 'N' of Tetra -methyl ammonium chloride (− OH------N) (Kaur et al. 2018, Dai et al. 2015). Further, broader band and high peak near 1169 $cm^{-1}$ is assigned to the C−N stretching in tetra -methyl ammonium chloride. Very broad band in OH stretching region near 2916 $cm^{-1}$ indicates the formation of additional more hydrogen bonds between DL-malic acid and tetra -methyl ammonium chloride in the form of − OH (malic acid)···$Cl^-$ and DL-malic acid − DL-malic acid hydrogen bonds (Kaur et al. 2018, Xin et al. 2017).

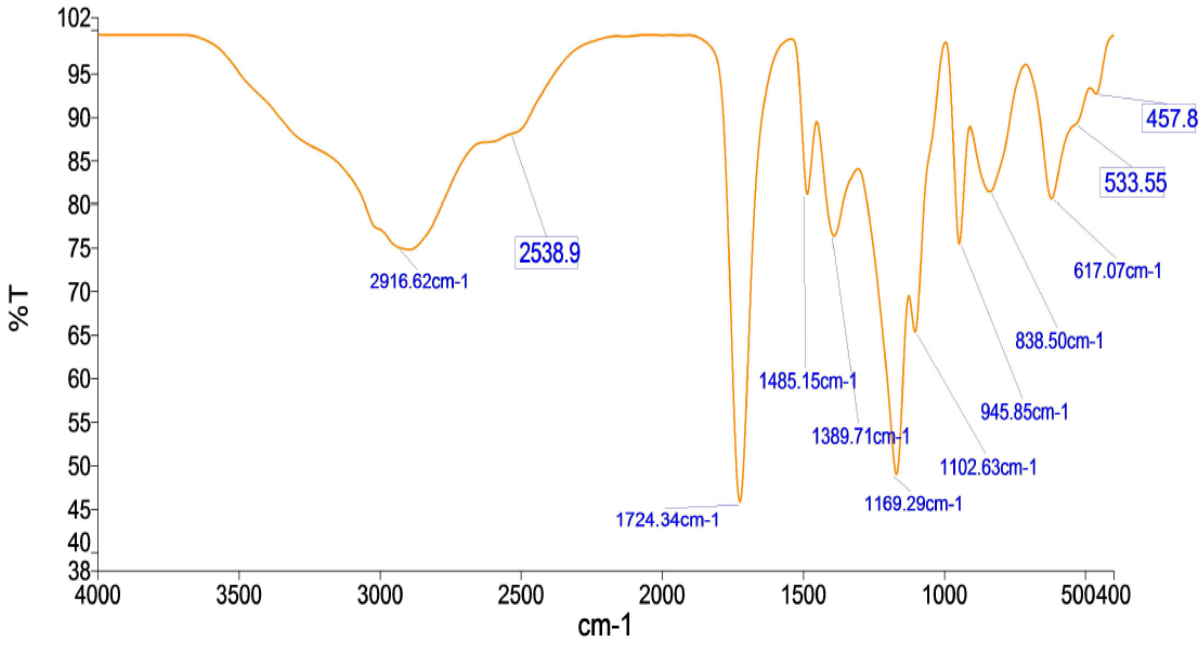


**Figure 4.32. FT-IR spectra for freshly prepared MTM1:1**

On the basis of above study, the hydrogen bonding between DL-malic acid and TMAC was proposed as shown in Figure 4.33. The formula unit of synthesized MTM1:1 is $(C_4H_{12}NO)^+NO^-.CH_2(CHOH)\text{-}2COOH$. The optimized structure studied by Gaussian 16 software is presented in Figure 4.34. $^1H$ NMR spectra of MTM1:1 was also determined and is given in Figure 4.35.

The viscosity, density and moisture Content of freshly prepared MTM1:1 was also determined by different analytical techniques discussed in chapter 3. Results of analysis are summarized in Table 4.16.

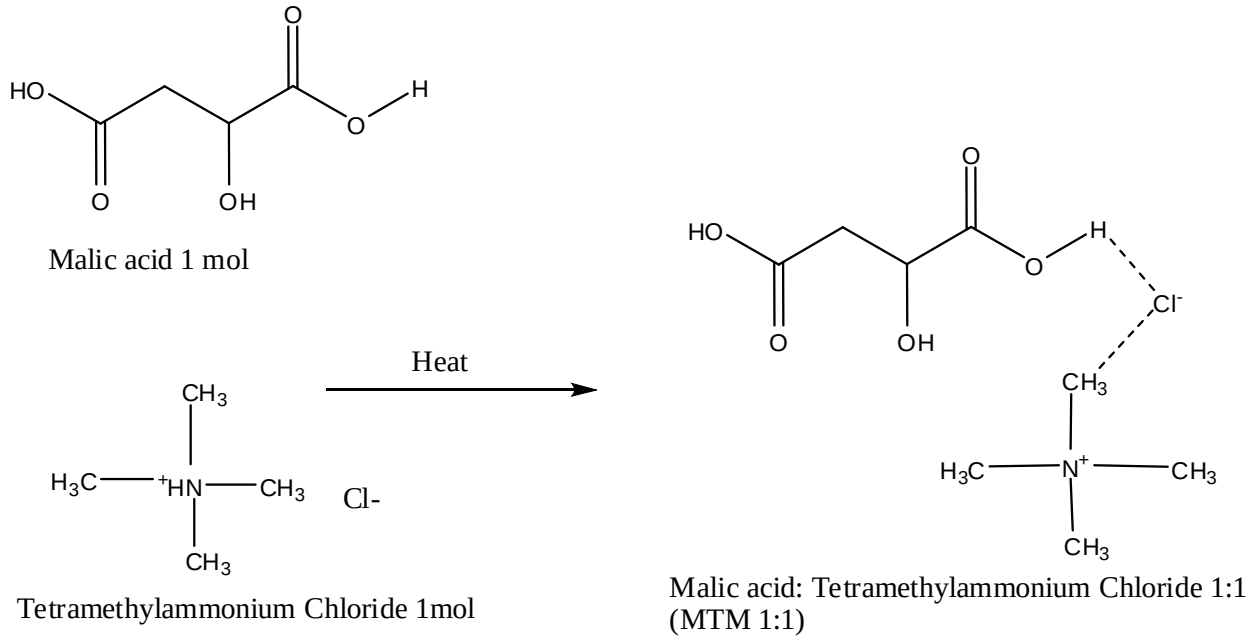


**Figure 4.33. Hydrogen Bonding Mechanism in Malic acid Tetramethylammonium Chloride 1:1 (MTM1:1)**

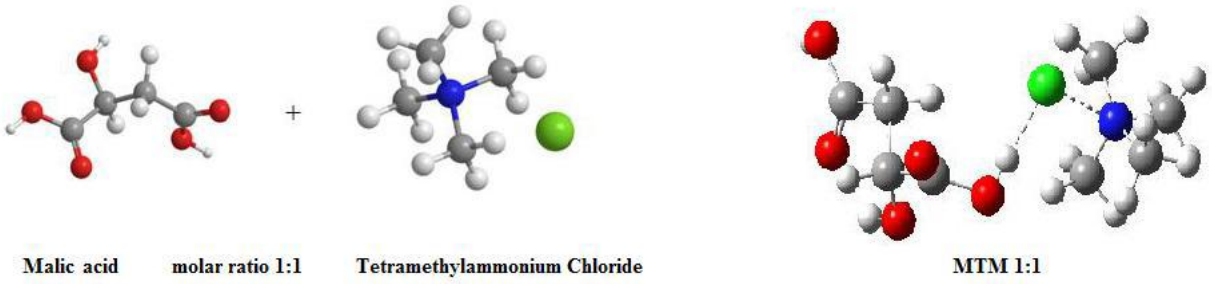


**Figure 4.34. Optimized Structure of MTM1:1**

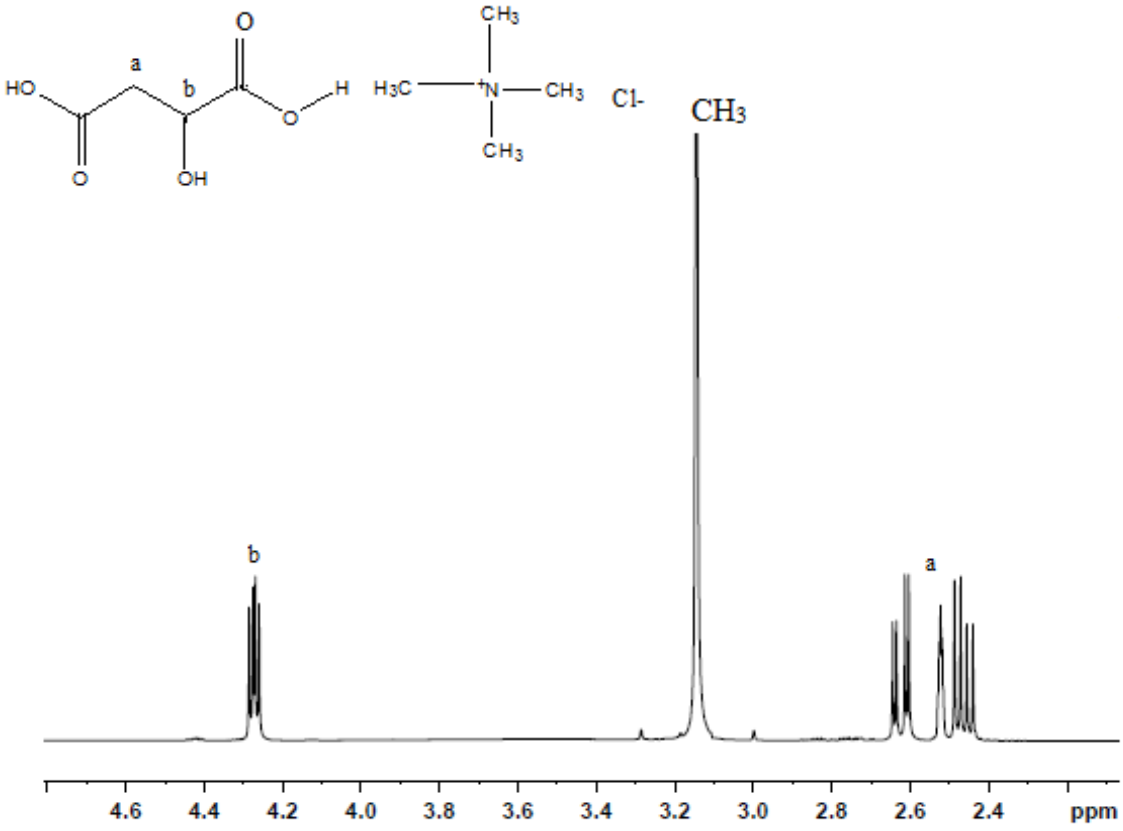


**Figure 4.35. $^{1}$NMR spectra of MTM1:1**

**Table 4.16. Physical Properties of MTM1:1**

| Properties | Value |
|---|---|
| Density (ρ) | 1.346 g/cm$^3$ |
| Viscosity (μ) | 36254.1 mPa/s |
| Moisture Content | 0.3 wt% |

#### 4.2.2.2 Vapor–liquid equilibrium (VLE) measurements using MTM1:1 as entrainer

To check the ability of MTM1:1 to break the ACN + water mixture, preliminary experiments were performed for azeotropic concentration of ACN + water system ($x_1' \approx$ 0.674). VLE data were generated for different MTM1:1 dosage ranging from 2 mol% to 20 mol% and relative volatility ($\alpha_{12}$) was evaluated. Experimental data are reported in Table 4.17. Variation in $\alpha_{12}$ of ACN to water with increase in MTM1:1 concentration is shown in Figure 4.36. MTM1:1 was found capable in enhancing the relative volatility of ACN to water, but this enhancement was less as compared to other used DESs (GC3:1, GTM3:1, MC1:1, MTM1:1).

**Table 4.17. Effect of MTM1:1 concentration on relative volatility $\alpha_{12}$ ($x_1' \approx$ 0.674) of ACN (1) + water (2) system, Relative volatilities $\alpha_{12}$ at atmospheric pressure (101.3 kPa): MTM1:1= (0 to 20) mol%**

| Mol% of MTM1:1 | Relative volatility $(\alpha_{12})$ |
|---|---|
| 0 | 1.06 |
| 2 | 1.24 |
| 5 | 1.55 |
| 7 | 1.72 |
| 10 | 2.10 |
| 12 | 2.49 |
| 15 | 3.08 |
| 20 | 3.97 |

Standard uncertainty $u(mol\%\ of\ MTM(1:1))$= 0.1, $u(\alpha)$ = 0.025.

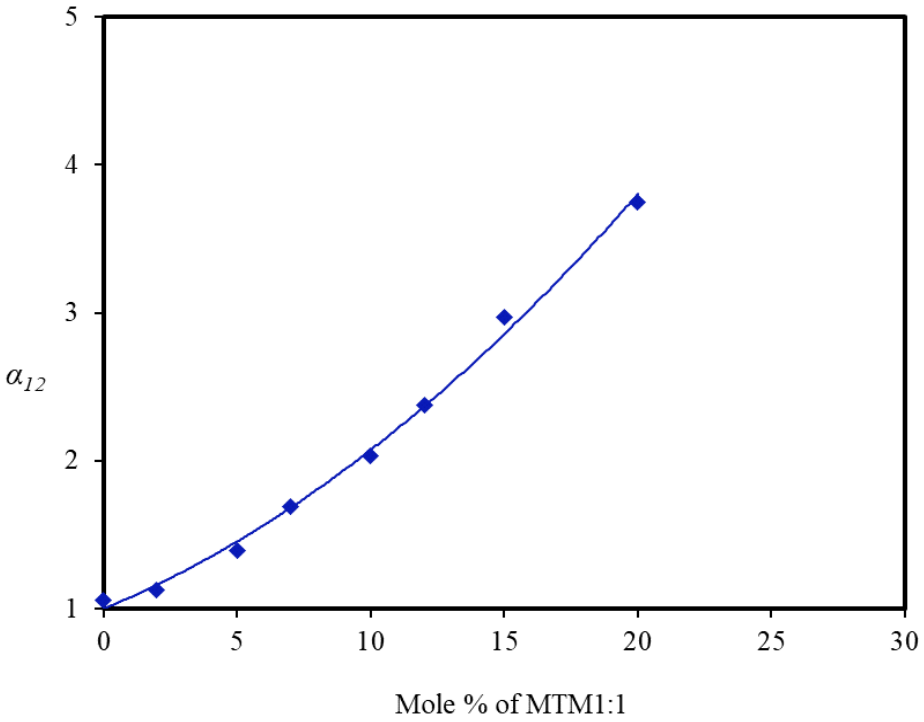


**Figure 4.36. Effect of MC1:1 concentration on relative volatility $\alpha_{12}$ ($x_1' \approx 0.674$) of ACN (1) + water (2) system at 101.3 kPa**

An experimental study for the isobaric VLE for the two pseudo-binary systems; ACN (1) + MTM1:1 (2) and water (1) + MTM1:1 (2) as well as pseudo-ternary system of ACN (1) + water (2) + MTM1:1 (3) was performed at 101.3 kPa, following the similar procedure. Pseudo-binary VLE data for both the systems are given in Table 4.18. Experimental data were also correlated with the NRTL model and deviations in activity coefficients $\Delta\gamma_i$ and temperature $\Delta T$ are also reported in Table 4.18. Variation in boiling points of water and ACN with the addition of MTM1: is shown in Figure 4.37 (a), (b) respectively. Pseudo-binary VLE data were correlated with the experimental data using NRTL model. The correlation results for the deviation in activity coefficient $\Delta\gamma_i$ and deviation in equilibrium temperature $\Delta T$ are presented in Tables 4.18 and average deviation in vapor mole fractions and temperature are presented in Tables 4.20. Results represent the good correlation between experimental VLE data and predicted values using NRTL model. Further, pseudo-ternary VLE studies were

performed for ACN (1) + water (2) + MTM1:1 (3) system by varying entrainer concentration (5 mol%, 10 mol% and 15 mol%) in the mixture. The results of experimental study are reported in Table 4.19.

**Table 4.18. Experimental VLE data and correlated results of pseudo-binary systems (Water + MTM1:1 and ACN + MTM1:1), Activity Coefficient $\gamma_i$, deviation in activity Coefficient $\Delta\gamma_i$ and deviation in equilibrium temperature $\Delta T$ at 101.3 kPa**

| **ACN (1) + MTM (1:1, mol/mol) (2)** | | | | | | |
|---|---|---|---|---|---|---|
| S. No. | $T\,(K)$ | Mole % of MTM (1:1) | $x_1$ | $\gamma_1^{\exp}$ | $\Delta\gamma_1^a$ | $\Delta T^b$ (K) |
| 1 | 354.7 | 0.0 | 1.000 | 0.999 | -0.0006 | 0.07 |
| 2 | 355.6 | 3.1 | 0.969 | 1.002 | 0.0016 | 0.00 |
| 3 | 356.6 | 6.3 | 0.937 | 1.005 | 0.0038 | -0.07 |
| 4 | 357.8 | 9.6 | 0.904 | 1.005 | 0.0019 | -0.01 |
| 5 | 358.9 | 13.1 | 0.869 | 1.011 | 0.0052 | -0.12 |
| 6 | 360.2 | 16.7 | 0.833 | 1.014 | 0.0051 | -0.12 |
| 7 | 361.6 | 20.5 | 0.795 | 1.019 | 0.0045 | -0.10 |
| 8 | 363.2 | 24.5 | 0.755 | 1.024 | 0.0007 | 0.03 |
| 9 | 364.7 | 28.7 | 0.713 | 1.037 | 0.0030 | -0.05 |
| 10 | 366.5 | 33.0 | 0.670 | 1.048 | 0.0002 | 0.04 |
| 11 | 368.5 | 37.6 | 0.624 | 1.062 | -0.0050 | 0.21 |
| 12 | 370.4 | 42.4 | 0.576 | 1.089 | -0.0035 | 0.16 |
| 13 | 372.5 | 47.5 | 0.525 | 1.125 | -0.0028 | 0.14 |
| 14 | 374.7 | 52.8 | 0.472 | 1.178 | 0.0041 | -0.08 |
| **Water (1) + MTM (1:1, mol/mol) (2)** | | | | | | |
| S. No. | $T\,(K)$ | Mole % of MTM (1:1) | $x_1$ | $\gamma_1^{\exp}$ | $\Delta\gamma_1^a$ | $\Delta T^b\,(K)$ |
| 1 | 373.1 | 0.00 | 1.000 | 1.002 | 0.0017 | 0.00 |
| 2 | 373.4 | 1.07 | 0.989 | 1.002 | 0.0021 | 0.01 |
| 3 | 373.9 | 2.23 | 0.978 | 0.995 | -0.0037 | -0.16 |
| 4 | 374.5 | 3.50 | 0.965 | 0.986 | -0.0096 | -0.32 |
| 5 | 375.2 | 4.89 | 0.951 | 0.976 | -0.0161 | -0.51 |

| | | | | | | |
|---|---|---|---|---|---|---|
| 6 | 375.8 | 6.41 | 0.936 | 0.971 | -0.0161 | -0.51 |
| 7 | 376.5 | 8.10 | 0.919 | 0.965 | -0.0155 | -0.50 |
| 8 | 377.2 | 9.97 | 0.900 | 0.961 | -0.0104 | -0.36 |
| 9 | 378.3 | 12.05 | 0.879 | 0.947 | -0.0133 | -0.45 |
| 10 | 379.6 | 14.40 | 0.856 | 0.930 | -0.0166 | -0.56 |
| 11 | 381.0 | 17.05 | 0.829 | 0.914 | -0.0153 | -0.53 |
| 12 | 382.6 | 20.08 | 0.799 | 0.898 | -0.0104 | -0.39 |
| 13 | 384.5 | 23.57 | 0.764 | 0.881 | -0.0024 | -0.13 |
| 14 | 386.8 | 27.63 | 0.724 | 0.862 | 0.0078 | 0.22 |
| 15 | 389.7 | 32.42 | 0.676 | 0.838 | 0.0196 | 0.68 |

Standard uncertainty $u(x_1) = 0.003, u(T) = 0.1\ K, u\left(mol\%\ of\ MTM(1:1)\right)$= 0.1, $u\left(P\right) = 0.05 kPa.$ [a] $\Delta\gamma_1 = \gamma_1^{\exp} - \gamma_1^{cal}$, [b] $\Delta T = T^{\exp} - T^{cal}$

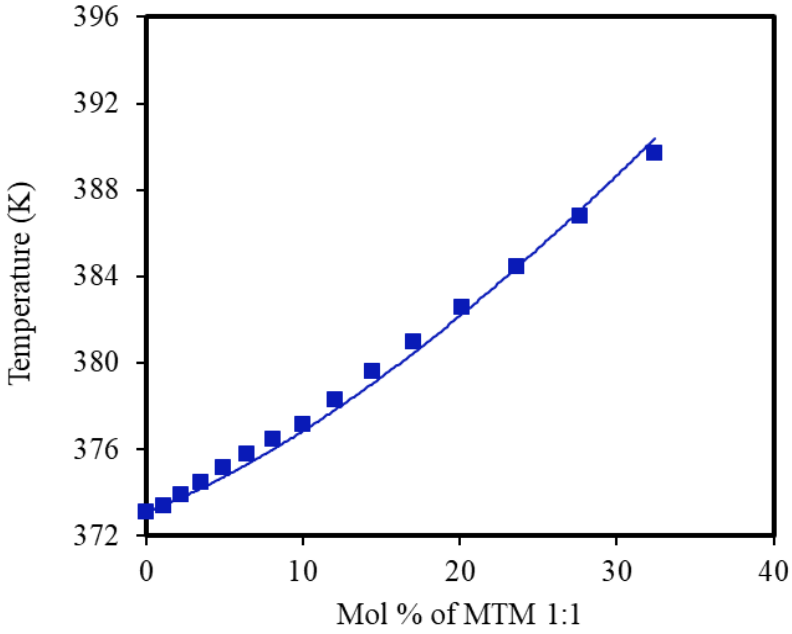


(a)

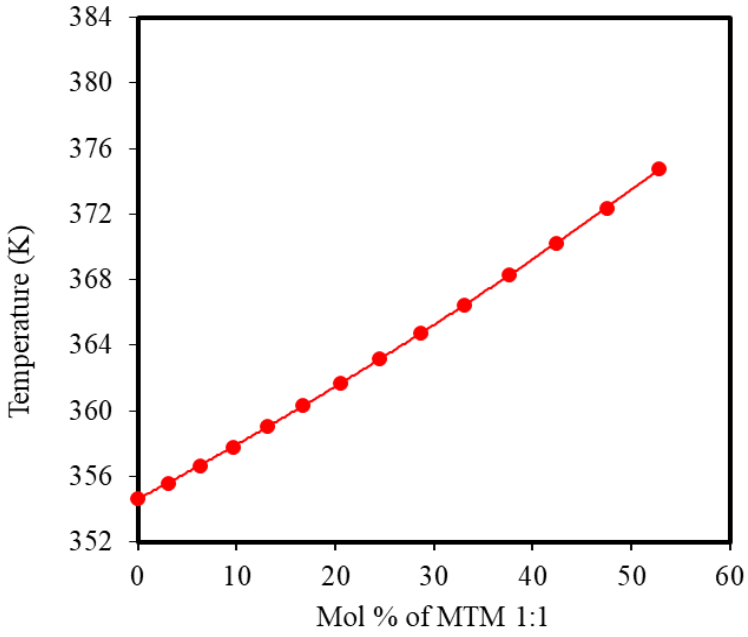


**(b)**

**Figure 4.37 (a), (b) Effect of MTM 1:1 on the normal boiling point of water and ACN at 101.3 kPa. Experimental data for water (■) and ACN (■); and solid lines, calculations based on NRTL model**

**Table 4.19. Experimental Isobaric VLE data for ACN (1) + water (2) + MTM1:1(3) system, experimental Activity Coefficient $\gamma_i^{exp}$ and Relative Volatilities $\alpha_{12}$ at 101.3 kPa**

| S. No. | $T$ (K) | $x_1^{'}$ | $x_1$ | $x_2$ | $y_1$ | $\gamma_1^{exp}$ | $\gamma_2^{exp}$ | $\alpha_{12}$ |
|---|---|---|---|---|---|---|---|---|
| **Malic acid/ TMAC 1:1= 5 mol%** | | | | | | | | |
| 1 | 356.5 | 1.000 | | | 1.000 | | | |
| 2 | 356.8 | 0.946 | 0.886 | 0.064 | 0.932 | 0.986 | 1.967 | 0.78 |
| 3 | 357.0 | 0.927 | 0.786 | 0.165 | 0.911 | 1.079 | 0.991 | 0.81 |
| 4 | 357.3 | 0.904 | 0.743 | 0.207 | 0.892 | 1.108 | 0.947 | 0.88 |
| 5 | 357.8 | 0.841 | 0.691 | 0.259 | 0.867 | 1.140 | 0.914 | 1.23 |
| 6 | 358.5 | 0.765 | 0.658 | 0.294 | 0.827 | 1.118 | 1.019 | 1.47 |
| 7 | 359.3 | 0.685 | 0.603 | 0.348 | 0.772 | 1.112 | 1.100 | 1.55 |
| 8 | 360.0 | 0.649 | 0.574 | 0.375 | 0.745 | 1.104 | 1.111 | 1.58 |
| 9 | 360.9 | 0.626 | 0.527 | 0.423 | 0.738 | 1.159 | 0.977 | 1.68 |
| 10 | 361.9 | 0.603 | 0.485 | 0.464 | 0.728 | 1.206 | 0.890 | 1.76 |
| 11 | 363.0 | 0.531 | 0.457 | 0.493 | 0.660 | 1.123 | 1.004 | 1.71 |
| 12 | 364.1 | 0.509 | 0.428 | 0.520 | 0.652 | 1.147 | 0.934 | 1.81 |
| 13 | 365.2 | 0.483 | 0.385 | 0.565 | 0.638 | 1.210 | 0.857 | 1.89 |
| 14 | 366.1 | 0.426 | 0.339 | 0.610 | 0.577 | 1.209 | 0.898 | 1.84 |
| 15 | 367.4 | 0.388 | 0.302 | 0.649 | 0.548 | 1.242 | 0.859 | 1.91 |
| 16 | 368.8 | 0.363 | 0.275 | 0.675 | 0.535 | 1.279 | 0.807 | 2.02 |
| 17 | 370.0 | 0.338 | 0.241 | 0.710 | 0.519 | 1.368 | 0.759 | 2.11 |
| 18 | 371.1 | 0.302 | 0.206 | 0.744 | 0.482 | 1.441 | 0.750 | 2.15 |
| 19 | 372.2 | 0.263 | 0.184 | 0.766 | 0.438 | 1.422 | 0.759 | 2.18 |
| 20 | 372.9 | 0.217 | 0.153 | 0.795 | 0.378 | 1.447 | 0.789 | 2.19 |
| 21 | 373.9 | 0.147 | 0.127 | 0.824 | 0.276 | 1.238 | 0.855 | 2.21 |
| 22 | 374.6 | 0.099 | 0.083 | 0.867 | 0.204 | 1.373 | 0.872 | 2.33 |
| 23 | 375.8 | 0.000 | | | 0.000 | | | |
| **Malic acid/TMAC 1:1= 10 mol%** | | | | | | | | |
| 1 | 358.0 | 1.000 | | | 1.000 | | | |
| 2 | 358.1 | 0.946 | 0.879 | 0.021 | 0.969 | 0.993 | 2.597 | 1.78 |
| 3 | 358.3 | 0.898 | 0.791 | 0.109 | 0.946 | 1.071 | 0.865 | 1.99 |
| 4 | 358.7 | 0.861 | 0.740 | 0.161 | 0.912 | 1.090 | 0.940 | 1.67 |
| 5 | 359.0 | 0.790 | 0.704 | 0.196 | 0.879 | 1.094 | 1.048 | 1.93 |
| 6 | 359.5 | 0.730 | 0.659 | 0.243 | 0.852 | 1.116 | 1.014 | 2.13 |
| 7 | 359.9 | 0.706 | 0.648 | 0.252 | 0.835 | 1.099 | 1.074 | 2.11 |
| 8 | 360.5 | 0.645 | 0.571 | 0.329 | 0.782 | 1.147 | 1.061 | 1.97 |
| 9 | 361.2 | 0.617 | 0.553 | 0.348 | 0.767 | 1.138 | 1.044 | 2.04 |
| 10 | 361.8 | 0.583 | 0.526 | 0.376 | 0.742 | 1.137 | 1.045 | 2.06 |

| | | | | | | | | |
|---|---|---|---|---|---|---|---|---|
| 11 | 362.7 | 0.529 | 0.462 | 0.439 | 0.696 | 1.182 | 1.019 | 2.04 |
| 12 | 363.8 | 0.471 | 0.430 | 0.470 | 0.648 | 1.145 | 1.057 | 2.07 |
| 13 | 364.8 | 0.445 | 0.389 | 0.512 | 0.635 | 1.205 | 0.969 | 2.17 |
| 14 | 366.0 | 0.408 | 0.362 | 0.541 | 0.608 | 1.197 | 0.941 | 2.25 |
| 15 | 367.3 | 0.370 | 0.345 | 0.555 | 0.578 | 1.150 | 0.941 | 2.33 |
| 16 | 368.7 | 0.317 | 0.291 | 0.609 | 0.524 | 1.187 | 0.919 | 2.37 |
| 17 | 370.1 | 0.274 | 0.247 | 0.654 | 0.479 | 1.229 | 0.889 | 2.44 |
| 18 | 371.3 | 0.246 | 0.227 | 0.674 | 0.450 | 1.214 | 0.872 | 2.51 |
| 19 | 372.3 | 0.213 | 0.187 | 0.723 | 0.407 | 1.296 | 0.846 | 2.54 |
| 20 | 373.5 | 0.175 | 0.173 | 0.727 | 0.352 | 1.172 | 0.880 | 2.56 |
| 21 | 374.6 | 0.146 | 0.127 | 0.774 | 0.306 | 1.346 | 0.851 | 2.58 |
| 22 | 375.9 | 0.104 | 0.094 | 0.807 | 0.232 | 1.330 | 0.863 | 2.60 |
| 23 | 377.5 | 0.000 | | | 0.000 | | | |
| **Malic acid/TMAC 1:1= 15 mol%** | | | | | | | | |
| 1 | 359.6 | 1.000 | | | 1.000 | | | |
| 2 | 359.9 | 0.932 | 0.792 | 0.058 | 0.991 | 1.067 | 0.254 | 8.03 |
| 3 | 360.1 | 0.887 | 0.771 | 0.079 | 0.959 | 1.055 | 0.844 | 2.98 |
| 4 | 360.5 | 0.838 | 0.735 | 0.115 | 0.946 | 1.078 | 0.752 | 3.39 |
| 5 | 360.8 | 0.782 | 0.712 | 0.140 | 0.932 | 1.087 | 0.769 | 3.82 |
| 6 | 361.3 | 0.745 | 0.609 | 0.241 | 0.909 | 1.221 | 0.586 | 3.42 |
| 7 | 361.9 | 0.681 | 0.571 | 0.279 | 0.856 | 1.205 | 0.783 | 2.78 |
| 8 | 362.7 | 0.611 | 0.513 | 0.337 | 0.799 | 1.222 | 0.878 | 2.53 |
| 9 | 363.4 | 0.562 | 0.469 | 0.380 | 0.759 | 1.244 | 0.909 | 2.45 |
| 10 | 364.3 | 0.521 | 0.438 | 0.414 | 0.729 | 1.246 | 0.907 | 2.47 |
| 11 | 365.4 | 0.479 | 0.417 | 0.433 | 0.703 | 1.222 | 0.911 | 2.57 |
| 12 | 366.9 | 0.435 | 0.348 | 0.501 | 0.679 | 1.355 | 0.805 | 2.75 |
| 13 | 368.3 | 0.367 | 0.307 | 0.543 | 0.615 | 1.336 | 0.846 | 2.76 |
| 14 | 369.5 | 0.339 | 0.276 | 0.574 | 0.598 | 1.396 | 0.799 | 2.90 |
| 15 | 370.8 | 0.309 | 0.251 | 0.600 | 0.574 | 1.421 | 0.773 | 3.01 |
| 16 | 371.8 | 0.278 | 0.238 | 0.612 | 0.545 | 1.383 | 0.780 | 3.11 |
| 17 | 372.9 | 0.256 | 0.206 | 0.644 | 0.526 | 1.495 | 0.743 | 3.23 |
| 18 | 373.8 | 0.223 | 0.179 | 0.673 | 0.482 | 1.538 | 0.752 | 3.24 |
| 19 | 375.0 | 0.189 | 0.157 | 0.692 | 0.435 | 1.531 | 0.764 | 3.30 |
| 20 | 376.3 | 0.158 | 0.141 | 0.711 | 0.387 | 1.463 | 0.771 | 3.36 |
| 21 | 377.5 | 0.134 | 0.119 | 0.731 | 0.348 | 1.509 | 0.765 | 3.45 |
| 22 | 378.9 | 0.098 | 0.106 | 0.745 | 0.278 | 1.303 | 0.791 | 3.54 |
| 23 | 380.4 | 0.000 | | | 0.000 | | | |

Standard uncertainty $u(x_1) = u(x_1') = u(y) = 0.003, u(T) = 0.1\ K, u(mol\%\ of\ MTM1{:}1)$ =0.1. $x_1'$ *is mole fraction of ACN in liquid phase expressed on MTM1:1 free basis.*

The $T - x, y$ diagrams for 5 mol%, 10 mol% and 15 mol% MTM1:1 dosage are shown in Figure 4.38 (a), (b) and (c) respectively, to represent the salting-out effect of MTM1:1.

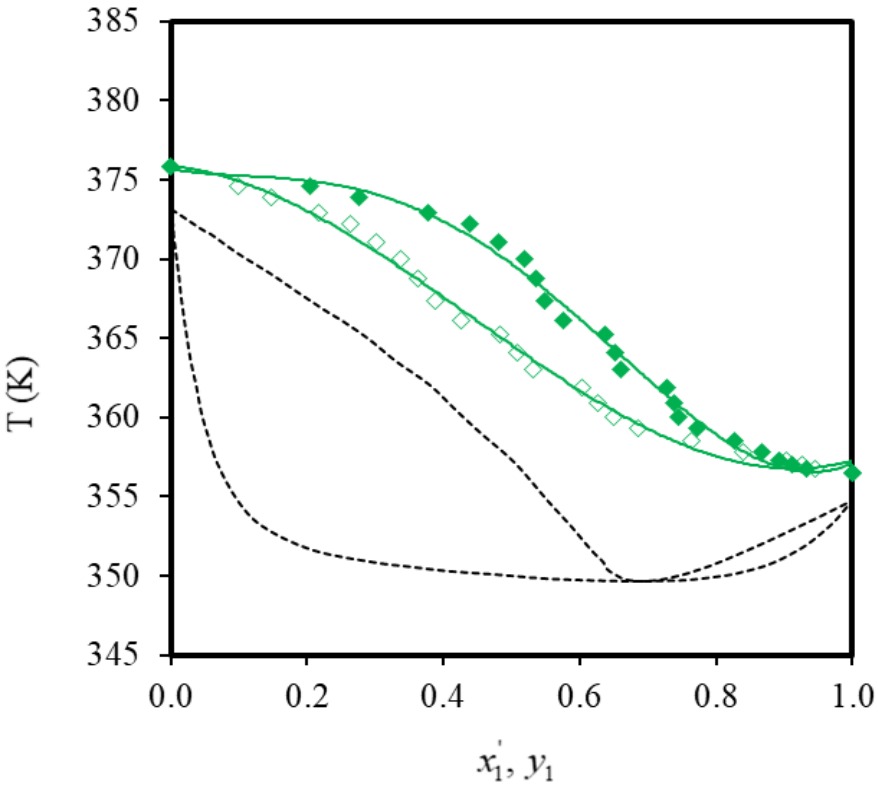


**Figure 4.38. (a) Temperature−composition diagram for the acetonitrile (1) + water (2) + MTM1:1 (3) system at 101.3 kPa with MTM1:1= 5 mol%. $x_1'$ vs T (♦) and $y_1$ vs T (◊), --- MTM1:1= 0%**

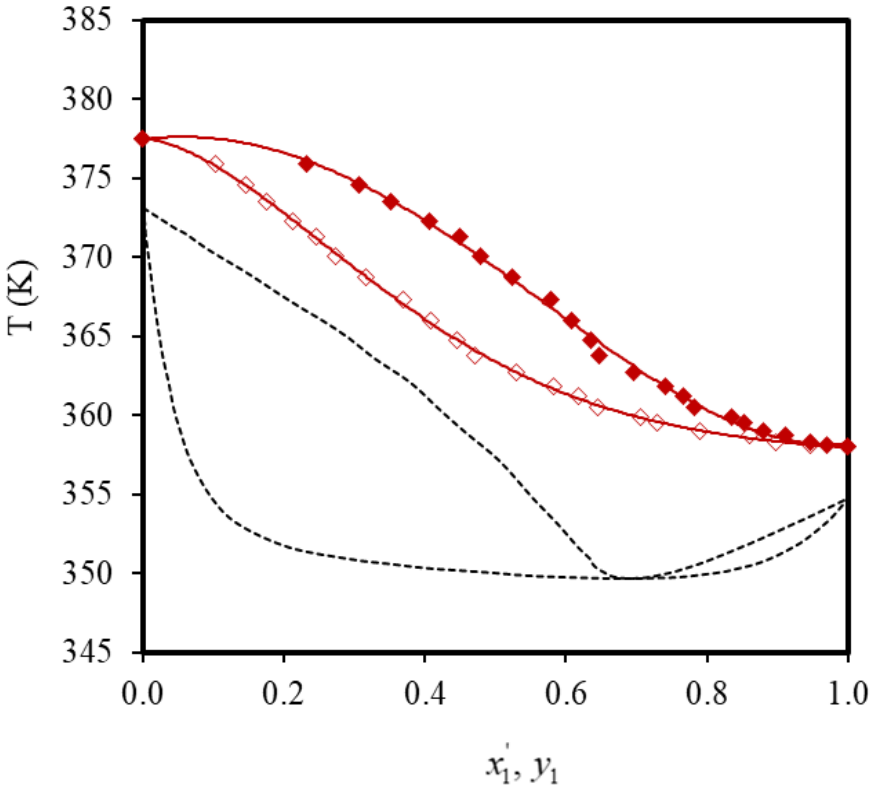


**Figure 4.38. (b) Temperature−composition diagram for the acetonitrile (1) + water (2) + MTM1:1 (3) system at 101.3 kPa with MTM1:1= 15 mol%. $x_1'$ vs T (♦) and $y_1$ vs T (◊), --- MTM1:1= 0%**

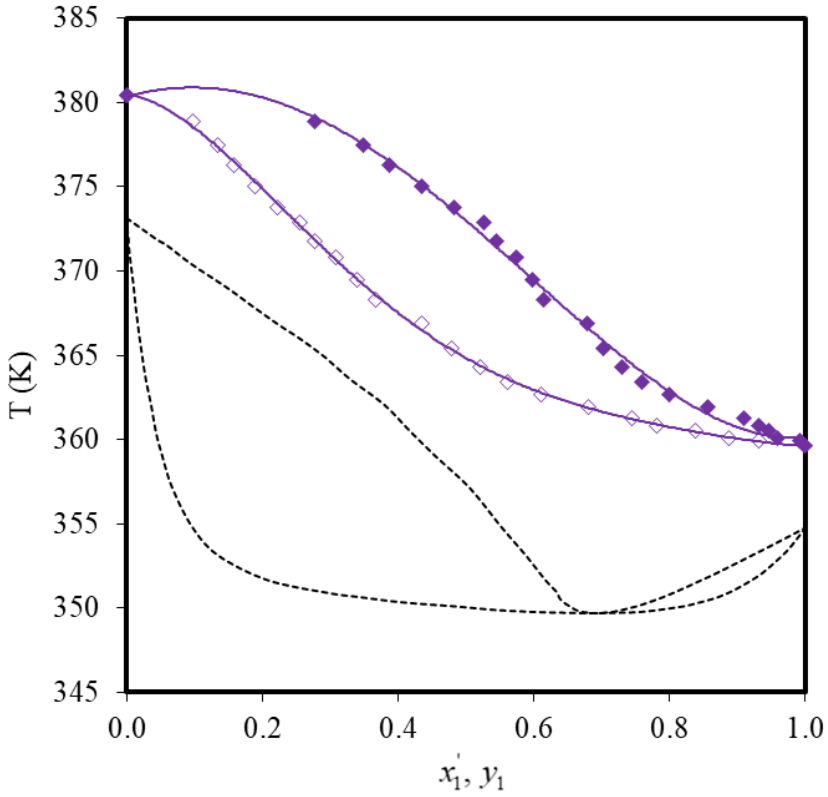


**Figure 4.38. (c) Temperature−composition diagram for the acetonitrile (1) + water (2) + MTM1:1 (3) system at 101.3 kPa with MTM1:1= 5 mol%.** $x_1'$ **vs T (♦) and** $y_1$ **vs T (◊), --- MTM1:1= 0%**

The equilibrium diagrams for these experimental conditions are also depicted in Figure 4.39. The results demonstrate that MTM1:1 could successfully eliminate ACN + water azeotrope but at higher entrainer dosage only. Addition of 5 mol% MTM1:1 enhances the relative volatility of ACN to water and considerable shifting in azeotrope was observed, but it could not break the azeotrope at this concentration. At higher dosage (10 mol% and 15 mol%) equilibrium curves were lying above the diagonal line for the entire concentration range. The experimental data for ACN (1) + water (2) + MTM1:1 (3) pseudo-ternary systems were also correlated successfully using NRTL model. The average absolute differences for the equilibrium temperature and the ACN mole fraction in the vapor phase were 0.45 and 0.0011 respectively. The deviations between experimental and predicted values are reported in Table 4.20 and shown in Figure 4.39. NRTL interaction parameters vales are reported.

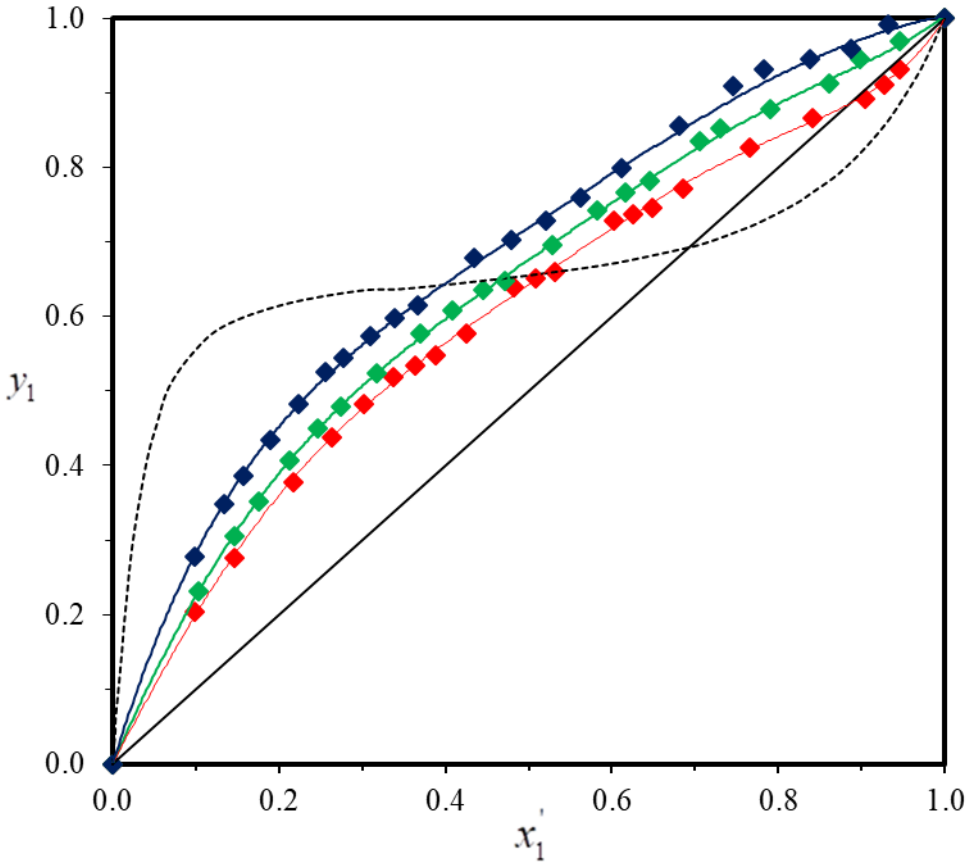


**Figure 4.39. Experimental and calculated VLE data for ACN (1) + water (2) + MTM1:1 (3) pseudo-ternary system at 101.3 kPa. For MTM1:1= 5 mol% (♦), for MTM1:1= 10 mol% (♦), for MTM1:1= 15 mol% (♦), --- MTM1:1= 0% and solid lines, calculations based on the NRTL model**

**Table 4.20. The parameters and correlation deviations of NRTL model for MTM1:1 containing systems at 101.3 kPa**

| Systems | $\Delta g_{12}$ | $\Delta g_{21}$ | $\alpha$ | $DT(K)$ | $dT(K)$ | $Dy_1$ | $dy_1$ |
|---|---|---|---|---|---|---|---|
| ACN (1)+MTM1:1 (2) | -1204.3 | 5005.9 | 0.3 | 0.09 | 0.22 | | |
| Water (1)+MTM1:1 (2) | 5586.6 | -6197.5 | 0.3 | 0.36 | 0.68 | | |
| ACN (1)+water (2) + MTM1:1 (3) | -1563.4 | 2632.9 | 0.3 | 0.45 | 0.4 | 0.0011 | 0.009 |

$\Delta g_{12}=(g_{12}-g_{22});\ \Delta g_{21}=(g_{21}-g_{11})$

$$DT=(1/n)\sum_{k=1}^{n}\left|T^{\exp}-T^{cal}\right|_k$$

$$dT=\max\left(\left|T^{\exp}-T^{cal}\right|\right)$$

$$Dy_1=(1/n)\sum_{k=1}^{n}\left|y_1^{\exp}-y_1^{cal}\right|_k$$

$$dy_1=\max\left(\left|y_1^{\exp}-y_1^{cal}\right|\right)$$

#### 4.2.2.3 Recoverability test of MTM1:1

MTM1:1 was recovered following the same procedure used for previously employed DESs. Figure 4.40 represents the FT-IR spectrum of recovered MTM1:1 after fifth cycle. No notable change was observed between FT-IR spectra of freshly prepared and recovered MTM1:1. Although the chemical properties were found stable but while reusing it slight decrease in performance was observed.

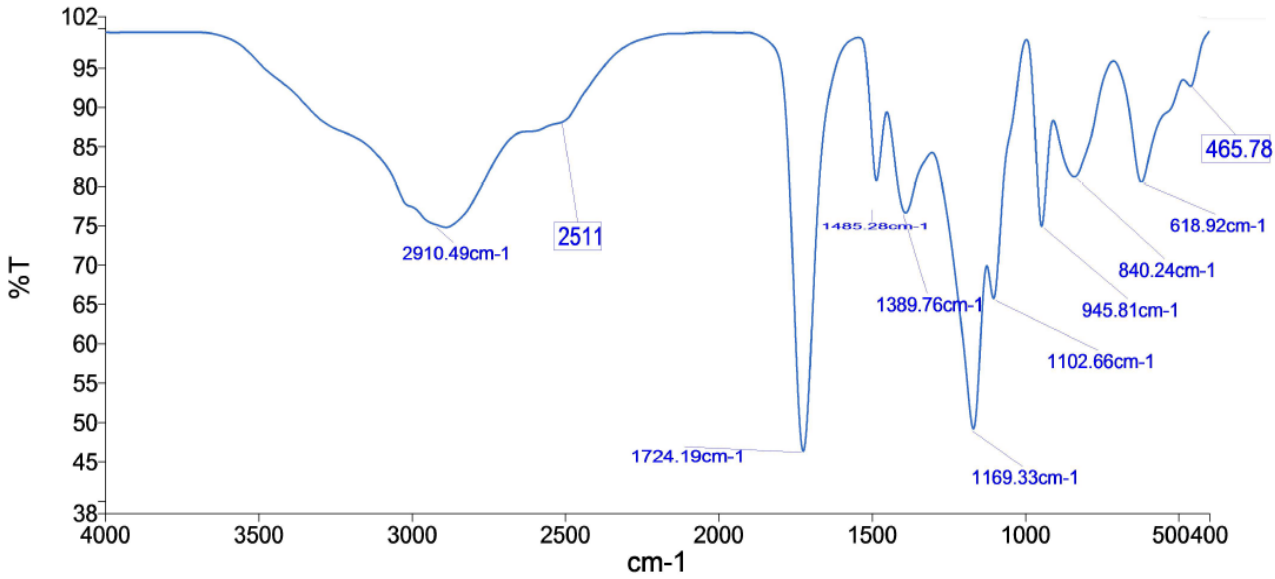


**Figure 4.40 FT-IR spectrum of MTM1:1 after use**

While comparing the performance of used NADESs as entrainer for separation of ACN + water mixture, MC1:1 was found more eligible than MTM1:1. As the value of basicity increases with the increment of the alkyl groups in the acid as well as the salt cation present in the DES. The chemical composition of MC1:1 contains more alkyl groups, due to which the basicity of the MC1:1 is higher than the MTM1:1. More the basicity of the compound, stronger the hydrogen bond will be (Teles et al. 2017). Also, in Choline chloride there is hydroxyl group present which enhance the hydrogen bonding between HBD and HBA. The hydrogen bond presents between the DES and water influence the activity coefficient of the water. Lower the value of activity coefficient indicates that there is strong bond present between the DES and water leads to the lower volatility of water. Hence the relative volatility of ACN/water will be higher. Due to which the azeotrope can be easily broken (Rodríguez et al. 2015).

*Chapter - 5*

# CONCLUSIONS

## 5.0. GENERAL

On behalf of the outcomes obtained in the results and discussion section of present study for synthesis and application of different types of DESs in breaking the ACN + water azeotrope, following major conclusions were drawn:

## 5.1. SUGAR BASED DEEP EUTECTIC SOLVENTS

- High relative volatility values of ACN to water for GC 3:1 and GTM 3:1 proves its applicability as entrainer for separation of ACN + water azeotropic mixture. These DESs can be excellent replacement of the ILs as well as volatile organic solvents.
- Deep eutectic solvents comprising carboxylic acids and ammonium-based salts present the greater ability to donate and accept protons while comparing with organic molecular solvents and most of the ILs.
- High separation ability presented by GTM 3:1 as compared to GC 3:1 proves that, DESs

  withouthydroxyl group in its HBA presents better separation ability than DESs containing hydroxyl group in its HBA. Due to the electron withdrawing nature of hydroxyl group, the chances of formation of hydrogen bonding with water becomes very low in case of GC3:1. On the other hand, in GTM3:1, tetramethylammonium chloride is used as HBA, which consists four methyl groups that are electron donating in nature. Therefore, strong hydrogen bond between water and DES results better separation of ACN + water mixture.
- The successful recovery and reuse of both DESs (GC 3:1 and GTM 3:1) till multiple cycles with stable chemical properties proves its applicability as entrainer for separation of azeotropic mixtures.
- Good agreement between experimental results (for pseudo-binary & pseudo-ternary systems) and predicted valueswith minor deviations, demonstrate that, NRTL model is capable in predicting the VLE data for sugar based DESs containing system.The average absolute deviation in vapor phase mole fraction of ACN in case of GC 3:1 and

GTM 3:1 were 0.009 and 0.007 respectively. The average absolute difference for the equilibrium temperature for GC 3:1 and GTM 3:1 was 0.42 K and 0.45K respectively.

- The distinctive features of sugar based DESs like; single step preparation, no further purification requirement, low cost, less toxicity and more biodegradable components than ILs makes them attractive solvent.

## 5.2. NATURAL DEEP EUTECTIC SOLVENTS

- Both constituents of DESs, hydrogen bond acceptors (HBAs) and hydrogen bond donors (HBDs) play important roles in breaking the ACN + water azeotrope.
- Comparing the performance of NADESs, the MC 1:1 was performing better than the MTM 1:1. The value of the basicity increases with the increment of the alkyl groups in the acid as well as the salt cation present in the DES. The chemical composition of MC 1:1 contains more alkyl groups due to which, the basicity of the MC1:1is higher than the MTM 1:1. More the basicity of the compound, stronger the hydrogen bond will be. The hydrogen bond presents between the DES and water influence the activity coefficient of the water. Lower the value of activity coefficient indicates that there is strong bond present between the DES and water which leads to the lower volatility of water. Hence the relative volatility of ACN to water will be higher. Due to which the azeotrope can be easily broken.
- Moreover, the required concentration of both studied NADESs for breaking ACN + water mixture is still higher than that of simple sugar based DESs and fewconventional solvents such as butyl acetate, which is also not economically attractive.
- High viscosity of MC1:1 and MTM1:1 NADESs is a great limitation for its industrial application as an entrainer, but by altering its properties, it can be used as an entrainer in future.
- Nonetheless, the additional features of NADESs like, natural and biodegradable starting compounds and non-corrosive nature adds more value than sugar based DESs for separation of azeotropic mixtures.

- NRTL model could successfully correlate the experimental data for NADES containing systems also. The average absolute deviation for vapor phase mole fraction of ACN in case of MC1:1 and MTM1:1 were0.002 and 0.001 respectively and the average absolute difference for the equilibrium temperature of MC 1:1 and MTM 1:1 was 0.15 K and 0.45 K respectively

**FUTURE RECOMMENDATION**

- Most of the DESs use salts as HBAs, so prior to industrial application of DESs, it is of great importance to study its corrosion potential, otherwise it may harm the industrial equipment.
- High viscosity of NADESs is a great limitation for its industrial application as an entrainer.

  In future more NADESs should be explored, which can give high separation performance with low viscosity, while retaining its positive feature of natural and biodegradable constituents.
- The possibility of esterification of the DESs at the time of recovery, should also be explored in detail.

# REFERENCES


Abbott, A. P., Barron, J. C., Ryder, K. S., & Wilson, D. (2007) Eutectic-Based Ionic Liquids with Metal-Containing Anions and Cations. *Chemistry—A European Journal*, *13* (22), 6495–6501.

Abbott, A. P., Boothby, D., Capper, G., Davies, D. L., & Rasheed, R. (2004) Deep Eutectic Solvents Formed Between Choline Chloride and Carboxylic Acids. *Journal of the American Chemical Society*, *126* (9), 9142.

Abbott, A. P., Capper, G., & Gray, S. (2006). Design of Improved Deep Eutectic Solvents Using Hole Theory. *Chemphyschem*, 7 (4), 803–806.

Abbott, A. P., Capper, G., Davies, D. L., Rasheed, R. K., & Tambyrajah, V. (2003) Novel Solvent Properties of Choline Chloride/urea Mixtures. *Chemical communications (Cambridge, England)*, 1, 70–71.

Abbott, A. P., Harris, R. C., Ryder, K. S., D'Agostino, C., Gladden, L. F., & Mantle, M. D. (2011). Glycerol Eutectics as Sustainable Solvent Systems. *Green Chemistry*, *13* (1), 82–90.

Abbott, A.P., Ahmed, E.I., Harrisa, R. C., &Rydera, K. S. (2014). Evaluating water miscible deep eutectic solvents (DESs) and ionic liquids as potential lubricants. *Green Chemistry*, 16, 4156–4161.

Abbott, A.P., Capper, G., McKenzie, K.J., & Ryder. K.S. (2007). Electrodeposition of zinc-tin alloys from deep eutectic solvents based on choline chloride, 599 (2), *Journal of Electroanalytical Chemistry*, 288–294.

Abbott, A.P., Cullis, P.M., Gibson, M.J., Harris, R.C., & Raven, E. (2007). Extraction of glycerol from biodiesel into a eutectic based ionic liquid. *Green Chemistry*, 9, 868–872.

Abdul Mudalip, S. K., Ripin, A., MohdYunus, R., Sulaiman, S. Z., & Che Man, R. (2011). Effects of Ultrasonic Waves on Vapor-Liquid Equilibrium of Cyclohexane/ Benzene. *International Journal on Advanced Science, Engineering and Information Technology*, *1* (1), 72.

Acosta, J., Arce, A., Rodil, E., & Soto, A. (2002). A thermodynamic study on binary and ternary mixtures of acetonitrile, water and butyl acetate, *Fluid Phase Equilibria*, 203, 83–98.

Acosta, J., Rodríguez, I., Jáuregui, U., Nuevas, L. &Pardillo, E. (2006). Recovery of acetonitrile from aqueous waste by a combined process: Solvent extraction and batch distillation. *Separation and Purification Technology*, 52, 95−101.

Adoor, S. G., Prathab, B., Manjeshwar, L. S., &Aminabhavi, T. M. (2007) Mixed matrix membranes of sodium alginate and poly(vinyl alcohol) for pervaporation dehydration of isopropanol at different temperatures. *Polymer*, 48 (18), 5417–5430.

Aparicio, S., Atilhan, M., &Karadas, F. (2010) Thermophysical Properties of Pure Ionic Liquids: Review of Present Situation. *Industrial & Engineering Chemistry Research,49* (20), 9580–9595.

Aptel, P., Challard, N., Cuny, J., & Neel, J. (1976) Application of the Pervaporation Process to Separate Azeotropic Mixtures.*Journal of Membrane Science, 1*, 271–287.

Arif, Z., Sethy, N.K., Mishra, P.K., Upadhayay, S.N. & Verma, B. (2017). Investigating the influence of sol gel derived PVA/SiO2 nanocomposite membrane on pervaporation separation of azeotropic mixture I. Effect of operating condition. *Journal of Porous Materials*, 1-9. Mishra

Bhat, S.D., &Aminabhavi, T.M. (2006). Novel sodium alginate composite membranes incorporated with SBA-15 molecular sieves for the pervaporation dehydration of aqueous mixtures of isopropanol and 1,4-dioxane at 30 C. *Microporous Mesoporous Material*, 91(1), 206–214.

Bhat, S.D., &Aminabhavi, T.M. (2007). Pervaporation separation using sodium alginate and its modified membranes—a review. *Separation and Purification Reviews*, 36(3), 203–229.

Boczkaj, G., Przyjazny, A., & Kaminski, M.(2014). New Procedures for Control of Industrial Effluents Treatment Processes. *Industrial & Engineering Chemistry Research*, 53, 1503−1514.

Bonhote, P., Dias, A.-P., Papageorgiou, N., Kalyanasundaram, K., &Gratzel, M. (1996). Hydrophobic, Highly Conductive Ambient-Temperature Molten Salts. *Inorganic Chemistry*, *35* (5), 1168–1178.

Brandt, A., Grasvik, J., Hallett, J. P., & Welton, T. (2013). Deconstruction of Lignocellulosic Biomass with Ionic Liquids. Green Chemistry, *15* (3), 550.

Brennecke, J. F., Maginn, E. J. (2001) Ionic Liquids: Innovative Fluids for Chemical Processing. *AIChE Journal*, 47(11), 2384–2389.

Brunjes,A. S., & Bogart, M.J.P. (1977). Vapor−Liquid Equilibria for commercially important systems of organic solvents. *Industrial* and *Engineering Chemistry*, 35, 255–260.

Calvar, N., Gonzalez, B., Gomez, E., & Dominguez, A. (2007). Study of the Behaviour of the Azeotropic Mixture Ethanol–water with Imidazolium-Based Ionic Liquids. *Fluid Phase Equilibria*, *259* (1), 51–56.

Chemat, F., Cravotto, G., (2013). Microwave-Assisted Extraction for Bioactive Compounds. *Food Engineering Series*, *Springer*.

Chronopoulos, T., Fernandez-Diez, Y., Maroto-Valer, M. M., Ocone, R., & Reay, D. A. (2014). $CO_2$Desorptionvia Microwave Heating for Post-Combustion Carbon Capture. *Microporous Mesoporous Materials*, *197*, 288–290.

Cui, X. B., Li, Y., Feng, T.Y., Sun, G. X., & Lin, L. (2007). Separation of acetonitrile and water by saline extractive distillation. *Petrochemical Technology*, 36, 1229−1233.

Dai, Y., Witkamp, G., Verpoorte, R., & Choi, Y.H. (2015). Tailoring properties of natural deep eutectic solvents with water to facilitate their applications. *Food Chemistry*, 187, 14–19.

Daubert, T. E., & Danner, R. P. (1992). Physical and Thermodynamic Properties of Pure Chemicals. Data Compilation, *American Institute of Chemical Engineers*.

De Haan, A., & Bosch, H. (2007).*Fundamentals of Industrial Separations*, 2nd Edition; De Haan& Bosh.

Dejanović, I., Matijašević, L., &Olujić, Ž. (2010). Dividing Wall column—A Breakthrough towards Sustainable Distilling. *Chemical Engineering* and *Processing - Process Intensification*, *49* (6), 559–580.

Del Pozo Gomez, M. T., Klein, A., Repke, J.-U., &Wozny, G. (2008). A new energy-integrated pervaporation distillation approach. *Desalination*, 224, 28.

Delazar, A., Nahar, L., Hamedeyazdan, S., &Sarker, S. D. (2012). Microwave-Assisted Extraction in Natural Products Isolation.*Methods in Molecular Biology*, *864*, 89–115.

Dhamole, P.B., Mahajan, P., & Feng, H. (2010). Sugaring out: a new method for removal of acetonitrile from preparative RP-HPLC eluent for protein purification. *Process Biochemistry*, 45, 1672-1676.

Docherty, K. M., &Kulpa, Jr., C. F. (2005). Toxicity and Antimicrobial Activity of Imidazolium and Pyridinium Ionic Liquids. *Green Chemistry*, *7* (4), 185.

Earle, M. J., Esperanca, J. M. S. S., Gilea, M. A., Lopes, J. N. C., Rebelo, L. P. N., Magee, J. W., Seddon, K.R., &Widegren, J. A. (2006). The Distillation and Volatility of Ionic Liquids. *Nature*, *439* (7078), 831–834.

Fang, J., Liu, J., Li, C., & Liu, Y. (2013). Isobaric vapor -liquid equilibrium for the acetonitrile + water system containing different ionic liquids at atmospheric pressure.*Journal* of *Chemical* & *Engineering Data*, 1483-1489.

Fang, J., Zhao, R., Wang, H., Li, C., & Liu, J. (2015). Functionalized ionic liquids based on [EMIM][OAC] for vapor-liquid phase equilibrium of acetonitrile and water by COSMO-RS method. *Chinese Journal of Chemical Engineering*, 23, 1369-1373.

Fang, J., Zhao, R., Wang, H., Li, C., & Liu, J. (2015). Salting-out effect of ionic liquids on isobaric vapor−liquid equilibrium of acetonitrile-water system. *Chinese Journal* of *Chemical Engineering*, 23, 1369–1373.

Feng, H., Yin, Y., & Tang, J. (2012). Microwave Drying of Food and Agricultural Materials: Basics and Heat and Mass Transfer Modeling. *Food Engineering Reviews*, *4* (2), 89–106.

Feng, Q. L., Wang, X. Q., Jia, Y., & Ning, P. (2013). Study on Microwave Desorption Azeotropic Distillation of Ethanol-Loaded Activated Carbon under Vacuum Condition.*Applied Mechanics and Materials*, *295-298*, 1240–1244.

Flieger, J., &Grushka, E. B. (2014). Ionic Liquids as Solvents in Separation Processes. *Austin Journal of Analytical and Pharmaceutical Chemistry*, *1* (2), 1–8.

Florindo, C., Oliveira, F. S., Rebelo, L. P. N., Fernandes, A. M., &Marrucho, I. M. (2014). Insights into the Synthesis and Properties of Deep Eutectic Solvents Based on Cholinium Chloride and Carboxylic Acids. *ACS Sustainable Chemistry* & *Engineering*, *2* (10), 2416–2425.

Francisco, M., Bruinhorst, A.V.D., Zubeir, L.F., Peters, C.J., Kroon, M.C. (2013). A new low transition temperature mixture (LTTM) formed by choline chloride+ lactic acid: characterization as solvent for $CO_2$ capture. *Fluid Phase Equilibria*, 340, 77–84.

Francisco,M., Van den Bruinhorst, A., &Kroon,M.C. (2012). New natural and renewable low transition temperature mixtures (LTTMs): screening as solvents for lignocellulosic biomass processing. *Green Chemistry*, 14, 2153–2157.

Gao, X., Li, X., Zhang, J., Sun, J., & Li, H. (2013). Influence of a Microwave Irradiation Field on Vapor–liquid Equilibrium. Chemical Engineering Science, *90*, 213–220.

Garcia, G., Aparicio, S., Ullah, R., &Atilhan, M. (2015). Deep Eutectic Solvents: Physicochemical Properties and Gas Separation Applications. *Energy & Fuels*, *29*, 2616–2644.

Gathergood, N., Garcia, M. T., &Scammells, P. J. (2004). Biodegradable Ionic Liquids: Part I. Concept, Preliminary Targets and Evaluation. *Green Chemistry*, *6* (3), 166.

Gathergood, N., Scammells, P. J., & Garcia, M. T. (2006). Biodegradable Ionic Liquids: Part III. The First Readily Biodegradable Ionic Liquids. *Green Chemistry*, *8* (2), 156.

Ghandi, K. (2014). A Review of Ionic Liquids, Their Limits and Applications. *Green and Sustainable Chemistry*, *4*, 44–53.

Gjineci, N., Boli, E., Tzani, A., Detsi, A. &Voutsas, E. (2016). Separation of the ethanol/water azeotropic mixture using ionic liquids and deep eutectic solvents. *Fluid Phase Equilibria*, 424, 1–7.

Gmehling, J., Menke, J., Krafczyk, J., & Fischer, K. (1994). *Azeotropic Data*, VCH Editor, Weinheim.

Godbole, S. P. (2005). *US Patent*,6843890.

Godbole, S. P., Wappelhorst, R. L., & Jacobson, P. A. (2001). *US Patent*,6326508.

Gu, T., Gu, Y., Zheng, Y., Wiehl, P. E., &Kopchick, J. J. (1994). Phase separation of acetonitrile-water mixture in protein purification. *Separation Science & Technology*, 4, 258-261.

Gu, Y., & Shih, P.-H. (2004). Salt-induced phase separation can effectively remove the acetonitrile from the protein sample after the preparative RP-HPLC.*Enzyme and MicrobialTechnology*, 35, 592.

Gupta, M. N., Tyagi, R., Sharma, S., Karthikeyan, S., & Singh, T.P. (2000). Enhancement of catalytic efficiency of enzymes through exposure to organic solvent at 70°C: Three-dimensional structure of a treated serine protease at 2.2 A° resolution. *Proteins*: *Structure*, *Function* and *Genetics*, 39-3, 226-234.

Gutierrez, M. C., Ferrer, M. L., Mateo, C. R., Monte, F. D., & del Monte, F. (2009). Freeze-Drying of Aqueous Solutions of Deep Eutectic Solvents: A Suitable Approach to Deep Eutectic Suspensions of Self- Assembled Structures. *Langmuir, 25* (10), 5509–5515.

Han, D., & Row, K. H. (2010). Recent Applications of Ionic Liquids in Separation Technology. *Molecules*, *15* (4), 2405–2426.

Hayyan, A., Mjalli, F. S., AlNashef, I. M., Al-Wahaibi, T., Al-Wahaibi, Y. M., & Hashim, M. A. (2012). Fruit Sugar-Based Deep Eutectic Solvents and Their Physical Properties.Thermochimica Acta, *541*, 70–75.

Hoof, V.V., Dotremont, C., &Buekenhoudt, A. (2006). Performance of Mitsui NaA type zeolite membranes for the dehydration of organic solvents in comparison with

commercial polymeric pervaporation membranes.*Separation and Purification Technology*, 48, 304–309.

Hosseini, S., Charkhi, A., &Minuchehr, A. (2017).Dehydration of acetonitrile using cross-linked sodium alginate membrane containing nano-sized NaA zeolite.*Chemical Papers*, 71, 1143.

http://pipeline.Corante.com. Lowe, D. (2009). The Great Acetonitrile Shortage. (Assessed on 28/08/ 2018).

http://www.chemmarket.info/en/home/article/2902; Acetonitrile Market in CIS and Worldwide. (2014) Eurasian Chemical Market International Magazine. (Assessed on 25/08/ 2018).

http://www.chromatographyonline.com/lcgc/Column%3A+Column+Watch/The-Continuing. (2009). Majors, R. E. The Continuing Acetonitrile Shortage: How to Combat it or Live with It. (Assessed on 28/08/ 2018).

http://www.ineos.com/businesses/ineos-nitriles. (Assessed on 28/08/2018).

http://www.ineos.com/businesses/ineos-nitriles/news/ineos-nitriles-breakthough-secures-global-supply-of-acetonitrile. (2009). Longden, R. INEOS Nitriles breakthough secures global supply of acetonitrile. (Assessed on 25/08/2018).

http://www.npi.gov.au/resource/acetonitrile. (Assessed on March 3, 2018).

https://www.ihs.com/products/acetonitrile-chemical-economics-handbook.html.(Assessed on 25/08/2018).

Imanishi, N., Fujiyoshi, M., Takeda, Y., Yamamoto, O., &Tabuchi, M. (1999). Preparation and $^{7}$Li-NMR study of chemically delithiated Li1−xCoO2 (0<x<0.5). *Solid State Ionics*, 118, 121−128.

Jiang, X.-C., Wang, J.-F., Li, C.-X., Wang, L.-M., & Wang, Z.-H. (2007). Vapour Pressure Measurement for Binary and Ternary Systems Containing Water Methanol Ethanol and an Ionic Liquid 1-Ethyl-3- EthylimidazoliumDiethylphosphate.*Journal of Chemical Thermodynamics*,*39* (6), 841–846.

Kareem, M. A., Mjalli, F. S., Hashim, M. A., &Alnashef, I. M. (2010). Phosphonium-Based Ionic Liquids Analogues and Their Physical Properties. *Journal* of *Chemical* & *Engineering Data*, *55* (11), 4632–4637.

Kaur, P., Rajani, N., Kumawat, P., Singh, N., & Kushwaha, J. P. (2018). Performance and mechanism of dye extraction from aqueous solution using synthesized deep eutectic solvents. *Colloids and Surfaces A*, 539, 85–91.

Khayet, M., Cojocaru, C., &Zakrzewska-Trnadel, G. (2008). Studies on pervaporation separation of acetone, acetonitrile and ethanol from aqueous solutions. *Separation Purification Technology*, 63, 303-310.

Kim, I., Svendsen, H. F., &Børresen, E. (2008). Ebulliometric determination of vapor-liquid equilibria for pure water, monoethanolamine, N-Methyldiethanolamine, 3-(methylamino)-propylamine, and their binary and ternary solutions. *Journal of Chemical & Engineering Data*, 53, 2521–2531.

Kim, K. W., Shin, J. S., Kim, S. H., Hong, S. K., Cho, J. H. & Park, S. J. (2013). A Computational Study on the Separation of Acetonitrile and Water Azeotropic Mixture Using Pressure Swing Distillation. *Journal* of *Chemical Engineering* of *Japan*, 46(5), 347-352.

Kim. K.-J., Diwekar, U.M., &Tomazi, K. G. (2004). Entrainer selection and solvent recycling in complex batch distillation.*Chemical Engineering Communications*, 191, 1606-1633.

Kishore, N., Sachan, S., Rai, K.N. & Kumar, A. (2003). Synthesis and characterization of a nanofiltration carbon membrane derived from phenol–formaldehyde resin.*Carbon 41*, 2961-2972.

Kittaka, S., Kuranishi, M., Ishimaru, S., &Umahara, O. (2007). Phase separation of acetonitrile–water mixtures and minimizing of ice crystallites from there in confinement of MCM-41.*Journal of Chemical Physics*, 126, 1-4.

Kober, P. A. (1917). Pervaporation, Perstillation and Percrystallization.*Journal of the American ChemicalSociety*,*39 (*5), 944–948.

Kulajanpeng, K., Suriyapraphadilok, U., &Gani, R. (2014). Ionic-Liquid Based Separation of Azeotropic Mixtures.*Chemical Engineering Transactions*, *39*, 517–522.

Kumar, S., & Prasad, R. (2010). Effect of Diaminomethanal on the Vapor-Liquid Equilibria of the Ethanol + Water System at Atmospheric Pressure. *Journal of Chemical & Engineering Data*, 55, 2581-2585.

Kumar, V., & Nigam, K.D.P. (2012). Process intensification in green synthesis. *Green Processing & Synthesis*, 1, 79–107.

Kurzin, A. V., Evdokimov, A. N., Antipina, V. B., & Pavlova, O. S. (2006). Measurement and correlation of isothermal vapor-liquid equilibrium data for the system acetonitrile + water + tetrapropylammonium bromide. *Journal of Chemical & Engineering Data*, 51, 1361−1363.

Kurzin, A.V., Evdokimov, A. N., Poltoratskiy, G.M., Platonov, A. Y., Gusev, V. E., &Golubeva, Y.M. (2004). *Journal of Chemical & Engineering Data*, 49, 208-211.

Leggett, D. C., Jenkins, T. F., &Miyares, P. H. (1990). Salting-out solvent extraction for preconcentration of neutral organic solutes from water.*Analytical Chemistry*, 62, 1355.

Li, J., Yang, X., Chen, K., Zheng, Y., Peng, C., & Liu, H. (2012). Shifting ionic liquids as additives for separation if acetonitrile and water azeotropic mixture using the COSMO-RS methods. *Industrial & Engineering Chemistry Research*, 51, 9376–9385.

Li, T., Yang, Q., Ding, H., Li, J., Peng, C., & Liu, H. (2015). Amino Acid Based Ionic Liquids as Additives for the Separation of an Acetonitrile and Water Azeotropic Mixture: COSMO-RS Prediction and Experimental Verification. *Industrial & Engineering Chemistry Research*, 54, 12143-12149.

Li, Y., & Armor, J.N. (1998). Ammoxidation of ethane to acetonitrile over metal-zeolite catalysts. *Journal of Catalysis*, 173(2), 511–518.

Liao, H.G., Jiang, Y.X., Zhou, Z.Y., Chen, S.P., & Sun, S.G. (2008). Shape-Controlled Synthesis of Gold Nanoparticles in Deep Eutectic Solvents for Studies of Struc-

ture–Functionality Relationships in Electrocatalysis. *AngewandteChemie*, 47, 9100 –9103.

Liu, O., Hao, J.W., Mo, L.P., & Zhang, Z.H. (2015). Recent advances in the application of deep eutectic solvents as sustainable media as well as catalysts in organic reactions. *RSC Advance*, 5, 48675–48704.

Ludwig, R. (2008). Ionic Liquids in Synthesis.Edited by *Peter Wasserscheid and Tom Welton*, Vol. 1.

Mahdi, T., Ahmad, A., Ripin, A., &Nasef, M. M. (2014). Ultrasonic Enhancement of Separation Azeotropic Mixtures via Single Distillation Column.*Advanced Materials Research*, 909, 83–87.

Mahdi, T., Ahmad, A., Ripin, A., &Nasef, M. M. (2014). Vapor-Liquid Equilibrium of Ethanol/ethyl Acetate Mixture in Ultrasonic Intensified Environment.*Korean Journal* of *Chemical Engineering*, 31 (5), 875–880.

Mandal, M.K., Sant, S.B., & Bhattacharya, P.K. (2011). Dehydration of aqueous acetonitrile solution by pervaporation using PVA–iron oxide nanocomposite membrane. *Colloids and surfaces. A: Physicochemical and Engineering Aspects*, 373, 11-21.

Marcotte, F. A., Rombouts, J. R. F., &Lubell, W. D. (2003). Diversity-oriented synthesis of functionalized pyrrolo [3, 2-d] pyrimidines with variation of the pyrimidine ring nitrogen substituents. *Journal of Organic Chemistry*, 68, 6984-6987.

Maslan, F., & Stoddard, E.J. (1956). Acetonitrile–water liquid-vapor equilibrium. *Journal of Physical Chemistry A*, 60(8), 1146–1147.

Masuda,T., Takatsuka, M., Tang, B.Z., &Higashimura, T. (1990). Pervaporation of organic liquid-water mixtures through substituted polyacetylene membranes.*Journal of Membrane Science*, 49, 69–83.

Mcloughlin, C. M., McMinn, W. A. M., & Magee, T. R. A. (2000). Microwave Drying of Pharmaceutical Powders. *Food and Bioproducts Processing*,*78* (2), 90–96.

Meier, M., Turner, M., Vallee, S., Conner, W. C., Lee, K. H., &Yngvesson, K. S. (2009). Microwave Regeneration of Zeolites in a 1 Meter Column. *AIChE Journal*, *55* (7), 1906–1913.

Meindersma, G. W., Podt, A. J. G., Klaren, M. B., & de Haan, A. B. (2006). Separation of Aromatic and Aliphatic Hydrocarbons with Ionic Liquids. *Chemical Engineering Communications*,193(11), 1384–1396.

Melnikov, S.M., Höltzel, A., Seidel-Morgenstern, A., &Tallarek, U. (2013). Adsorption of Water−Acetonitrile Mixtures to Model Silica Surfaces. *Journal of Physical Chemistry C*, 117, 6620−6631.

Mishra, S.B., Sachan, S., Upadhyay, S.N. & Mishra, P.K. (2016). Synthesis, Characterization and Performance Evaluation PVDF-SPES-$ZrO_2$, Membrane. *Desalination and Water Treatment*, 57, 17333-17342.

Miyanaga, S., Tamura, K. & Murakami, S. (1992). Excess molar volumes, isentropic and isothermal compressibities, and isochoric heat capacities of (acetonitrile + benzene), (benzene + dimethylformamide), and (acetonitrile + dimethylformamide) at the temperature 298.15 K, *J. Chem. Thermodynamics*, 24, 1077−1086.

Mulyono, S., Hizaddin, H.F., Wazeer, I., Alqusair, O., Ali, E., Hashim, M.A. &Hadj-Kali, M.K. (2019). Liquid-liquid equilibria data for the separation of ethylbenzene/styrene mixtures using ammonium-based deep eutectic solvents. *Journal of Chemical Thermodynamics*, 135, 296–304.

Naidu, B., Bhat, S.D., Sairam, M., Wali, A.C., Sawant, D.P., Halligudi, S.P., Mallikarjuna, N.N. &Aminabhavi, T.M. (2005). Comparison of the pervaporation separation of a water–acetonitrile mixture with zeolite-filled sodium alginate and poly (vinyl alcohol)–polyaniline semi-interpenetrating polymer network membranes. *Journal of Applied Polymer Science*, 96(5), 1968–1978.Kishore

Nigiz, F.U., &Hilmioglu, N.D. (2012) Pervaporation of ethanol/water mixtures using clinoptilolite and 4A filled sodium alginate membranes. *Desalination*, 300, 24–31.

Olivier-Bourbigou, H., Magna, L., &Morvan, D. (2010). Ionic Liquids and Catalysis: Recent Progress from Knowledge to Applications.*Applied Catalysis A: General, 373* (1-2), 1–56.

Orchillés, A. V., Miguel, P. J., Vercher, E., &Martínez-Andreu, A. (2010). Using 1-Ethyl-3-Methylimidazolium Trifluoromethanesulfonate as an Entrainer for the Extractive

Distillation of Ethanol + Water Mixtures.*Journal* of *Chemical* & *Engineering Data*,*55* (4), 1669–1674.

Othmer, D.F., Gilmont, R., & Conti, J.J. (1960). An Adiabatic Equilibrium Still. *Industrial & Engineering Chemistry*, 52, 625–628.

Othmer, D.F., & Josefowitz S. Composition of Vapors from Boiling Binary Solutions Acetonitrile-Water System. (1947). *Ind. Eng. Chem.* 39, 1175−1177.

Parmentier, D., Paradis, S., Metz, S. J., Wiedmer, S. K., & Kroon, M. C. Continuous Process for Selective Metal Extraction with an Ionic Liquid. (2016). *Chemical Engineering Research & Design, 109, 553-560*.

Paulechka, Y. U., Zaitsau, D. H., Kabo, G. J., &Strechan, A. A. (2005). Vapor Pressure and Thermal Stability of Ionic Liquid 1-Butyl-3-Methylimidazolium Bis(trifluoromethylsulfonyl)amide. *Thermochimica Acta*, *439* (1-2), 158–160.

Pena-Pereira, F., &Namienik, J. (2014) Ionic Liquids and Deep Eutectic Mixtures: Sustainable Solvents for Extraction Processes. *ChemSusChem, 7* (7), 1784–1800.

Peng, Y., Lu, X., Liu, B., & Zhu, J. (2017). Separation of azeotropic mixtures (ethanol and water) enhanced by deep eutectic solvents. *Fluid Phase Equilibria*, 448, 128–134.

Perkins, L.S., Painter, P., &Colina, C.M. (2014) Experimental and computational studies of choline chloride-based deep eutectic solvents. *Journal of Chemical & Engineering Data*, 59, 3652–3662.

Perry, R.H. (1934).*Perry's Chemical Engineers' Handbook*. McGraw-Hill, 7th Edition.

Pfenning, D., &Woermann, D. (1987) Modification of the transport properties of a membrane by selective solvation: hyperfiltration of acetonitrile/water mixtures, *Journal of Membrane Science*, 32, 105–116.

Phadtare, S.B., &Shankarling, G.S. (2010). Halogenation reactions in biodegradable solvent: efficient bromination of substituted 1-aminoanthra-9,10-quinone in deep eutectic solvent (choline chloride:urea). *Green Chemistry*, 12, 458–462.

Pirkanniemi, K., &Sillanpää, M. (2002). Heterogeneous water phase catalysis as an environmental application: a review. *Chemosphere*, 48, 1047–1060.

Plechkova, N. V, & Seddon, K. R. (2008). Applications of Ionic Liquids in the Chemical Industry.*Chemical Society Reviews*,*37*, 123–150.

Presson, R. D., Wu, H. C., &Sockell, E. J. (1982). *US Patent*,4362603.

Rao, C.V., Rao, K.V., Raviprasad, A., &Chiranjivi, C. (1978). Extraction of Acetonitrile from Aqueous Solutions. 1. Ternary Liquid Equilibria, *Journal of Chemical & Engineering Data*, 2, 23-25.

Rao, D.S., Rao, K.V., Raviprasad, A., &Chiranjivi, C. (1979). Extraction of Acetonitrile from Aqueous Mixtures. 2. Ternary Liquid Equilibria, *Journal of Chemical & Engineering Data*, 24, 241-244.

Rebelo, L. P. N., Canongia Lopes, J. N., Esperanca, J. M. S. S., & Filipe, E. (2005). On the Critical Temperature, Normal Boiling Point, and Vapor Pressure of Ionic Liquids. *Journal of Physical Chemistry B*, *109* (13), 6040–6043.

Rehm, B.H. (2009). Alginate production: precursor biosynthesis, polymerization and secretion. *Alginates: biology and applications. Springer*, Berlin, 55–71.

Renon, H., &Prausnitz, J.M. (1968). Local compositions in thermodynamic excess functions for liquid mixtures. *AIChE Journal*, 14, 135–144.

Repke, J.U., Forner, F., Klein, A. (2005). Separation of homogeneous azeotropic mixtures by pressure-swing distillation-analysis of the operation performance. *Chemical Engineering & Technology*, 28, 1151–1157.

Repke, J.U., Klein, A., &Forner, F. (2004). Homogeneous azeotropic distillation in an energy- and mass-integrated pressure swing column system. *Computer Aided Chemical Engineering*, 18, 757–762.

Ripin, A., Abdul Mudalip, S. K., &Mohd. Yunus, R. (2008). Effects of Ultrasonic Waves on Enhancement of Relative Volatilities in Methanol–Water Mixtures.*JurnalTeknologi*, *48* (1), 61–73.

Rocha, M. A. A., Neves, C. M. S. S., Freire, M. G., Russina, O., Triolo, A., Coutinho, J. A. P., & Santos, L.M. N. B. F. (2013). Alkylimidazolium Based Ionic Liquids: Impact of Cation Symmetry on Their Nanoscale Structural Organization. *Journal of Physical Chemistry B,117* (37), 10889–10897.

Rocha, M. A. A., Ribeiro, F. M. S., Ferreira, A. I. M. C. L., Coutinho, J. A. P., & Santos, L. M. N. B. F. (2013). Thermophysical Properties of [CN−1C1im][PF6] Ionic Liquids. *Journal of Molecular Liquids, 188*, 196–202.

Rodriguez, A., Pereiro, B.A. (2011). Ionic Liquids: Applications and Perspectives. *Kokorin* edition.

Rodriguez, N.R., &Kroon,M.C. (2015) Isopropanol dehydration via extractive distillation using low transition temperature mixtures as entrainers. *Journal of Chemical Thermodynamics*, 85, 216–221.

Rodríguez, N.R., Gonz_alez, A.S.B., Tijssen, P.M.A., &Kroon,M.C. (2015). Low transition temperature mixtures (LTTMs) as novel entrainers in extractive distillation. *Fluid Phase Equilibria*, 385, 72–78.

Rodriguez-Donis, I., Esquijarosa, J. A., Gerbaud, V., &Joulia, X. (2003). Heterogenous batch- extractive distillation of minimum boiling azeotropic mixtures, *AIChE Journal*, 49, 3074.

Rodriguez-Donis, I., Gerbaud, V., &Joulia, X. (2001). Heterogeneous Entrainer Selection for the Separation of Azeotropic and Close Boiling Temperature Mixtures by Heterogeneous Batch Distillation. *Industrial & Engineering Chemistry Research*, 40, 2729.

Rodriguez–Donis, I., Pardillo–Fontdevilla, E., Gerbaud, V., &Joulia, X. (2001). Synthesis, experiments and simulation of heterogeneous batch distillation processes. *Computers & Chemical Engineering*, 25, 799–806.

Rosen, J., &Hellenas, K. E. (2002). Analysis of acrylamide in cooked foods by liquid chromate- graphy tandem mass spectrometry. *Analyst*, 127, 880−882.

Ruiz, R.A., Borda, B. N., Alexander, L.R., Javier, R., Guevara, L., Ivan, D., & Gil, C. (2011). Control of an azeotropic distillation process to acetonitrile production, *21st EuropeanSymposium on Computer Aided Process Engineering – ESCAPE 21*.

Salusjärvi, L., Havukainen, S., Koivistoinen, O., &Toivari, M. (2019). Biotechnological production of glycolic acid and ethylene glycol: current state and perspectives, *Applied Microbiology and Biotechnology*, 103, 2525-2535.

Samarov, A. A., Smirnov M.A., Sokolova, M.P., Popova, E.N., &Toikka, A.M. (2017). Choline chloride based deep eutectic solvents as extraction media for separation of n-hexane-ethanol mixture, *Fluid Phase Equilibria*, 448, 123–127.

Samarov, A.A., Smirnov, M.A., Toikka, A.M., &Prikhodko, I.V. (2018). Study of Deep Eutectic Solvent on the Base Choline Chloride as Entrainer for the Separation Alcohol–Ester Systems. *Journal of Chemical & Engineering Data*, 63, 6, 1877.

Sangal, V.K., Kumar, V., & Mishra, I.M. (2012). Optimization of structural and operational variables for the energy efficiency of a divided wall distillation column. *Computers & Chemical Engineering*, 40, 33-40.

Sangal, V.K., Kumar, V., & Mishra, I.M. (2014). Process Parametric Optimization of a Divided Wall Distillation Column. *Chemical Engineering Communications (ISSN: 0098- 6445)*, 201, 72-87.

Saravanan, G., & Mohan, S. (2012). Structure, composition and corrosion resistance studies of Co–Cr alloy electrodeposited from deep eutectic solvent (DES).*Journal of Alloys and Compounds*, 522, 162–166. Pirkanniemi

Sazonova, A.Y., &Raeva, V.M. (2015). Recovery of Acetonitrile from Aqueous Solutions by Extractive Distillation–Effect of Entrainer.International *Journal* of *Chemical* and *Molecular Engineering*, 9, 288–291.

Scholtz, J., &Grimsehl, U. (2002). Characterisation of the pervaporative separation of water and acetonitrile by PVA membranes. *South African Journal* of *Chemical Engineering*, 14(1), 1–14.

Seiler, M., Jork, C., Karvanou, A., Arlt, W., & Hirsch, R. (2004). Separation of azeotropic mixtures using hyperbranched polymers or ionic liquids. *AIChE Journal*, 50, 2439−2454.

Smith, J.M., Van, N.H.C., & Abbott, M.M. (2001). Introduction to chemical engineering thermodynamics, *McGraw-Hill, New York*, 6th Edition.

Sorensen, J. M., Magnussen, T., Rasmussen, P., &Fredenslund, A. (1979). Liquid-Liquid Equilibrium Data: Their Retrieval, Correlation and Prediction Part I: Retrieval. *Fluid Phase Equilibria*, *2* (4), 297–309.

Soukup, J., &Jandera, P. (2014). Adsorption of water from aqueous acetonitrile on silica-based stationary phases in aqueous normal-phase liquid chromatography. *Journal of Chromatography A*, 1374, 102–111.

Srinivasu, M. K., Raju, A. N., & Reddy, G. O. (2002). Determination of lovastatin and simvastatin in pharmaceutical dosage forms by MEKC. *Journal of Pharmaceutical and Biomedical Analysis*, 29, 715−721.

Tadesse, H., &Luque, R. (2011). Advances on Biomass Pretreatment Using Ionic Liquids: An Overview.*Energy & Environmental Science*, *4* (10), 3913.

Takamuku, T., Noguchi, Y., Yoshikawa, E., Kawaguchi, T., Matsugami, M., &Otomo, T. (2007). Alkali chlorides-induced phase separation of acetonitrile-water mixtures studied by small-angle neutron scattering. *Journal of Molecular Liquids*, 131, 131-138.

Tan, S. S. Y., & Macfarlane, D. R. (2010). Ionic Liquids in Biomass Processing. *Topics in CurrentChemistry*, *290*, 311–339.

Teles, A.R., Capela, E.V., Carmo, R.S., Coutinho, J.A.P., Silvestre, A.J.D., & Freire, M.G. (2017). Solvatochromic parameters of deep eutectic solvents formed by ammonium-based salts and carboxylic acids. *Fluid Phase Equilibria*, 448, 15-21.

Therdthai, N., & Zhou, W. (2009). Characterization of Microwave Vacuum Drying and Hot Air Drying of Mint Leaves (Mentha CordifoliaOpiz Ex Fresen). *Journal of Food Engineering*, *91* (3), 482–489.

Tsonopoulos, C. (1974). An empirical correlation of second virial coefficient. *AIChE Journal*, 20, 263–272.

Tsuru, T. &Tsuru, W. (2000).*Pervaporation Kirk-Othmer Encyclopedia of Chemical Technology*. John Wiley & Sons, Inc.: Hoboken, NJ, USA.

Valente, I.M., Goncalves, L.M., & Rodrigues, J.A. (2013). Another glimpse over the salting-out assisted liquid-liquid extraction in acetonitrile/water mixtures. *Journal of Chromatography A*, 58–62, 1308.

Valkenburg, M. E. V., Vaughn, R. L., Williams, M., & Wilkes, J. S. (2005). Thermochemistry of Ionic Liquid Heat-Transfer Fluids. *Thermochimica Acta*, *425* (1-2), 181–188.

Van Assche, T.R.C., Remy, T., Desmet, G., Baron, G.V., &Denayer, J.F.M. (2011). Adsorption separation of liquid water/ acetonitrile mixtures.*Separation and PurificationTechnology*, 82, 76-86.

Van Osch, D. J. G. P., Zubeir, L. F., van den Bruinhorst, A., Rocha, M. A. A., & Kroon, M. C. (2015). Hydrophobic Deep Eutectic Solvents as Water-Immiscible Extractants. *Green Chemistry,17* (9), 4518–4521.

Verevkin, S.P., Sazonova, A.Y., Frolkova, A.K., Zaitsau, D.H., Prikhodko, I.V.,& Held, C. (2015). Separation Performance of BioRenewable Deep Eutectic Solvents. *Industrial & Engineering Chemistry Research*, 54, 13, 3498-3504.

Wang, B., Feng, H., Ezeji, T., &Blaschek, H. (2008). Sugaring-Out Separation of Acetonitrile from Its Aqueous Solution. *Chemical Engineering & Technology*, 31, 1869–1874.

Wazeer, I., Hayyanb, M., &Hadj-Kali, M.K. (2018). Deep Eutectic Solvents: Designer Fluids for Chemical Processes. *Journal of Chemical Technology & Biotechnology*, 93, 945–958.

Welton, T. (1999). Room-Temperature Ionic Liquids. Solvents for Synthesis and Catalysis. *Chemical Reviews*, *99* (1), 2071–2083.

Welton, T. (2004). Ionic Liquids in Catalysis. *Coordination Chemistry* Reviews,*248* (21-24), 2459–2477.

Wilkes, J. S. (2002). A Short History of Ionic Liquids-from Molten Salts to Neoteric Solvents. *Green Chemistry,4* (2), 73–80.

Xin, R., Qi, S., Zeng, C., Iqbal Khan, F., Yang, B., & Wang, Y. (2017) Functional natural deep eutectic solvent based on trehalose: Structural and physicochemical properties. *Food Chemistry*, 217, 560–567.

Xu, K.X. (2002). *Handbook of fine organic chemical raw materials and intermediates*. Chemical Industry Press: Beijing, 2nd edition.

Yang, H., & Bard, A. J. (1991). The application of rapid scan cyclic voltammetry and digital simulation to the study of the mechanism of diphenylamine oxidation, radical cation dimerization, and polymerization in acetonitrile. *Journal of ElectroanalyticalChemistry and InterfacialElectrochemistry*, 306, 87−109.

Yu, M., Yang, J., Zheng, Z. (2014). Simulation and optimization for separation of acetonitrile and water by pressure swing distillation and extractive distillation. *Journal of Central South University (Science and Technology)*, 45 (9), 2966–2971.

Zerry, R., Repke, J.U., Wusterhausen, M., &Wozny, G. (2005). Novel Heat Integration Concepts for Hybrid Distillation/Pervaporation Processes. *Berlin Technical University, Dep. of Process and Plant Technology, Berlin, Germany*.

Zhang, Q., De Oliveira Vigier, K., Royer, S., & Jerome, F. (2012). Deep Eutectic Solvents: Syntheses, Properties and Applications. *Chemical Society Reviews*, *41* (21), 7108–7146.

Zhang, Q., Zhang, S., & Deng, Y. (2011). Recent Advances in Ionic Liquid Catalysis. *Green Chemistry*, *13* (10), 2619.

Zhang, Z., Lv, M., Huang, D., Jia, P., Sun, D., & Li, W. (2013). Isobaric vapor-liquid equilibrium for the extractive distillation of acetonitrile + water mixtures using dimethyl sulfoxide at 101.3 kPa. *Journal of Chemistry*, 58, 3364-3369.

Zhao, J., Jiang, X.-C., Li, C.-X., & Wang, Z.-H. (2006). Vapor Pressure Measurement for Binary and Ternary Systems Containing a Phosphoric Ionic Liquid. *Fluid Phase Equilibria*, *247* (1), 190–198.

Zhou, J.B., Cui, X.B., Dong, B.L., Wang, Y.F., & Chen, Z. K. (2009). Separation of acetonitrile and water mixture by batch extractive distillation.*Industrial* & *Engineering Chemistry*, 26, 482−486.

# APPENDICES

## Appendix 1

### A1. Step by step methodology of calculation for activity coefficient and fugacity coefficient using the Tsonopoulos correlation

The step by stepmethodology of calculation for activity coefficient and fugacity coefficient estimation using the Tsonopoulos correlation are as following:

1. **Second virial coefficient estimation-**

The Tsonopoulos correlation given for second virial coefficients is as following:

$$\frac{BP_c}{RT_c} = f^{(0)}(T_R) + \omega f^{(1)}(T_R) + f^{(2)}(T_R)$$

Where

$$f^{(0)}(T_R) = 0.1445 - \frac{0.330}{T_R} - \frac{0.1385}{T_R^2} - \frac{0.0121}{T_R^3} - \frac{0.000607}{T_R^8}$$

$$f^{(1)}(T_R) = 0.0637 + \frac{0.331}{T_R^2} - \frac{0.423}{T_R^3} - \frac{0.008}{T_R^8}$$

$$f^{(2)}(T_R) = \frac{a}{T_R^6}$$

where

$B =$ Second virial coefficient

$P_c =$ Critical pressure

$R =$ Gas constant

$T_c =$ Critical temperature

$f^{(0)}, f^{(1)}, f^{(2)} =$ Dimensionless terms of Tsonopoulos equation

$T_c =$ Reduced temperature

$\omega =$ Acentric factor

$a =$ Parameter of polar contribution term to second virial coefficient

2. **Fugacity coefficient estimation-**

$$ln\widehat{\emptyset}_i^v = \frac{B \times P}{R \times T}$$

$$ln\widehat{\emptyset}_i^s = \frac{B \times P_i^s}{R \times T}$$

where

$\widehat{\emptyset}_i^v$ =Fugacity coefficient of the component $i$

$\widehat{\emptyset}_i^s$ =Fugacity coefficient of saturated component $i$

$P$ = Pressure

**3. Activity coefficient calculation-**

$$\gamma_i = \frac{y_i \times P \times \left(\widehat{\emptyset}_i^v \Big/ \widehat{\emptyset}_i^s\right)}{x_i \times P_i^s}$$

Where

$\gamma_i$ = Activity coefficient of component $i$

$x_i$ = Mole fraction of component $i$ in liquid phase

$y_i$ = Mole fraction of component $i$ in vapor phase

$P_i^s$ =Saturated vapor pressure of the component $i$

# Appendix 2

## A2.1 Calculation of Relative Volatility

The relative volatility α of ACN + water system at various concentrations of extracting agents was calculated using the following equation:

$$\alpha = \frac{\frac{y_1}{1-y_1}}{\frac{x_1'}{1-x_1'}}$$

Where,

$x_1'$ = mole fraction of ACN in liquid on extracting agent-free basis

$y_1$ = mole fraction of ACN in equilibrium vapour

# Appendix 3

## CALCULATION OF UNCERTAINTIES

### A3.1 Standard Uncertainties in $x_1'$ and $y_1$

By analysing an ACN + water sample, the uncertainty in mole fraction $x_1'$ and $y_1$ were calculated. Calculation procedure is shown by using the raw data for the triplicate measurements for Table 4.6. The uncertainty in mole fractions are calculated as under in Table A3.1:

**Table A3.1 Calculation of Standard Uncertainties in $x_1'$ and $y_1$**

| | Measurement No. | $x_1'$ | $x_1' - \overline{x_1'}$ | $\left(x_1' - \overline{x_1'}\right)^2$ |
|---|---|---|---|---|
| | 1. | 0.903 | 0.00167 | 0.000003 |
| | 2. | 0.896 | -0.00533 | 0.000028 |
| 1. | 3. | 0.901 | 0.00367 | 0.000013 |
| | | | | $\sum\left(x_1' - \overline{x_1'}\right)^2 = 0.000045$ |
| | | | | $u(x_1') = 0.00273$ |
| | 1. | 0.837 | -0.00500 | 0.000025 |
| | 2. | 0.844 | 0.00200 | 0.000004 |
| 2. | 3. | 0.845 | 0.00300 | 0.000009 |
| | | | | $\sum\left(x_1' - \overline{x_1'}\right)^2 = 0.000038$ |
| | | | | $u(x_1') = 0.00252$ |
| | 1. | 0.810 | 0.00400 | 0.000016 |
| | 2. | 0.807 | 0.00100 | 0.000001 |
| 3. | 3. | 0.801 | -0.00500 | 0.000025 |
| | | | | $\sum\left(x_1' - \overline{x_1'}\right)^2 = 0.000042$ |
| | | | | $u(x_1') = 0.00265$ |
| | 1. | 0.761 | 0.00433 | 0.000019 |
| 4. | 2. | 0.758 | 0.00133 | 0.000002 |

| | | | | |
|---|---|---|---|---|
| | 3. | 0.751 | -0.00567 | 0.000032 |
| | | | | $\sum\left(x_1' - \overline{x_1'}\right)^2 = 0.000053$<br>$u(x_1') = 0.00296$ |
| | 1. | 0.703 | -0.00567 | 0.000032 |
| | 2. | 0.712 | 0.00333 | 0.000011 |
| 5. | 3. | 0.711 | 0.00233 | 0.000005 |
| | | | | $\sum\left(x_1' - \overline{x_1'}\right)^2 = 0.000049$<br>$u(x_1') = 0.00285$ |
| | 1. | 0.684 | -0.00467 | 0.000022 |
| | 2. | 0.689 | 0.00033 | 0.000000 |
| 6. | 3. | 0.693 | 0.00433 | 0.000019 |
| | | | | $\sum\left(x_1' - \overline{x_1'}\right)^2 = 0.000041$<br>$u(x_1') = 0.00260$ |
| | 1. | 0.663 | 0.00500 | 0.000025 |
| | 2. | 0.653 | -0.00500 | 0.000025 |
| 7. | 3. | 0.658 | 0.00000 | 0.000000 |
| | | | | $\sum\left(x_1' - \overline{x_1'}\right)^2 = 0.000050$<br>$u(x_1') = 0.00289$ |
| | 1. | 0.596 | -0.00533 | 0.000028 |
| | 2. | 0.606 | 0.00467 | 0.000022 |
| 8. | 3. | 0.602 | 0.00067 | 0.000000 |
| | | | | $\sum\left(x_1' - \overline{x_1'}\right)^2 = 0.000051$<br>$u(x_1') = 0.00291$ |
| | 1. | 0.540 | -0.00267 | 0.000007 |
| | 2. | 0.548 | 0.00533 | 0.000028 |
| 9. | 3. | 0.540 | -0.00267 | 0.000007 |
| | | | | $\sum\left(x_1' - \overline{x_1'}\right)^2 = 0.000043$<br>$u(x_1') = 0.00267$ |
| | 1. | 0.417 | 0.00367 | 0.000013 |

| | | | | |
|---|---|---|---|---|
| | 2. | 0.408 | -0.00533 | 0.000028 |
| | 3. | 0.415 | 0.00167 | 0.000003 |
| 10. | | | | $\sum\left(x_1' - \overline{x_1'}\right)^2 = 0.000045$<br>$u(x_1') = 0.00273$ |
| | 1. | 0.389 | -0.00300 | 0.000009 |
| | 2. | 0.398 | 0.00600 | 0.000036 |
| 11. | 3. | 0.389 | -0.00300 | 0.000009 |
| | | | | $\sum\left(x_1' - \overline{x_1'}\right)^2 = 0.000054$<br>$u(x_1') = 0.00300$ |
| | 1. | 0.349 | 0.00233 | 0.000005 |
| | 2. | 0.350 | 0.00333 | 0.000011 |
| 12. | 3. | 0.341 | -0.00567 | 0.000032 |
| | | | | $\sum\left(x_1' - \overline{x_1'}\right)^2 = 0.000049$<br>$u(x_1') = 0.00285$ |
| | 1. | 0.311 | -0.00533 | 0.000028 |
| | 2. | 0.319 | 0.00267 | 0.000007 |
| 13. | 3. | 0.319 | 0.00267 | 0.000007 |
| | | | | $\sum\left(x_1' - \overline{x_1'}\right)^2 = 0.000043$<br>$u(x_1') = 0.00267$ |
| | 1. | 0.288 | -0.00300 | 0.000009 |
| | 2. | 0.289 | -0.00200 | 0.000004 |
| 14. | 3. | 0.296 | 0.00500 | 0.000025 |
| | | | | $\sum\left(x_1' - \overline{x_1'}\right)^2 = 0.000038$<br>$u(x_1') = 0.00252$ |
| | 1. | 0.261 | -0.00600 | 0.000036 |
| | 2. | 0.271 | 0.00400 | 0.000016 |
| 15. | 3. | 0.269 | 0.00200 | 0.000004 |
| | | | | $\sum\left(x_1' - \overline{x_1'}\right)^2 = 0.000056$<br>$u(x_1') = 0.00306$ |

| | | | | |
|---|---|---|---|---|
| | 1. | 0.249 | 0.00133 | 0.000002 |
| | 2. | 0.251 | 0.00333 | 0.000011 |
| 16. | 3. | 0.243 | -0.00467 | 0.000022 |
| | | | | $\sum\left(x_1' - \overline{x_1'}\right)^2 = 0.000035$<br>$u(x_1') = 0.00240$ |
| | 1. | 0.200 | -0.00200 | 0.000004 |
| | 2. | 0.199 | -0.00300 | 0.000009 |
| 17. | 3. | 0.207 | 0.00500 | 0.000025 |
| | | | | $\sum\left(x_1' - \overline{x_1'}\right)^2 = 0.000038$<br>$u(x_1') = 0.00252$ |
| | 1. | 0.171 | -0.00567 | 0.000032 |
| | 2. | 0.178 | 0.00133 | 0.000002 |
| 18. | 3. | 0.181 | 0.00433 | 0.000019 |
| | | | | $\sum\left(x_1' - \overline{x_1'}\right)^2 = 0.000053$<br>$u(x_1') = 0.00296$ |
| | 1. | 0.142 | 0.00367 | 0.000013 |
| | 2. | 0.135 | -0.00333 | 0.000011 |
| 19. | 3. | 0.138 | -0.00033 | 0.000000 |
| | | | | $\sum\left(x_1' - \overline{x_1'}\right)^2 = 0.000025$<br>$u(x_1') = 0.00203$ |
| | 1. | 0.105 | -0.00500 | 0.000025 |
| | 2. | 0.114 | 0.00400 | 0.000016 |
| 20. | 3. | 0.111 | 0.00100 | 0.000001 |
| | | | | $\sum\left(x_1' - \overline{x_1'}\right)^2 = 0.000042$<br>$u(x_1') = 0.00265$ |
| | 1. | 0.089 | 0.00333 | 0.000011 |
| | 2. | 0.087 | 0.00133 | 0.000002 |
| 21. | 3. | 0.081 | -0.00467 | 0.000022 |
| | | | | $\sum\left(x_1' - \overline{x_1'}\right)^2 = 0.000035$ |

$$u(x_1') = 0.00240$$

$$u(x_1') = \left[\frac{1}{n(n-1)}\sum\left(x_1' - \overline{x_1'}\right)^2\right]^{1/2}$$

$u = 0.0027$ (say 0.003)

### A3.2 Combined Relative Uncertainty in α

The experimental data on ACN composition in liquid (DES free basis) and vapor at 5 mol% concentration of DES (GC 3:1) are given in Table A3.3. The relative volatility $\alpha$ has been calculated and tabulated in Table 4.2. The calculation of relative uncertainty in $\alpha$ is given below:

Table A3.2 Calculation of Combined Relative Uncertainty in α

| $x_1'$ | $y_1$ | $\alpha$ | B | C | D |
|---|---|---|---|---|---|
| 0.912 | 0.965 | 2.65 | 0.00852961 | 0.09 | 0.034851 |
| 0.87 | 0.947 | 2.64 | 0.00375846 | 0.06 | 0.023222 |
| 0.821 | 0.926 | 2.72 | 0.00194827 | 0.04 | 0.016228 |
| | | | | | ∑D = 0.074301 |

$B = (0.003/y_1)^2 + \{0.003/(1-x_1')\}^2 + (0.003/x_1')^2 + \{0.003/(1-y_1)\}^2$

$C = B^{1/2}$

$D = C/\alpha$

$u_{c,r}(\alpha) = (\sum D)/n$

$= 0.074301/3$

$= 0.024767$ (say 0.025)

### A3.3 Uncertainty in Barometric Pressure

The uncertainty in barometric pressure $u(p)$ has been reported as 0.05 kPa within which the atmospheric pressure was observed to vary.

# PUBLICATIONS FROM THESIS

## Papers published in SCI Journals

1. Bandhana Sharma, Neetu Singh and Jai Prakash Kushwaha. Ammonium-based deep eutectic solvent as entrainer for separation of acetonitrile–water mixture by extractive distillation, **Journal of Molecular Liquids** 285 (2019) 185–193. (**Impact factor**: 5.065)
2. Bandhana Sharma, Neetu Singh and Jai Prakash Kushwaha. Natural deep eutectic solvent (NADES)-mediated extractive distillation for separation of Acetonitrile+ water azeotropic mixture. **Journal of Chemical & Engineering Data** 65 (2020) 1497–1505. (**Impact factor**: 2.369)
3. Bandhana Sharma, Neetu Singh, Tarun Jain, Jai Prakash Kushwaha and Parminder Singh. Acetonitrile dehydration via extractive distillation using low transition temperature mixtures as entrainer, **Journal of Chemical & Engineering Data** 63 (2018) 2921–2930. (**Impact factor**: 2.369)

## International Conference

1. Bandhana Sharma, Neetu Singh and Jai Prakash Kushwaha , Dehydration of Aqueous Acetonitrile by Extractive Distillation using deep eutectic solvent as Extracting agent, ***CHEMCON 2018*** *– Seamless Chemical Engineering in Service of Humanity: Innovations, Opportunities & Challenges* (December 27–30, 2018), Dr. B. R. Ambedkar National Institute of Technology, Jalandhar, India

## National Conference

1. Bandhana Sharma, Neetu Singh, and Jai Prakash Kushwaha, Recovery of acetonitrile from industrial waste stream: A review, *National Conference on Advances in Chemical and Environment Engineering - 2016* ***(ACEE 2016)*** (April 22–23, 2016), Dr. B. R. Ambedkar National Institute of Technology, Jalandhar, India.